Experimental Investigation of the At Rest and Active Lateral Earth Pressure of Overconsolidated Sand

Riad Al-Romhein

A Thesis
in
The Department
of
Civil Engineering

Presented in Partial Fulfillment of the requirements
for the Degree of Master of Applied Science at

Concordia University
Montreal, Quebec, Canada

October 1995

ISBN 0-612-05132-3

ABSTRACT

Experimental Investigation of the At Rest and Active Lateral Earth Pressures of Overconsolidated Sand

Riad Al-Romhein

The present study is an experimental investigation on the effect of soil stress history expressed in terms of the overconsolidation ratio, on the at rest and active earth pressures.

Prototype experimental model was instrumented to measure the total and the distribution of the earth pressure on the retaining wall as well as the vertical and the horizontal stresses in predetermined points in the sand mass, behind the wall.

In order to produce an overconsolidated sand mass in the lab, two sand placing techniques were developed. First, the sand was overconsolidated by applying a surface static uniform load for a period of time (In order to allow the consolidation process to be completed) and then unloading. Second, the sand was overconsolidated by means of placing the sand in layers, and compacting each mechanically by an air compressor.

The results revealed that the overconsolidation ratios affect substantially the values of the earth pressure at rest, while they have no effect on the active earth pressure.

Semi-empirical formula and design charts were developed to predict the coefficient of earth pressure at rest for a given angle of shearing resistance, ϕ, and overconsolidation ratio, OCR.

ACKNOWLEDGMENTS

I wish to acknowledge my sincere gratitude to Professor A.M.Hanna for his abiding encouragement, constant interest, talented support, suggestions and ideas during the preparation of this thesis. His helpful criticism, supervision, valuable guidance and concentration on producing a good report brought about this research.

I also would like to thank all the professors and the staff in the department for their collaboration, advice and information.

For their helpful assistance during the development of the process first, I would like to thank Mr.Andrew Chociwski in the Structural Laboratory, Concordia University for his help during the testing program and his instructions concerning safety. Besides, I owe thanks to Mr.Daniel Roy for taking the photographs presented here and writing the computer programming for the data acquisition system with providing assistance to manufacture and install the equipments. Furthermore, I would like to thank the employees who helped in manufacturing all requested parts within logical periods of time.

Besides, I would like to thank all my colleagues in the department of civil engineering and Mr.Gilles Champigny for offering their help and suggestions in the use of the computer software.

Finally, I am indebited to my wife, Rita, for her constant encouragement throughout my studies.

TABLE OF CONTENTS

LIST OF FIGURES

CHAPTER 4

LIST OF TABLES

LIST OF SYMBOLS

Symbol	Represents	Chapter
ENGLISH		
a	The slope of the straight line showing in logarithmic scale OCR vs. σ_3 / σ_1	2
c	Cohesion of the soil.	2
Cc	The uniformity coefficient.	2
Cu	The Coefficient of curvature.	2
d	The width of the plate.	2
Dr	The relative density.	2
Gs	The specific gravity.	2
H	The height of the wall.	2
k	Coefficient from Rowe's stress dilatancy that equal to: $0.5 \times \left(1 - \frac{d\varepsilon_v^p}{d\varepsilon_a^p}\right)$	2
K_a	Coefficient of the active lateral earth pressure.	2
Ko	Coefficient of the at rest lateral earth pressure.	2
$K_{o(nc)}$	Coefficient of the at rest lateral earth pressure for normally consolidated soils.	2

$K_{o(ocr)}$	Coefficient of the at rest lateral earth pressure for overconsolidated soils.	2
K_p	Passive lateral earth pressure.	2
K'o	The intercept with $\sigma_{1max}/\sigma_1 = 1$ This is the last point of the primary	2
	loading in the logarithmic graph OCR vs. σ_3/σ_1.	2
Kr	Coefficient of lateral earth pressure in rebound.	2
n	The exponent of OCR that could be taken from a special graph for Alpan	2
OCR	Over Consolidation Ratio.	2
P_a	Active force on the retaining wall.	2
p_c	The maximum isotropic consolidation stress in the triaxial test.	2
p'_c	The maximum effective stress in the soil.	2
p_o	The minimum isotropic stress	2
p'_o	The present overburden effective stress in the soil	2
p_h	Horizontal stress on the element base.	2
p_v	Normal stress on the element base.	2
R	The ratio of the axial stress to the lateral stress in the triaxial tests.	2
V	Volume of the sample.	2

GREEK

α	Diversion of the slip angle due to densification.	2

β	Angle of the trial wedge failure.	2
γ	The unit weight of the soil.	2
γ_d	Actual in place soil density	2
γ_{min}	Loosest density of the soil.According ASTM D2049.	2
δ	Angle of friction between the soil and the wall.	2
ε_v	Volumetric strain	2
ε_a	Axial strain	2
θ	Angle of inclination of the wall.	2
λ	The ratio of the change in effective horizontal stress to the change in	2
	effective vertical stress	2
μ	Poisson's Ratio.	2
σ_1	Minor principal stress	2
σ_3	Major principal stress	2
σ_a	Axial stress	2
σ_c	Maximum vertical pressure ever applied on an element.	
σ_h	The horizontal stress on an element in the soil.	2
σ_r	Lateral stress	2
σ_v	The vertical stress on the soil.	2

σ_1'	Minor effective principal stress.	2
σ_3'	Major effective principal stress.	2
τ	Shear strength.	2
ϕ	Angle of shearing resistance	2
ϕ'	Effective angle of shearing resistance.	2
ϕ_{cv}	Angle of interangular friction with constant volume test.	2
Φ_μ	Angle of interangular friction.	2

CHAPTER 1

INTRODUCTION

1-1 GENERAL.

The technology of construction shows that old scientists had good common sense in dealing with geotechnical problems. However, documents in this field started early in the nineteenth century when major geotechnical problems were solved.

Few attempts were made to evaluate the earth pressure either theoretically or experimentally by means of laboratory testing. These kinds of research continue to advance due to the development of instruments and powerful computer facilities. However, due to the difficulty in duplicating overconsolidated cohesionless soils in the laboratory, the effects of overconsolidation ratios in the performance of this sand mass under loading and unloading remain undefined.

In the literature the lateral earth pressure on retaining walls has been studied by several researchers. However, it was limited to the case of normally consolidated sand or normally and overconsolidated clay. Some attempts were made on overconsolidated sand which was overconsolidated by means of compaction in the laboratory. This proven to be not simulating the field condition. Furthermore, there is no available literature showing the effect of the stress history on active lateral earth pressure.

1-2 RESEARCH OBJECTIVES

The objective of this research program is to study the influence of the stress history in the case of homogeneous sand on both the at rest and active lateral earth pressures behind retaining structures. For this purpose, a prototype experimental set-up was developed to allow the measuring of the earth pressure on a retaining wall subjected to at rest or active condition, as well as the overconsolidation ratio of the sand.

Chapter one represents an introduction to the subject and the objective of this thesis. Chapter two reports the literature review. The properties of the sand, the experimental Set-UP and the laboratory test techniques are shown in chapter three. In chapter four the experimental results are recorded together with the analysis and discussion. Finally, in chapter five the conclusion is given and the recommendation for future researches is presented.

CHAPTER 2

REVIEW OF PREVIOUS STUDIES.

2-1 GENERAL.

The stresses in soil mass are the result of the soil's own weight and any other external loading. These stresses are function of the existing loading condition as well as the ones imposed on this soil in the past. Evaluation of these stresses under any existing loading condition is well documented in literature. However, such evaluation is rather complicated for the case of previous loading. The stress history plays an important role in the determination of the earth pressure on the walls.

2-2 Active Lateral earth pressure.

The problem of earth pressure generated on retaining structures was studied in 1776 by Coulomb C.A. (8), who presented the theory of lateral earth pressure for both the active and the passive lateral cases. In developing his theory he assumed that the soil is homogeneous i.e $\tau = \sigma$ tang ϕ, (where: τ is the shearing resistance of the sand, σ is the normal pressure on the failure plane and ϕ is angle of shearing resistance) and the friction forces either in the soil or on the wall are uniform and finally the rupture surface is a plane surface. Figure (2- 1) shows the equilibrium of the free body where:

$$P_a = \frac{1}{2} K_a \gamma H^2 \qquad (2\text{-}1)$$

$$K_a = \frac{\cos^2 \cdot (\Phi - \theta)}{\cos^2(\Theta)\cos(\delta+\theta)\left[1+\sqrt{\frac{\sin(\delta+\phi)\sin(\Phi-\alpha)}{\cos(\delta+\theta)\cos(\theta-\alpha)}}\right]^2} \qquad (2\text{-}2)$$

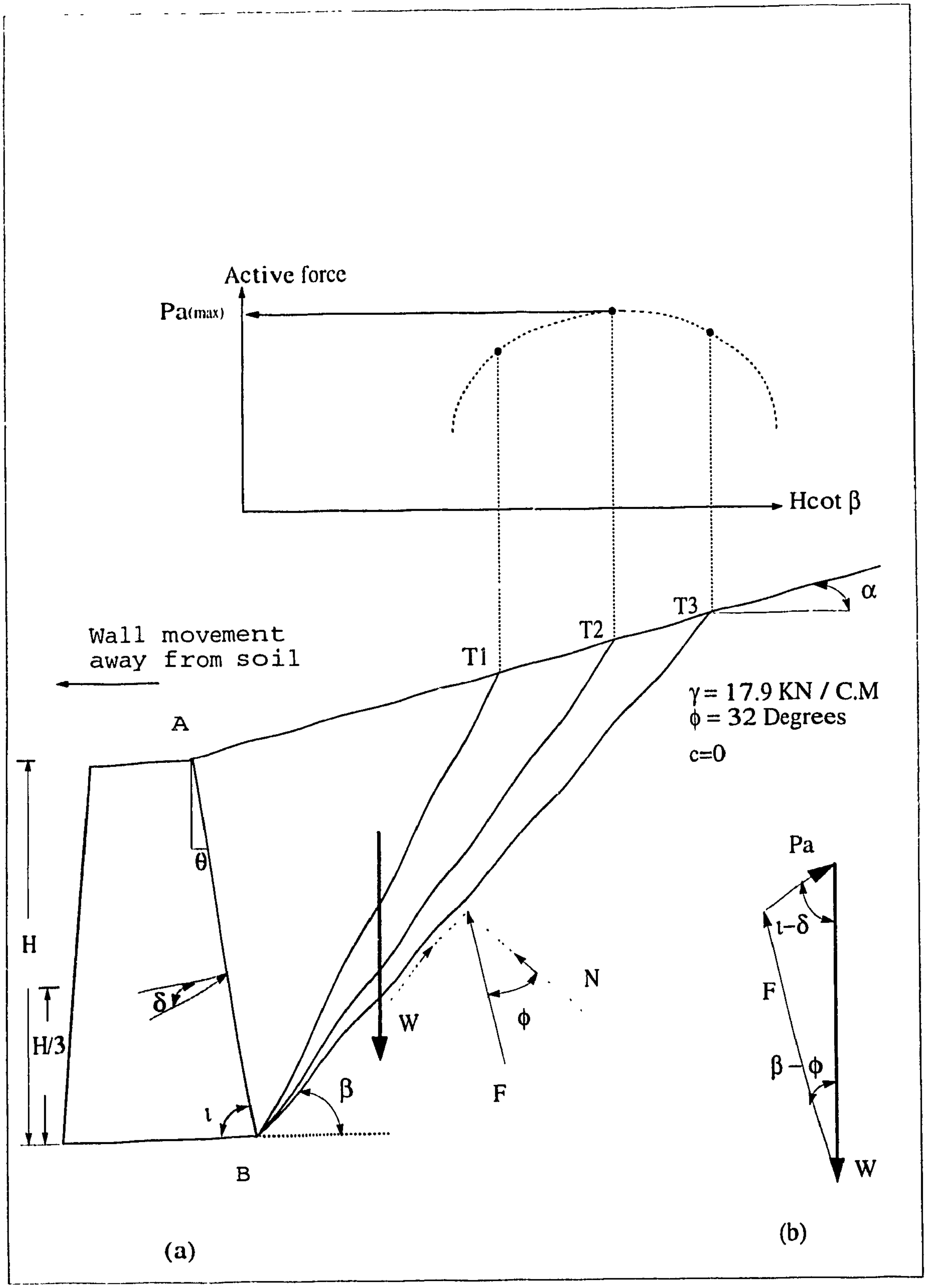

Figure 2-1 Coulomb's active earth pressure. a) trial failure wedge, b) force polygon

Where Ka is Coulomb's active earth pressure coefficient. The maximum Pa could be calculated by making several trials with different values of β.

In 1857, Rankine, W. J. M. (22), presented his theory to predict the earth pressures by assuming that every point in a soil mass is on the verge of failure (state of plastic equilibrium). In this theory the failure mechanism is developed simultaneously through out a semi-finite mass of soil subjected to its own weight and the wall is frictionless and extends to infinite depth. Fig (2-2) illustrates the Rankine states where the considered element has a unit cross section. The normal stress on the element base is:

$$P_v = \gamma H \qquad (2\text{-}3)$$

The state of plastic equilibrium is represented by the Mohr circle where the vertical stress could be either the minor or the major principal stress according to the situation of the retaining wall, i.e (the wall is pushed by the sand or the wall is pushing the sand). Pv is the major principal stress and Ph is the minor principal stress in the case when the retaining wall is pushed by the sand as a result, the following equations can be developed:

$$\sin\Phi = \frac{OaA}{NOa} \qquad (2\text{-}4)$$

$$\sin\Phi = \frac{\sigma'_1 - \sigma'_3}{\sigma'_1 + \sigma'_3} \qquad (2\text{-}5)$$

where σ'_1 is the major principal effective stress and σ'_3 is the minor principal effective stress and By rearranging the last equation we can get:

$$K_a = \frac{P_h}{P_v} = \frac{\sigma'_3}{\sigma'_1} \qquad (2\text{-}6)$$

$$K_a = \frac{(1 - \sin\Phi)}{(1 + \sin\Phi)} \qquad (2\text{-}7)$$

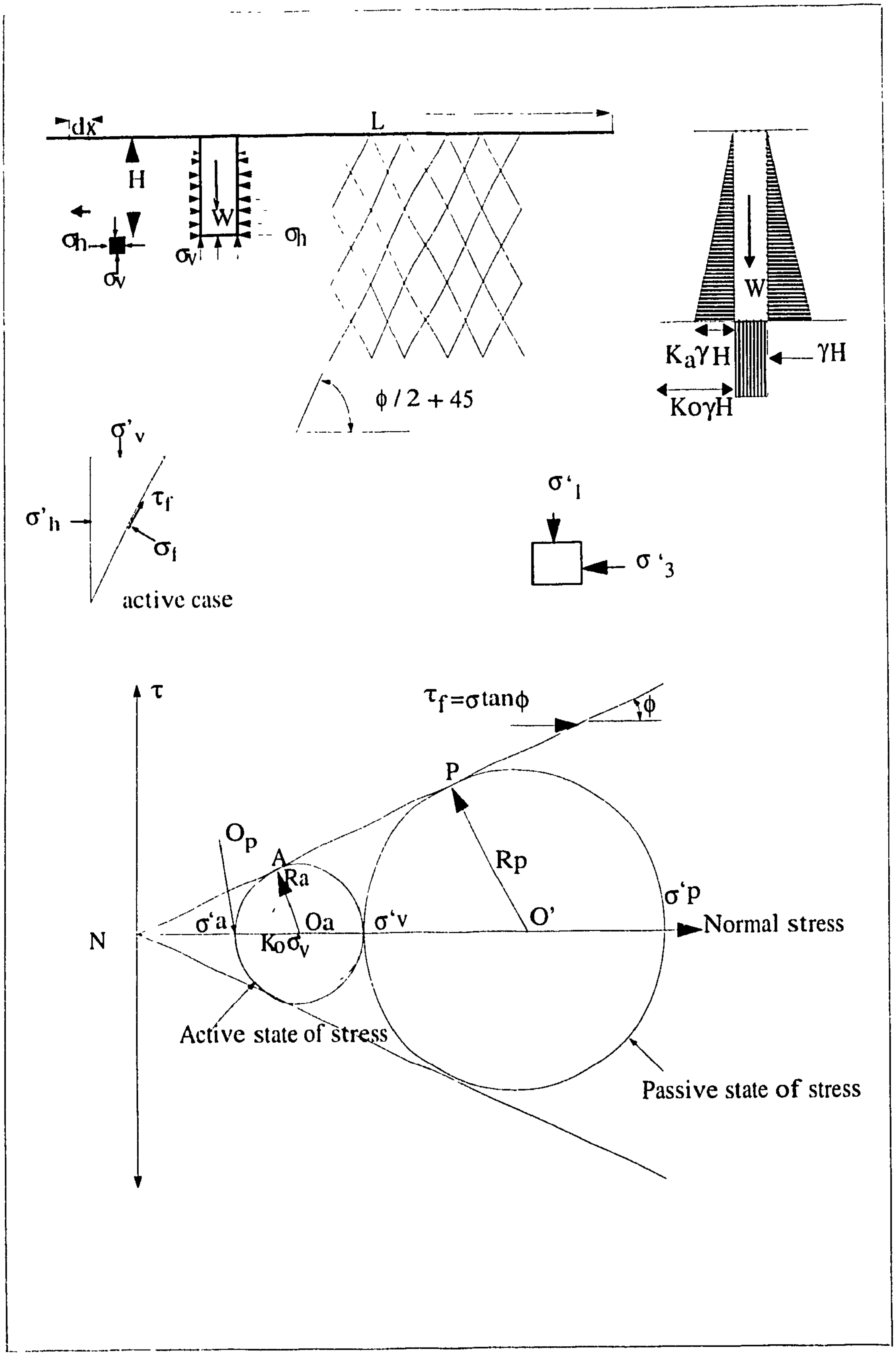

Fig 2 - 2 diagram illustrating active Rankine state in semi-infinite mass of sand (active case)

Which is the maximum value of Ka, or in another way we can express it by:

$$\sigma'_1 = \frac{(1+\sin\Phi)}{(1-\sin\Phi)} \times \sigma'_3 \quad \text{.......... (2-8)}$$

$$\sigma'_3 = \frac{1-\sin\Phi}{1+\sin\Phi} \times \sigma'_1 \quad \text{.......... (2-9)}$$

For the passive case i.e the wall is pushing the sand and accordingly σ'_h is The major principal effective and Kp reaches its maximum value, thus:

$$\sigma'_1 = K_p \times \gamma H \quad \text{.......... (2-10)}$$

$$K_p = \frac{\sigma_1}{\sigma'_3} \quad \text{.......... (2-11)}$$

$$K_p = \frac{(1+\sin\Phi)}{(1-\sin\Phi)} \quad \text{.......... (2-12)}$$

Furthermore, Ka and Kp represent the lower and higher limits of the sand equilibrium states. The intermediate states are the states of elastic equilibrium which include the condition of the at rest state that is the subject of the following paragraph.

In 1957, Janbu, N (16). Proposed, according to his study of lateral earth pressure by generalized procedure of slices, a method to evaluate lateral forces for both the active and passive conditions: $Pa = Ka(0.5\ \gamma\ H^2 + qH)$ where Ka could be taken from his proposed graph.

In 1963, Rowe. P. W. (23) demonstrated that the force on a smooth retaining wall behind dense sand is less than the case of loose sand. This is due to the fact that the failure wedge which is directly supported by the wall is relatively smaller for the case of dense sand as compared to loose sand.

In 1971, Clough G.W & Duncan J. (7) according to their finite element analysis performed for smooth walls translating away from the backfill, the active condition was reached for displacement equal to $\Delta/H = 0.0026$

In 1984, Rahardjo, H. & Al (21). According to their study using General Limit Equilibrium method for lateral earth forces for horizontal cohesionless backfill against vertical wall they found that all: Coulomb (planar slip surface), Krey (curved slip surface) and GLE (Circular slip surface) are similar. Besides, they studied the location of the critical center of rotation and they found that the wall friction angle results in an increase in the curvature of the critical slip surface.

2-3 At Rest Lateral Earth Pressure.

2-3.1 General.

Historically, when natural superposition of soil layers occurred in a large area, it couldn't exist a lateral movement or horizontal compression between soil elements this condition is known as the at rest condition or Ko condition where Ko is the coefficient of at rest earth pressure. For sand layers where there is no external forces during formation, Ko will be within a range of 0.4 and 0.5. On the other hand, Ko could reach higher value if there were a load in the past i.e. additional overburden without pressure dissipation (i.e completion of the consolidation process).

2-3-2 Theoretical Estimation of Ko

The first trial to theoretically estimate Ko was done by Jaky, (15) In 1944: who assumed a semi-infinite granular mass and divided it into Rankine zone and transitional zone as shown in Figure(2-3), and that the shear distribution on any horizontal plane is parabolic. Based on these assumptions Jaky was able to express the coefficient of earth pressure Ko as a function of angle of shearing resistance, ϕ.

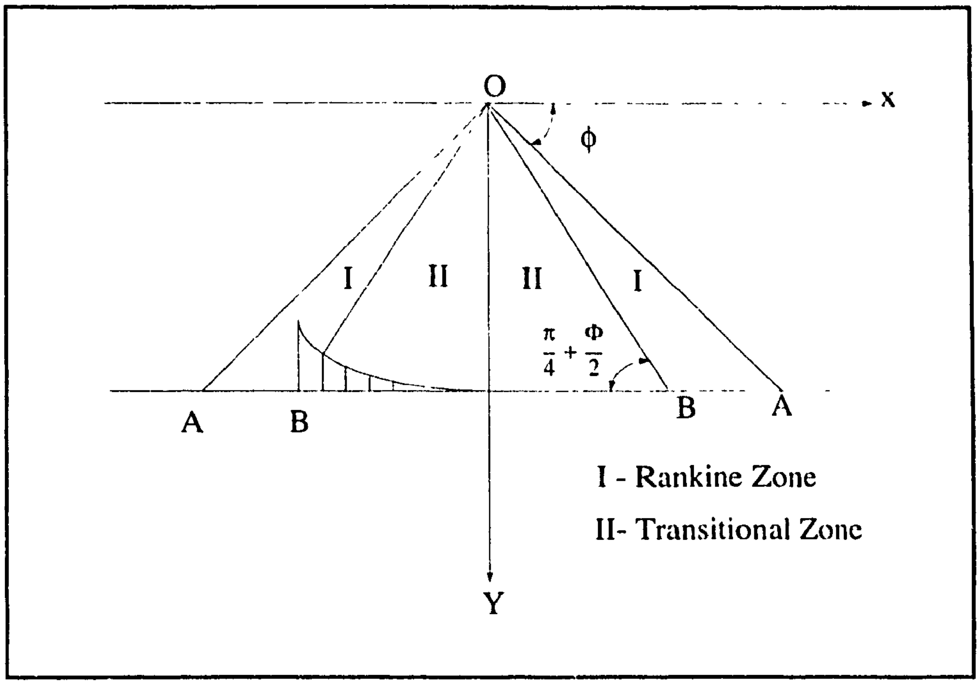

Fig 2-3 Jaky's solution

$$K_o = \frac{1-\sin\phi}{1+\sin\Phi} \times \left(1+\frac{2}{3}\times\sin\Phi\right) \qquad \text{2-13)}$$

Later on, Jaky proposed another simplified formula without giving any explanation

$$K_o = (1-\sin\Phi) \qquad (2-14)$$

The second attempt to evaluate Ko theoretically was done in 1963 by Hendron, A.(14). He assumed that a rounded, uniform and dense sand could be simulated to a face-centered array of equiradii spheres. Having subjected the array of spheres to one dimensional compression, then Ko can be evaluated by the following equation:

$$Ko = \frac{1}{2}\left[\frac{1+\frac{\sqrt{6}}{8}-3\frac{\sqrt{6}}{8}(\sin\Phi')}{1-\frac{\sqrt{6}}{8}+3\frac{\sqrt{6}}{8}(\sin\Phi')}\right] \qquad (2-15)$$

He also reported that Ko is also influenced by the shape of the granular soil. For example round sand having similar angle of shearing resistance to angular sand has a smaller value of Ko.

2-3-3 Experimental estimation of Ko.

In 1883, G.H. Darwin.(10) studied how a talus will stand and he defined the angle of repose as the inclination to the horizontal (in this way it has uninteresting meaning from the geotechnical point of view).

In 1891, A. Donath. (11) was the first who introduced Ko as the coefficient of the lateral earth pressure at rest, which is the ratio of the horizontal to the vertical stresses under no lateral deformation.

In 1920, Terzaghi.C. (27) conducted his tests in the field accordingly he could estimate Ko. Then he reported the value of Ko = 0.42 for coarse sand. Later on, in 1923 he introduced the empirical equation

$$K_o = \frac{1 - \sin\Phi}{1 + \sin\phi} \qquad (2-16)$$

Besides, he studied in details the importance of no lateral movement in retaining wall where he called the ratio of the horizontal to vertical stresses Ko in such situation and he reported that the Ko increases with the increase of the degree of the sand compaction.

In 1936, Kjellman, W. (17) found that Ko has an amount between 0.5 and 1.5 by using a complicated triaxial device on sand samples.

In 1957, Bishop, W.A. & Henkel.D.J. (5) found that Ko =.47 for loose sands and.38 for dense sands which depends on the soil type, stress history and pore water pressure.

In 1958, Bishop, W.A (4) gave Ko more deep explanation by using the ratio of the horizontal effective stress to the vertical effective stress.

In 1961, Bjerrum, L. & Al. (6) provided a plot of Ko against initial porosity where Ko is equal to 0.25 in dense sands and to 0.654 in very loose sands.

In 1966, Schmidt. B. (24) in his discussion on the results of Brooker and Ireland proposed a simplified relation:

$$\left(\frac{\sigma_3}{\sigma_1}\right) = K_r = K'o\left[\frac{\sigma_{1max}}{\sigma_1}\right]^a \quad \ldots\ldots (2-17)$$

where OCR is = σ_{1max}/σ_1 , (a) is the slope of the straight line showing in logarithmic scale OCR vs.σ_3 / σ_1. And K'o is the intercept with σ_{1max} / σ_1=1. Besides, he suggested to carry out tests with different values of σ_{1max}, to demonstrate the results of unpublished tests on sand which states that the curvature of odometer load-deformation curves in rebound is independent of σ_{1max} this means that the factor (a) in the proposed relation in rebound is also independent from σ_{1max}.

In 1967, Alpan. I. (2) proposed this empirical relation for overconsolidated sands where the exponent n for sands could be determined from a special graph:

$$K_{o(ocr)} = K_{o(nc)} \times OCR^n \quad \ldots\ldots (2-18)$$

In 1973, Andrawes, K. & El-Sohby, M. (3) declared that in the triaxial test there is no lateral strain when the axial strain equal the volumetric strain, i.e $\varepsilon_v = \varepsilon_a$ which is measured from the burette:

$$\frac{dV}{V} = \varepsilon_v = \frac{dH \times A}{H \times A} = \varepsilon_a \quad \ldots\ldots (2-19)$$

Furthermore, when the triaxial tests are done with constant $R = \sigma_a/\sigma_r$ First, it can be executed with $\varepsilon_v/\varepsilon_a > 1$ next, with $\varepsilon_v/\varepsilon_a < 1$ then we can find the quantity of R for $\varepsilon_v/\varepsilon_a = 1$ which gives Ko=1/R.

In 1975, Saglamer, A. (24) mentioned that OCR has big influence on Ko and gave the following equation for normally consolidated sand:

$$K_{o(nc)} = 0.97\,[1 - 0.97\sin\phi] \quad \ldots\ldots (2-20)$$

In 1976 Meyerhof, G. (20) proposed the following equation:

$$K_{o(oc)} = (1 - \sin\phi)\sqrt{OCR} \quad \ldots\ldots (2-21)$$

In 1980, Daramola, O. (9) developed Wroth's(1973) formula:

$$K_{o(oc)} = K_{o(nc)} \times OCR - \left[\frac{\mu}{1-\mu}\right](OCR - 1) \quad \ldots\ldots (2-22)$$

to

$$K_{o(oc)} = K_{o(nc)} \times OCR - \lambda\,(OCR - 1) \quad \ldots\ldots (2-23)$$

where, $\lambda = \dfrac{1-\beta}{1+\beta}$ and β could be taken from his proposed graph.

In 1982, Mayne, P.W. & Kulhawy, F.H. (18) presented the following relation according to statistical analysis conducted on Ko(nc) for cohesionless soils:

$$K_{o(nc)} = 1 - 0.998\sin\Phi \quad \ldots\ldots (2-24)$$

Besides, from linear regression analysis for clay and dense sands he suggested the following equations:

$$K_{o(nc)} = 1 - 1.003\sin\phi \quad \ldots\ldots (2-25)$$

$$K_{o(oc)} = (1-\sin\Phi)\left(\frac{OCR}{OCR_{max}}\right) + \frac{3}{4}\times\left(1-\frac{OCR}{OCR_{max}}\right) \qquad (2-26)$$

In 1983, Handy, R. (13) stated that Ko decreases when densification continues and he proposed the following:

$$K_{o(nc)} = \frac{1-\sin(\phi+\alpha)}{1-\sin(\phi+\alpha)} \qquad (2-27)$$

Where, α is the diversion of the slip angle due to densification.

In 1984, Sherif, M.& Fang,R. (26) recommended based on their Laboratory tests Jacky relation for loose sands. But, for dense sand backfill they proposed the following relation

$$K_0 = (1-\sin\phi) + \left(\frac{\gamma_d}{\gamma_{min}} - 1\right)x5.5 \qquad (2-28)$$

where γ_d is the field actual unit weight and γ_{min} is the minimum unit weight.

In 1984, Feda, J (12) declared based on his results that Ko(oc) increases until a maximum value with OCR increasing then decreases with increasing OCR. Also he studied the relation between porosity and relative density and Ko(nc) and he found that maximum Ko(oc) corresponds to Rankine coefficient of passive earth pressure.Finally, he proposed the following equation:

$$K_{onc} = \frac{1}{4k}\cdot\left[\frac{1}{\tan^2\left(\frac{\pi}{4}+\frac{\Phi_\mu}{2}\right)} + \frac{1}{\tan^2\left(\frac{\pi}{4}+\frac{\Phi_{cv}}{2}\right)}\right] \qquad (2-29)$$

where ϕ_μ is the angle of interangular friction, and ϕ_{cv} is the angle of inter angular friction with constant volume test and k is the coefficient from Rowe's stress dilatancy which is equal to $0.5\left(1-\frac{d\varepsilon_v}{d\varepsilon_a}\right)$ Where $d\varepsilon_v$ and $d\varepsilon_a$ are the plastic volumetric and axial strain increments in the triaxial test.

In 1993, Ting.C. M. & Al (28) declared according to their experimental results on Kaolin the sedimentable samples differ from remolded samples and they provided the equations:

$$Ko = -0.22e + 0.9 \text{ for remolded Kaolin} \quad (2\text{-}30)$$

and

$$Ko = -0.25e + 0.87 \text{ for sedimentable Kaolin} \quad (2\text{-}31)$$

In 1993, Mesry.G. & Hayat. (19) In their experimental study during the decrease of σ'_v on granular soils they provided the following equation:

$$Ko = (1 - \sin\phi)\, OCR^{\sin\phi'_{cv}} \quad (2\text{-}32)$$

2-4 Stress History of the soil represented by OCR.

A soil in the field at some depth has been subjected to certain maximum effective overburden pressure in its geological history. This maximum effective overburden pressure may be equal to or less than the existing overburden pressure at the time of sampling. The reduction of the pressure in the field may be due to natural geologic process or to human process. During the soil sampling, the existing overburden pressure is also released, resulting in some expansion. When this sample is subjected to consolidation test, a small amount of compression (that is a small change in void ratio) will occur when the total pressure applied is less than the maximum effective overburden pressure to which the soil has been subjected in the past. When the total applied pressure on the sample is greater than the maximum past effective overburden pressure, the change of the void ratio is much larger, and the log p relationship is practically linear with a steeper slope. Such plot is used by Casagrand for the estimation of OCR for clayey soils. But, for a specific sand deposits there is no known technique to predict OCR maximum other than a knowledge of the local geology and the stress history of the soil deposits.

2.5 Discussion and Scope of the Present Research.

It can be noted that most of the theories reported in literature to predict the Active and At Rest lateral earth pressures are based on the study of normally consolidated sands. Besides, mostly experimental studies were focusing on normally consolidated or compacted soils. Furthermore, some scientists during their special triaxial tests for the evaluation of Ko during loading and unloading assume that OCR is the ratio of the maximum vertical pressure to the available vertical pressure in that specific point of the test graph. Others assume that OCR is the ratio between the maximum confined pressure applied to the sample and the minimum confining pressure applied to the tested sample in the triaxial tests.

In addition, no trial has been made to study the effect of OCR that is caused by the extended superficial static loads on the lateral earth pressure of overconsolidated sand under the at rest or active conditions.

The present analysis is directed to evaluate the coefficients Ko and Ka of overconsolidated sand as a function of OCR and ϕ.

CHAPTER 3

EXPERIMENTAL INVESTIGATION

3 - 1 GENERAL.

In order to achieve the objectives mentioned in chapter two in this thesis, an experimental set-up was designed to simulate the condition of a retaining wall subjected to at rest and active earth pressures. Measuring devices were installed to record the pressures on the wall and in the sand mass.The pressures measured on the wall will be the at rest or active pressures which depend on the movement. The pressures measured in the sand mass allow for the calculation of the overconsolidation ratio.The case of the active earth pressure condition was produced by allowing the wall to move horizontally without any rotation. Figure 3-1 presents a schematic flow chart of the experimental set-up. Figure 3-2 presents the general view of the experimental set -up, while figure 3-3 shows a photograph of the executed set-up.

3-2 EXPERIMENTAL SET-UP.

A- The Tank.

The inner dimensions are 1080 mm, 197 mm and 405 mm length, width and depth respectively. Figures (3-4) and figure (3-5) show a sketch and photo of the tank used in the present investigation. The longitudinal sides are manufactured from sheets of Plexiglas (Acrylic Cast Sheet) which is transparent in order to show the sand movement behind the retaining wall and, accordingly, the failure mechanism. The plexiglas sheet has a thickness of 10 mm and a Tensile Strength of 65 MPa. The tank is reinforced from outside by a steel frame to prevent deflection under the maximum loading condition. Mechanical dial gages are installed to measure the deflection of the sides of the tank if there is any. The results showed that the sides of the tank do not deflect, and, accordingly, the retaining wall is considered to be loaded in a two dimensional condition.

B- The retaining wall.

A steel plate was manufactured with the dimensions 197mm x 215 mm x 19 mm width, depth and thickness respectively. The retaining wall was allowed to move horizontally and no rotation was permitted. Five displacement transducers were installed firmly within the wall to measure the horizontal soil pressure on the wall. Figure (3-6) to (3-8) show a sketch and the photograph of the retaining wall with the transducers in location. For easy reference the transducers were given the symbols (W1,W2,W3,W4,W5). These pressure transducers are manufactured by Data Instruments Lexington, USA. The transducers were connected to the data acquisition system(D.A.S.) which allows registering the transducers' reading at predetermined intervals. DAS was consequently connected to a personal computer to record and print the transducers' pressure readings according to their calibration in Kpa.

The wall movements were measured by the electrical sensor (Linear Variable Displacement Transducer LVDT) which is manufactured by Sangaho Schlumberger. The LVDT after calibration was connected to the D.A.S. and the personal computer. The displacement was recorded in mm. Figure (3-9) shows the Dial Gage (LVDT) used in the present investigation.

C- The Loading System.

The loading system consist of a gear box which was manufactured by Wikehan Farranc Eng. LTD. Slought England. The fixed gear box will generate horizontal force which will produce a horizontal movement along the axis which is connected to the retaining wall. Figure (3-10) shows the Gear Box used in the present investigation. The forces generated by the gear box are measured by a Load cell which is connected on one side to the horizontal retaining wall axis and on the other side to the gear box horizontal axis. The load cell is also connected to the Data acquisition system which registers these forces according to the calibration factor previously established. Figure (3-11) shows the Force transducer (Load Cell) used in the present investigation. The wall movements could be forward movements i.e towards the sand mass which generate compressive force on the soil mass (Passive condition) or backwards movements i.e away from the sand mass which generate tensile force on the soil (Active condition) or no movement at all (At rest condition).

D- Laboratory production of Overconsolidated sands.

In this investigation, the sand was overconsolidated by two different techniques. First, by applying an external static load on the surface of the sand in the testing tank for a period of time and then unloading, the stresses in the sand mass were measured by a set of transducers embedded in a predetermined locations at three different levels. The transducers were given the symbols of b1,to b9 (see figure 3-4). Special boxes were manufactured to house such transducers. Figure (3-13) and (3-14) show these boxes units for vertical, and vertical and horizontal transducers respectively. Second, the sand was overconsolidated by means of compacting the sand mechanically for each sub-layer of 100mm.

E- Sand placing technique.

The sand placing technique was developed to minimize the sand disturbance and to produce the requested unit weight. The equipment used for placing the sand is presented in Figure (3-15). The sand was placed in the tank in the form of layers suitable for placing the transducers in the predetermined levels. The containers of measuring the unit weight were also placed in their designed levels. Figure (3-16) shows the location of these containers.

Each layer was compacted by an air compressor with an end steel plate. The range of the compact duration varied from 1 to 11 seconds, depending on the required unit weight of the sand. Figure (3-17) shows the compact duration versus unit weight. The thickness of the sand layers was fixed to be 100mm for the entire experimental program.

In case of surfaced loads, the sand was placed in the tank by spreading it in its loose state for the entire height of the tank. Next, the sand was covered by sheet of Plexiglas to ensure a uniform distributed stress on the top layer of the sand and to allow the settlement of the static loads used to overconsolidate the sand. Afterwards, the static loads were applied for a period of time (For test No 3 the period of loading and unloading the static loads took more than three months.) Afterwards, the sand was overconsolidated due the residual plastic deformation in the sand mass which increased the interlocking between the sand particles.

3 - 3 SAND CHARACTERISTICS.

A-General.

The sand used in the present investigation was a 99.9% high Silica sand "MORIE Sand" imported from the United States.The MORIE sand was selected due to its homogeneous quality.

B - Grain size distribution (Sieve analysis).

Figure (3-18) represents the grain size distribution curve of the sand used in the present investigation. From the grain-size distribution curves the following parameters were determined:

a) The Uniformity Coefficient Cu:

$$C_u = \frac{D_{60}}{D_{10}} \qquad (3-1)$$

b) The Coefficient of curvature

$$C_c = \frac{D_{30}^2}{D_{10}D_{60}} \qquad (3-2)$$

For the sand used in this investigation Cc was found to be 1.63 and Cu to be 5.5. According the Unified Soil Classification System the sand is WELL GRADED CLEAN SAND.

C - The Shear Strength.

The shear strengths of the sand were determined from the results of Direct Shear Tests. Figure (3-19) shows the shear strengths of the sands and the corresponding unit weights.

D- Particle shape

The shape of the individual particle is at least as important as the grain size distribution which affect the engineering response of granular soils: in our case it is angular, clean, cohesionless, homogeneous and quartz sand. This shape affects the frictional characteristics of the investigated sand.

E - The Unit Weight.

The unit weight was measured before and after loads application by placing containers having 62.7 mm as diameter and 45 mm as depth. Table (3-1) shows the results.

F- The Relative Density

There are two possibilities to evaluate the relative density either by:

$$D_r = \frac{e_{max} - e}{e_{max} - e_{min}} \qquad (3-3)$$

or from:

$$D_r = \frac{\gamma_f - \gamma_{min}}{\gamma_{max} - \gamma_{min}} \times \frac{\gamma_{max}}{\gamma_f} \qquad (3-4)$$

According to The American Society for Testing and Materials (ASTM) D-2049 procedure for the estimation of the minimum and the maximum dry unit weights of cohesionless granular soils, the following characteristics of the soil used in the present investigation were obtained: $\gamma_{min} =$ 17.41 KN / C.M and $\gamma_{max} =$ 19.95 KN / C.M. Figure (3-20) shows Angle of shearing resistance versus relative density.

Table (3-1) The physical properties of the tested sand (where ϕ^o is computed from the shear box test results).

SAND PROPERTY	γ / KN	ϕ^o	RELATIVE DENSITY Dr%
LOOSE	17.67	31	12
LOOSE	17.90	33	21
MEDIUM	18.32	36	39
MEDIUM	18.80	40	58
DENSE	19.02	42	67
DENSE	19.25	45	75

3-4 Computer and Data acquisition system.

The Data Acquisition System (D.A.S) Figure (3-21), which is designed by H.P (H.P 3852 A), gets voltage signals from the transducers that differ according to the intensity of the stress applied on each transducer. The computer translates the signals to stresses according to a program that has the scales of transformation. This program should be prepared according to the requirement of the tests. All the signals are memorized according to chosen intervals for all connected transducers where the capacity of the panel is 200 transducers.

3 - 5 Test Procedure.

A)- Transducers calibration:

Transducers were calibrated individually. Figure (3-22) illustrates the lay-out of the transducer method of calibration. Each transducer was subjected to different levels of air pressure through plastic pipe that could be measured by a pressure test gauge. The excitation power was 5 Volts according to the manufacturer's recommendation. The output signals were recorded for each level of pressure. According to the results, the calibration factor was calculated for each transducer. These factors were entered in the computer program to convert the output signals registered by the D.A.S. to pressures. Figure (3-23) shows the instrument used for the transducers' calibration.

After installing all the transducers, the connection of each transducer was checked with its characterized computer output data, and they were initialized by giving them zero values as an initial pressure.

B - Applying static loads.

In this case the tank was filled up by spreading sand in its loose state. The plexiglas cover overlaid by a rigid cover was put in place to ensure the uniform distribution of the load on the entire sand mass. Then, the static load was applied on the rigid cover gradually to achieve different levels of pressure. For each individual static load pressure the change of the horizontal and vertical pressures in transducers were monitored until no change was recorded with time. The next increment of static pressure was added after the stabilization of the previous pressures in the transducers. The same process was used during unloading where the increments of unloading were similar to the loading increments.

C - The test records.

C - 1 General.

The Data Acquisition System is programmed to read and record the output voltages from the transducers and the load cell according to the predetermined interval periods. Furthermore, the Data Acquisition System has the possibility to record results manually at a given time which was used during the application of the static loads.

C - 2 Computer records.

During loading the following measurement were recorded and printed by the computer system for each level of static pressure where the registration intervals were controlled manually:

- All transducers pressures "in Kpa ";

- The horizontal displacement of the plate (the retaining wall) "in mm";

- The forces inside the load cell "in Newton ".

C - 3 Manual records.

During loading the following displacements were measured and recorded manually:

- The horizontal Displacement of the tank side walls;

-The vertical displacement of the tank upper cover;

-The horizontal displacement of the gear box axle.

D -The records of the Displacement of the wall and the applied forces.

The wall was pulled backwards away from the sand by the gear box according to the displacement steps of approximately 0.5 mm in order to generate the active earth pressure condition. The deviation of stresses on the wall and in the soil mass, the wall displacement, and the total force on the wall were recorded. The test was ended when there were no changes in the forces deduced by the load cell.

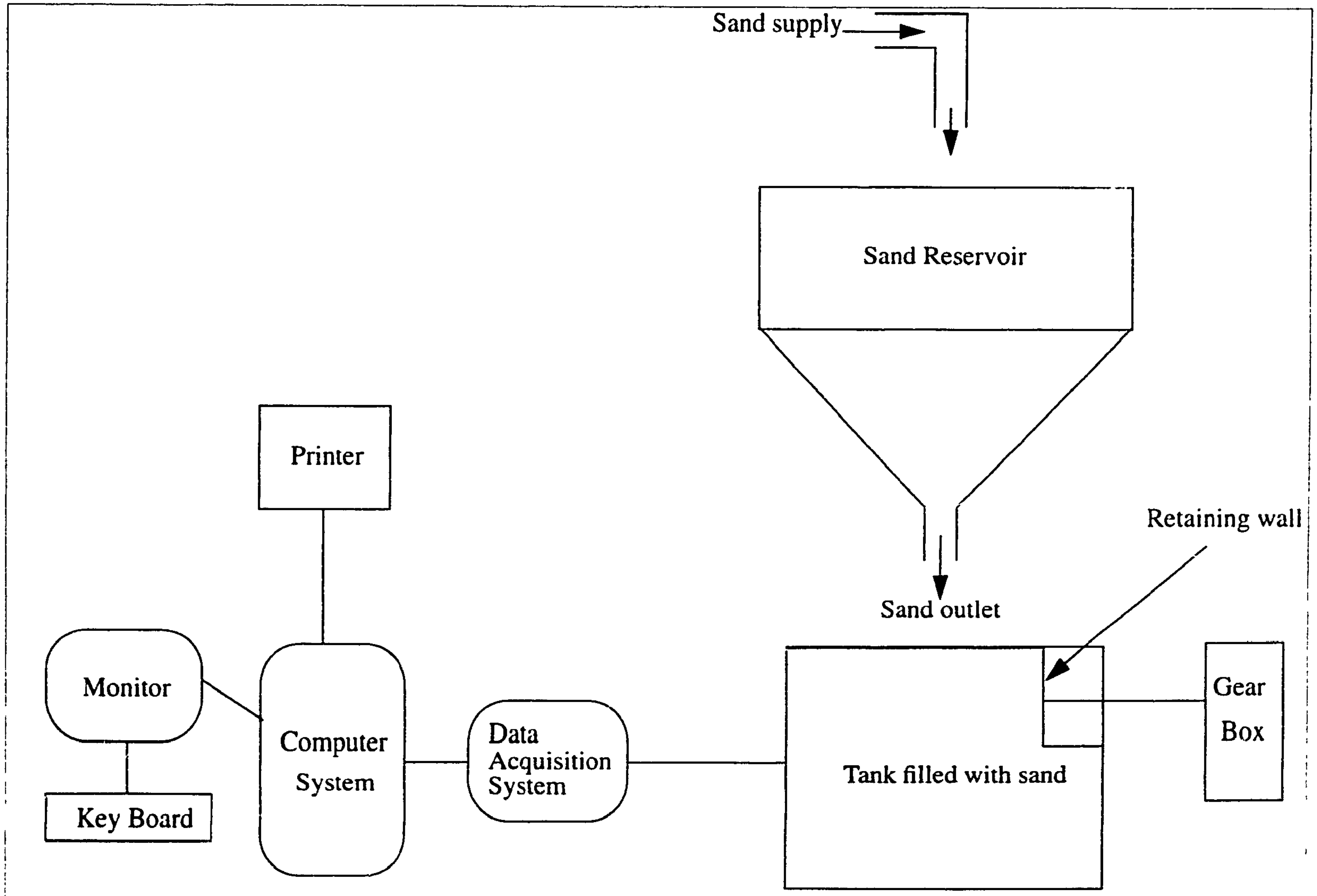

Figure 3-1 Layout for the experimental set-up.

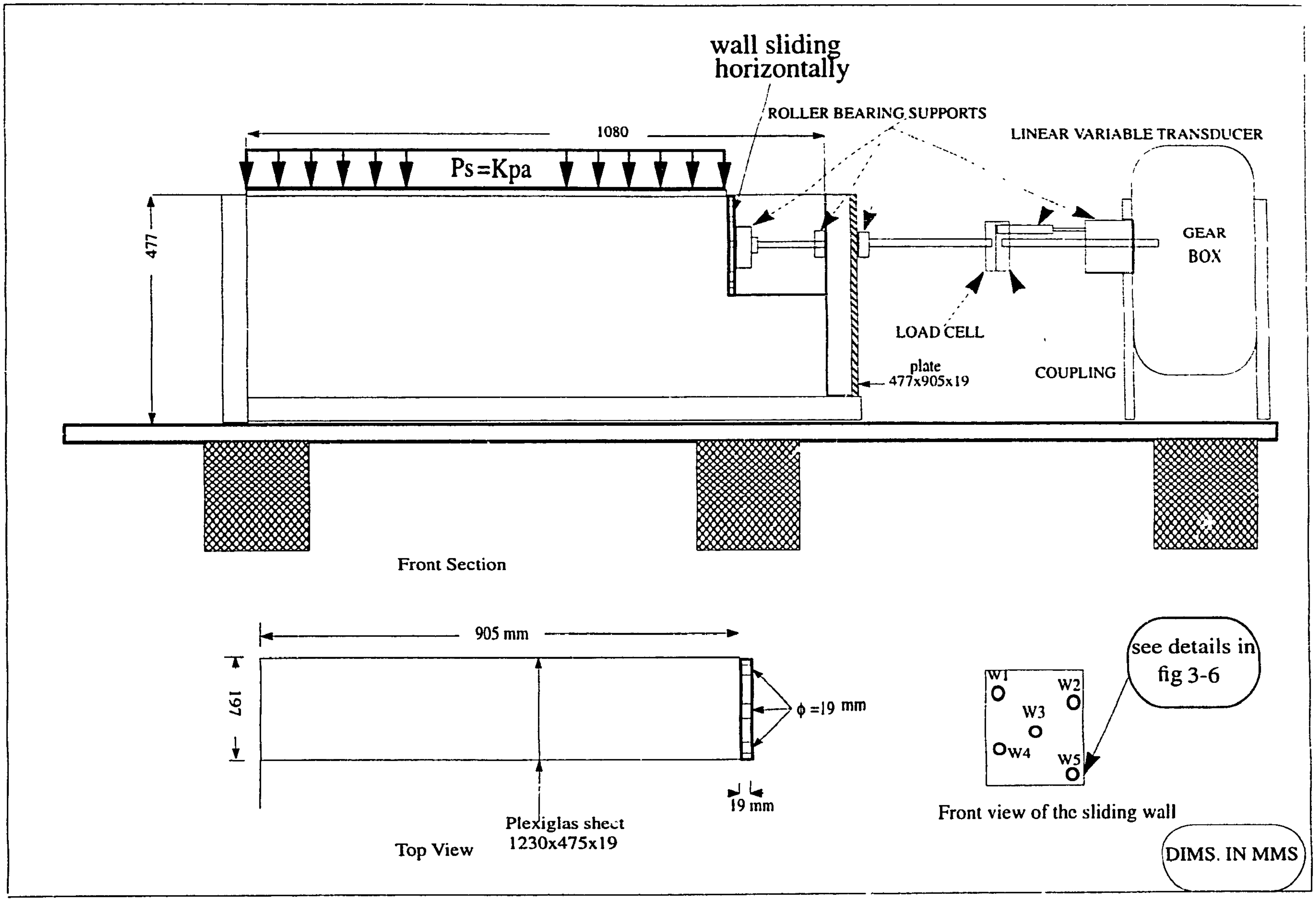

Figure 3-2 General view of the experimental set-up.

Figure 3-3 Photograph shows the tank

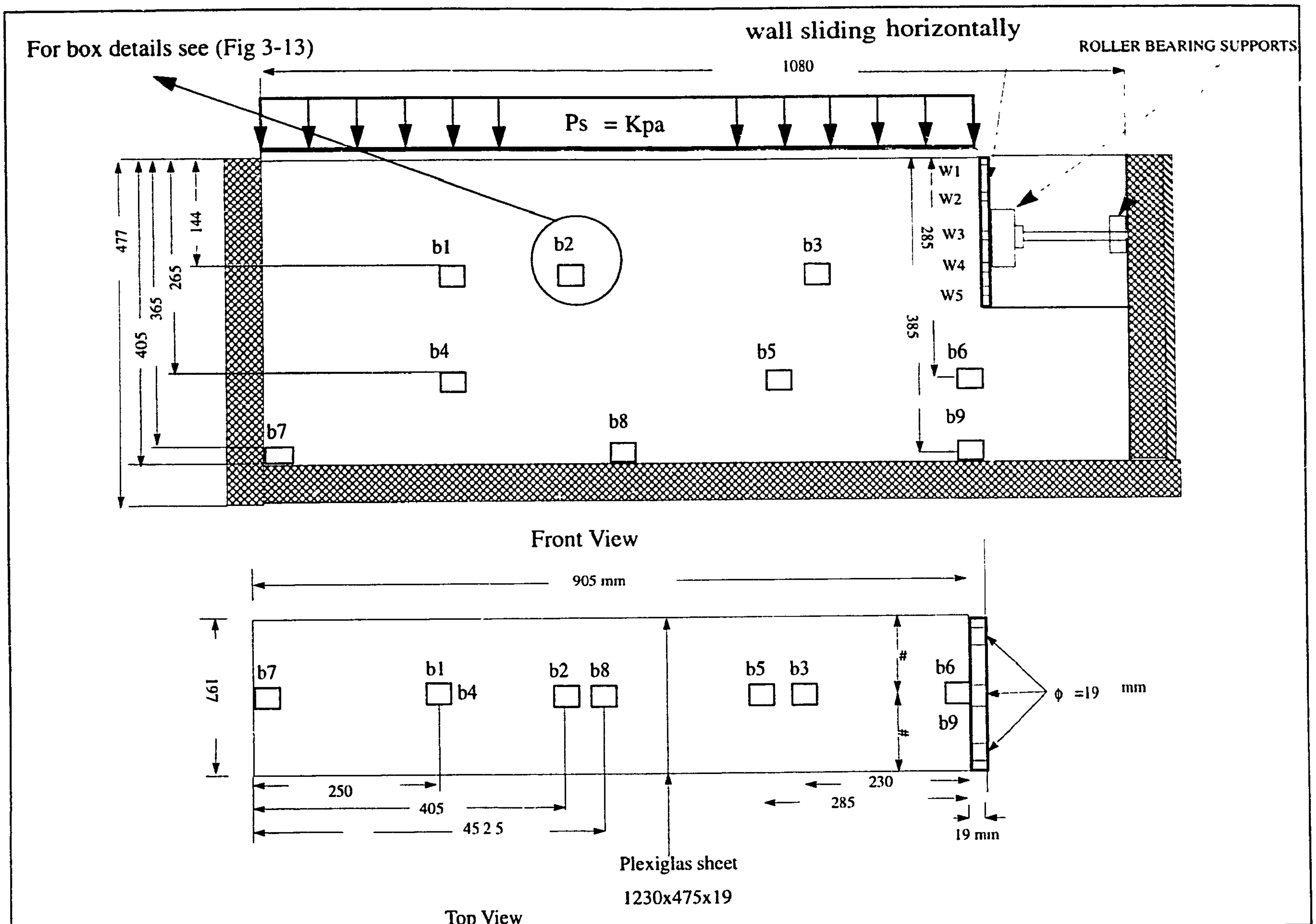

Figure 3-4 Sketch of the testing tank.

Figure 3-5 Photograph shows the application of the surface loading.

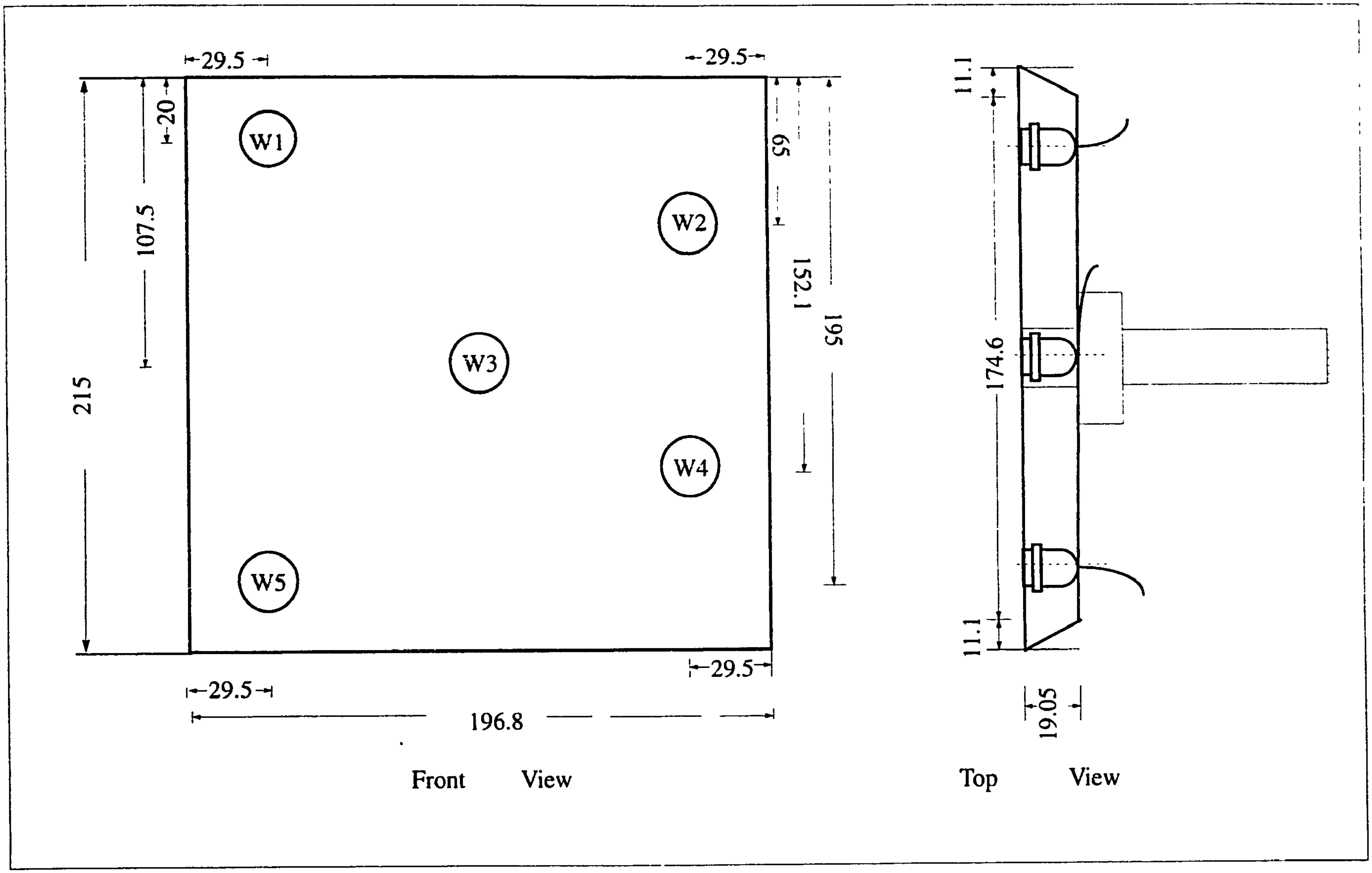

Figure 3-6 Location of Transducers on the wall

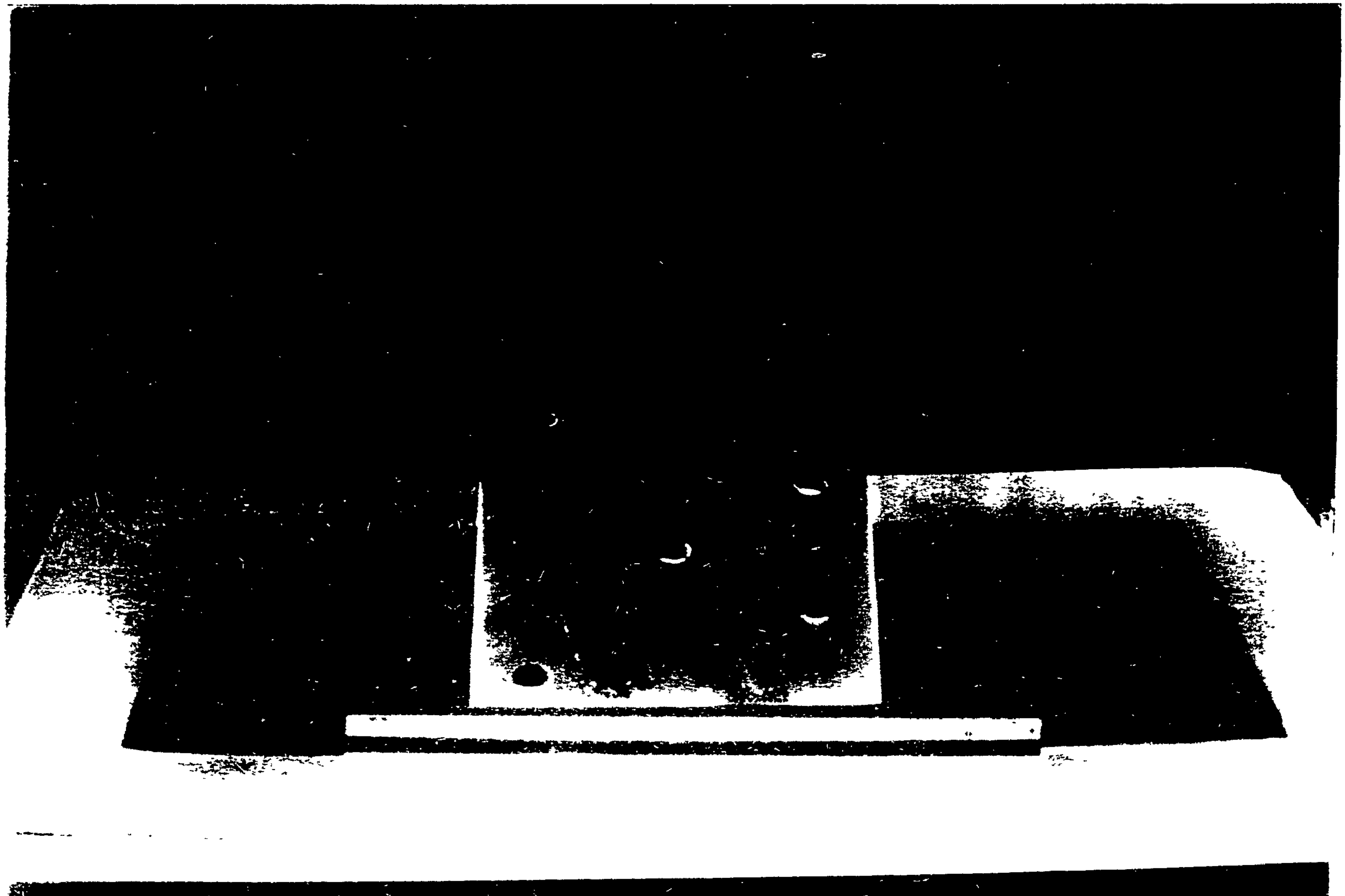

Figure 3-7 Photograph of the retaining wall (Front View)

Figure 3-8 Photograph of the retaining wall (Back View).

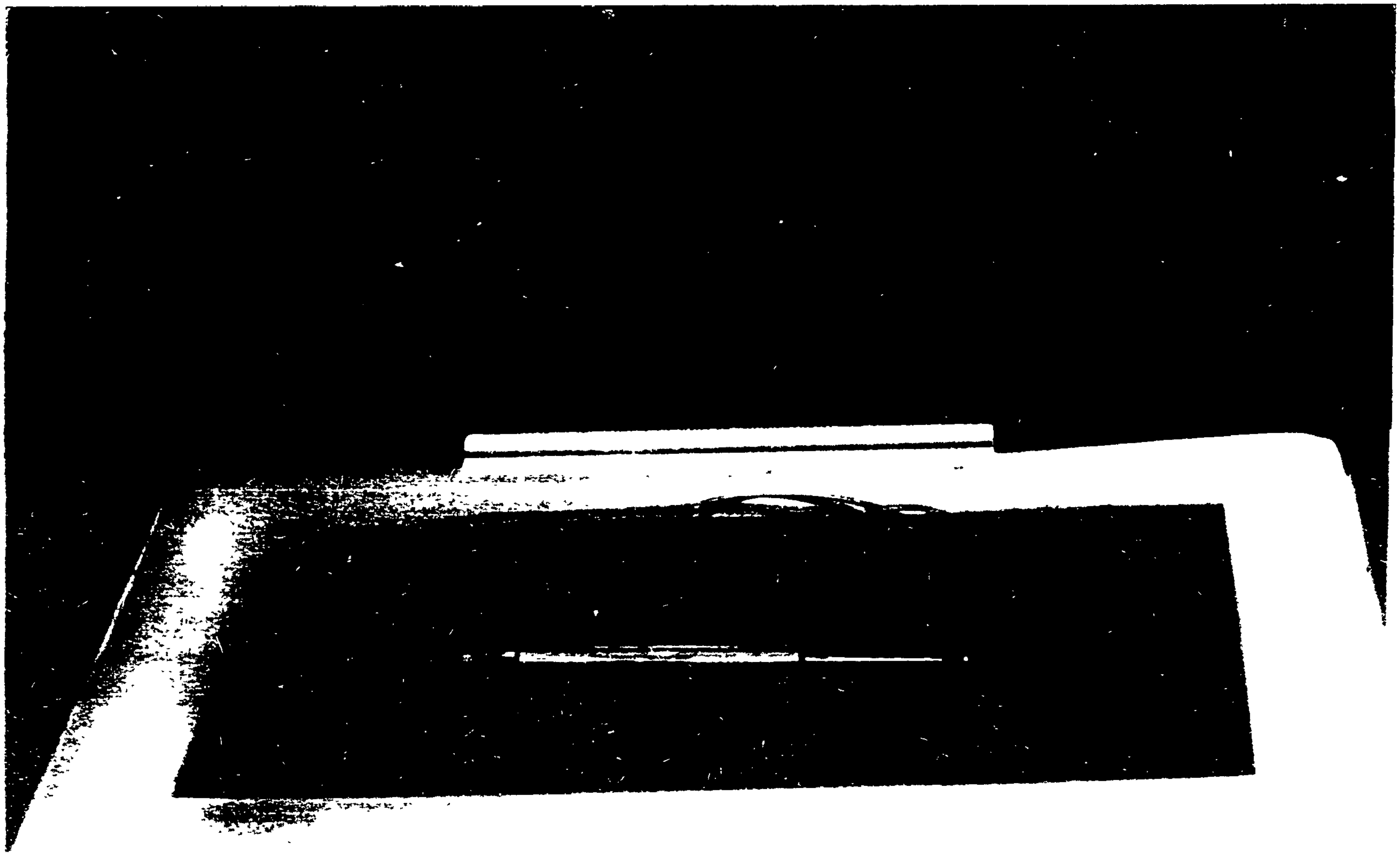

Figure 3-9 Photograph shows the Linear Variable Displacement Transducer (LVDT)

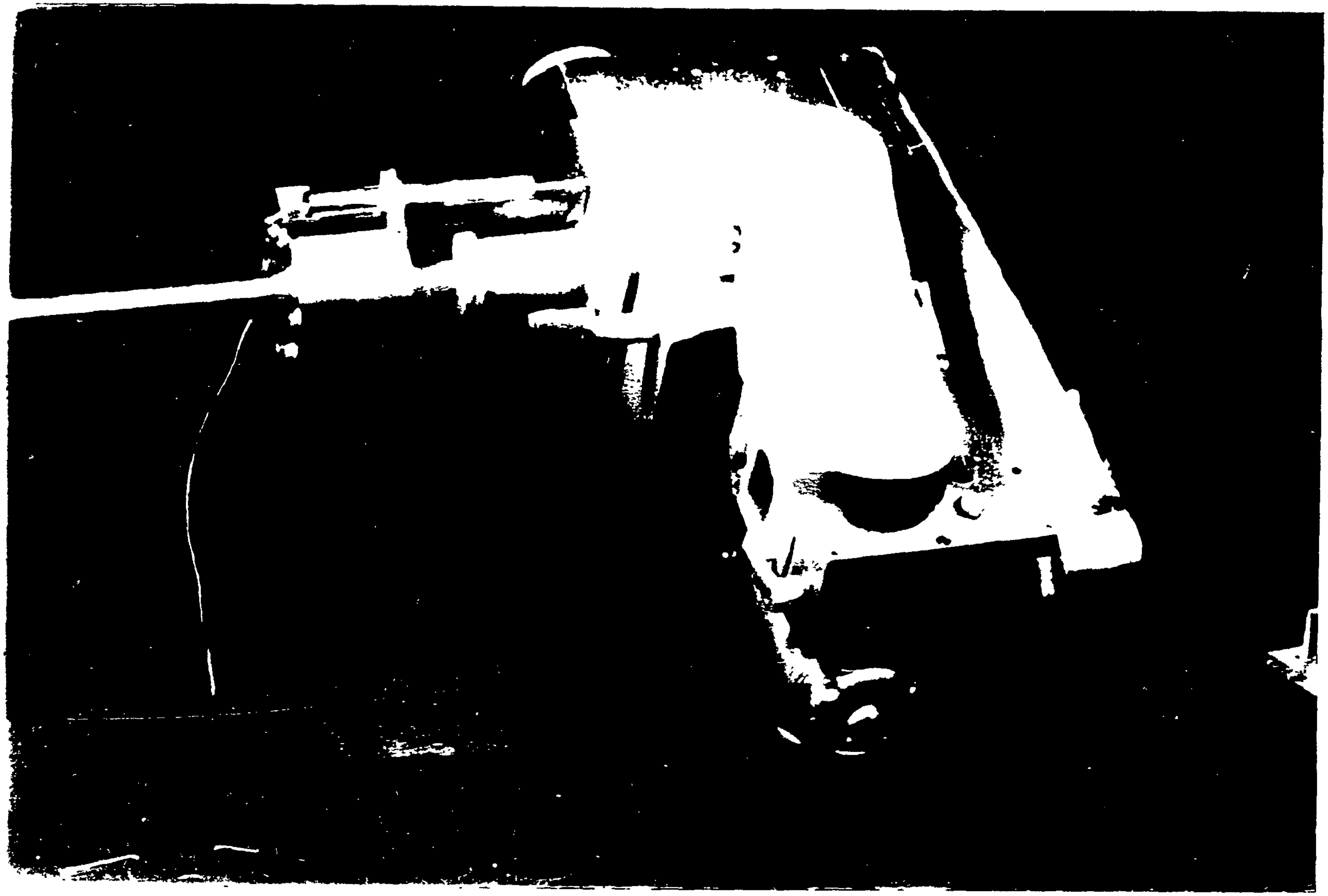

Fig 3-10 Photograph shows the Gear Box connected to the Load Cell and the Variable Displacement Transducer (LVDT).

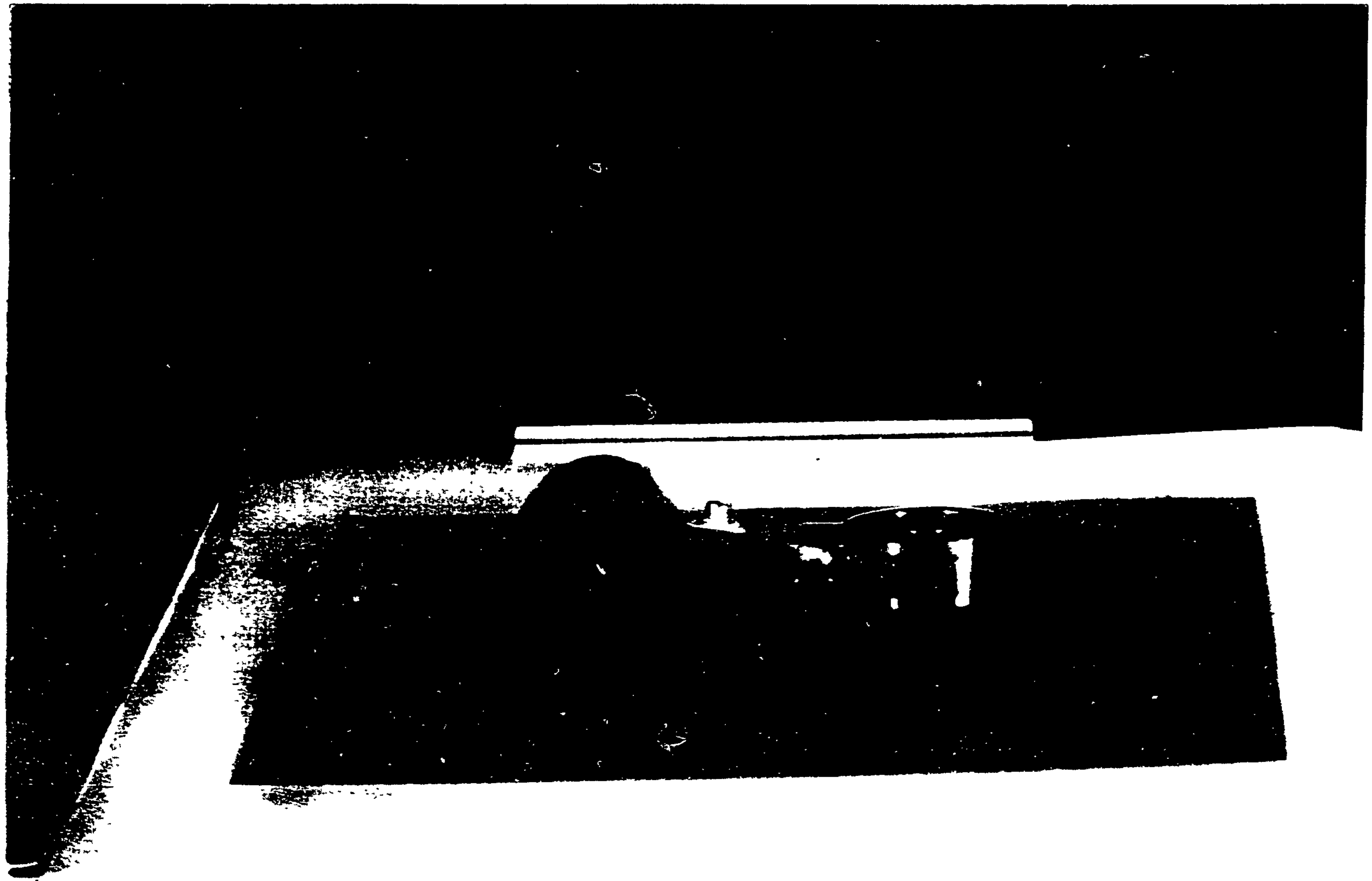

Fig 3-11 Photograph shows the Load Cell

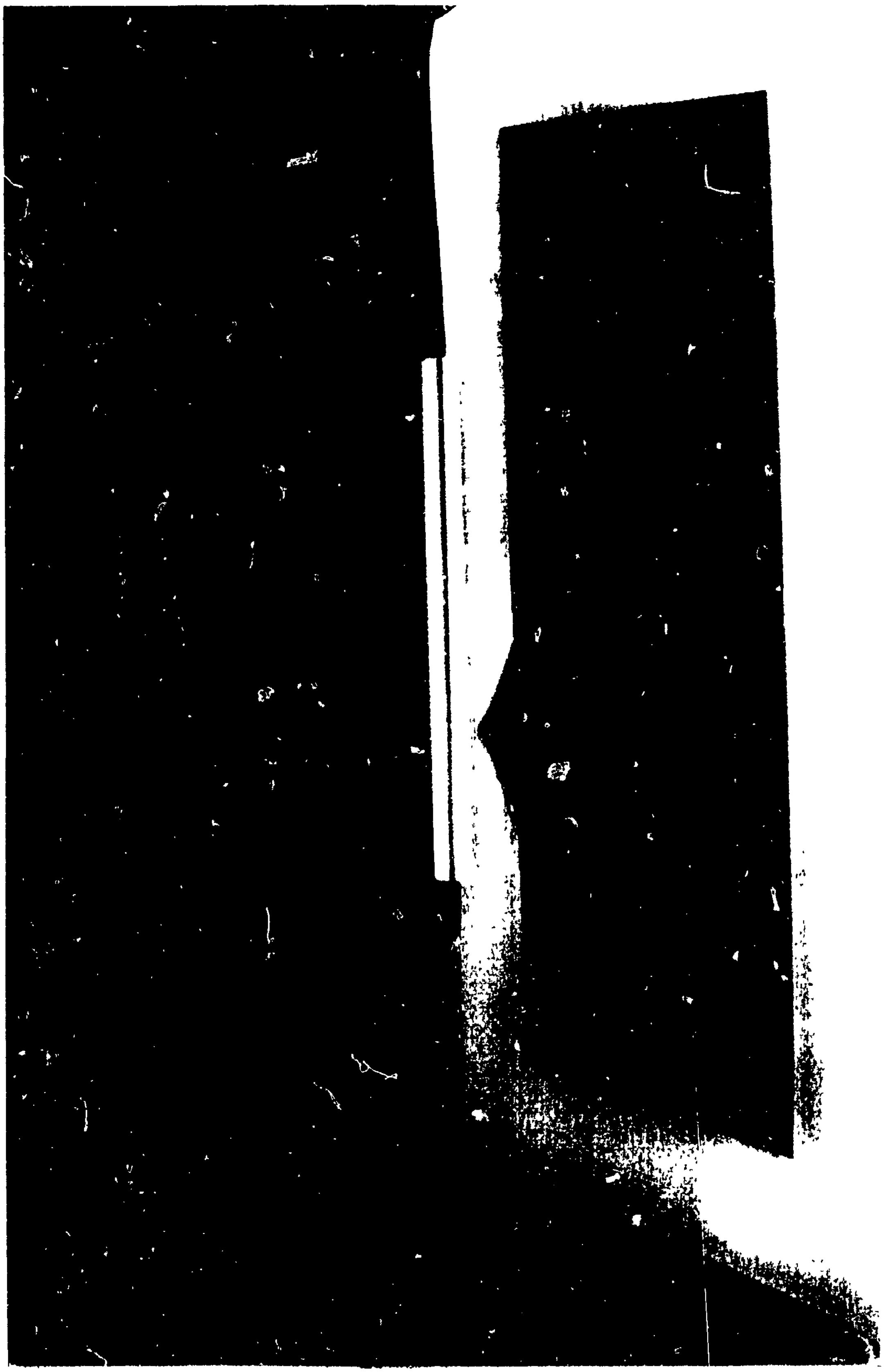

Figure 3-12 Photograph shows the static loads.

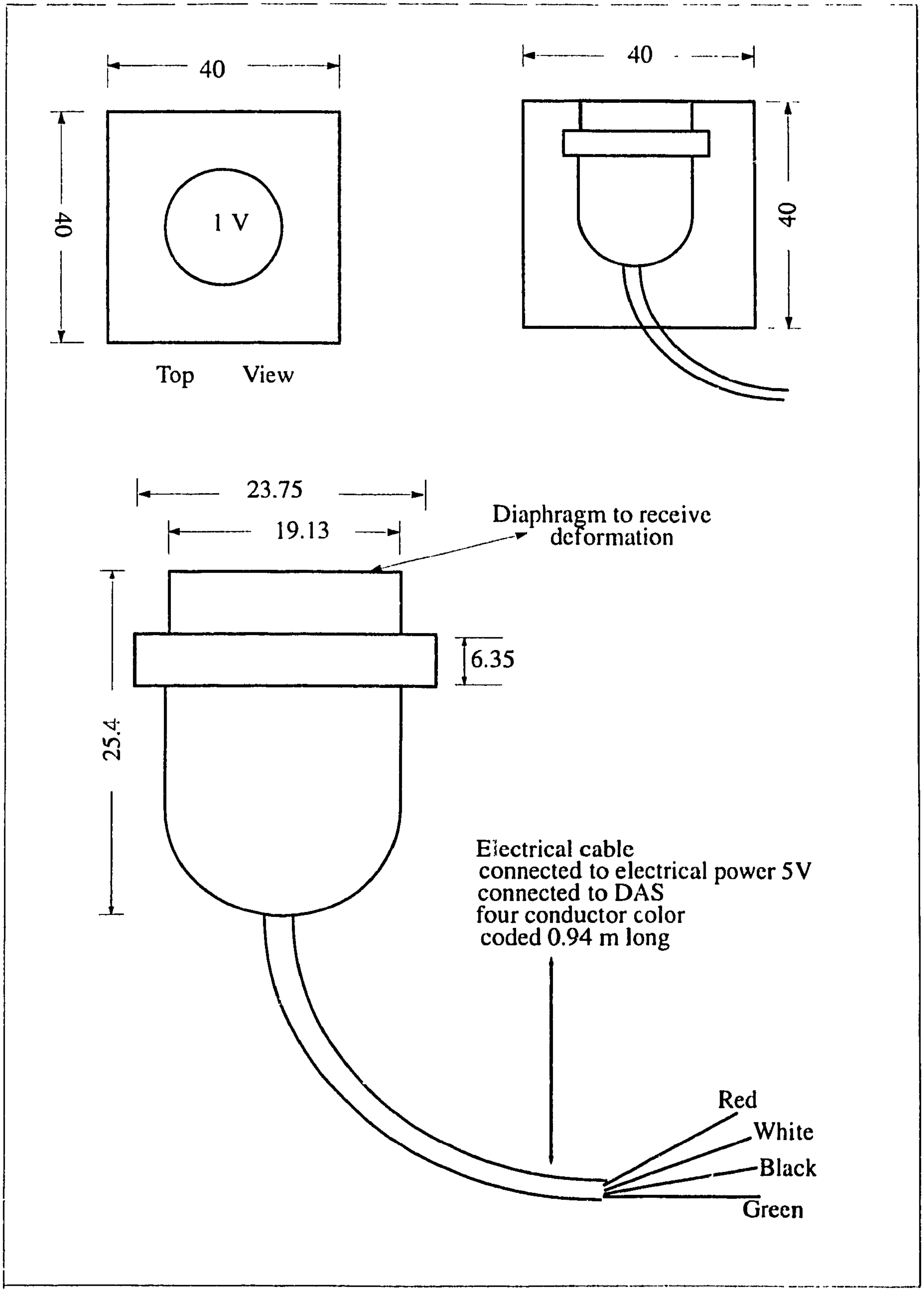

Figure 3 -13 Transducers box unit to measure vertical stresses

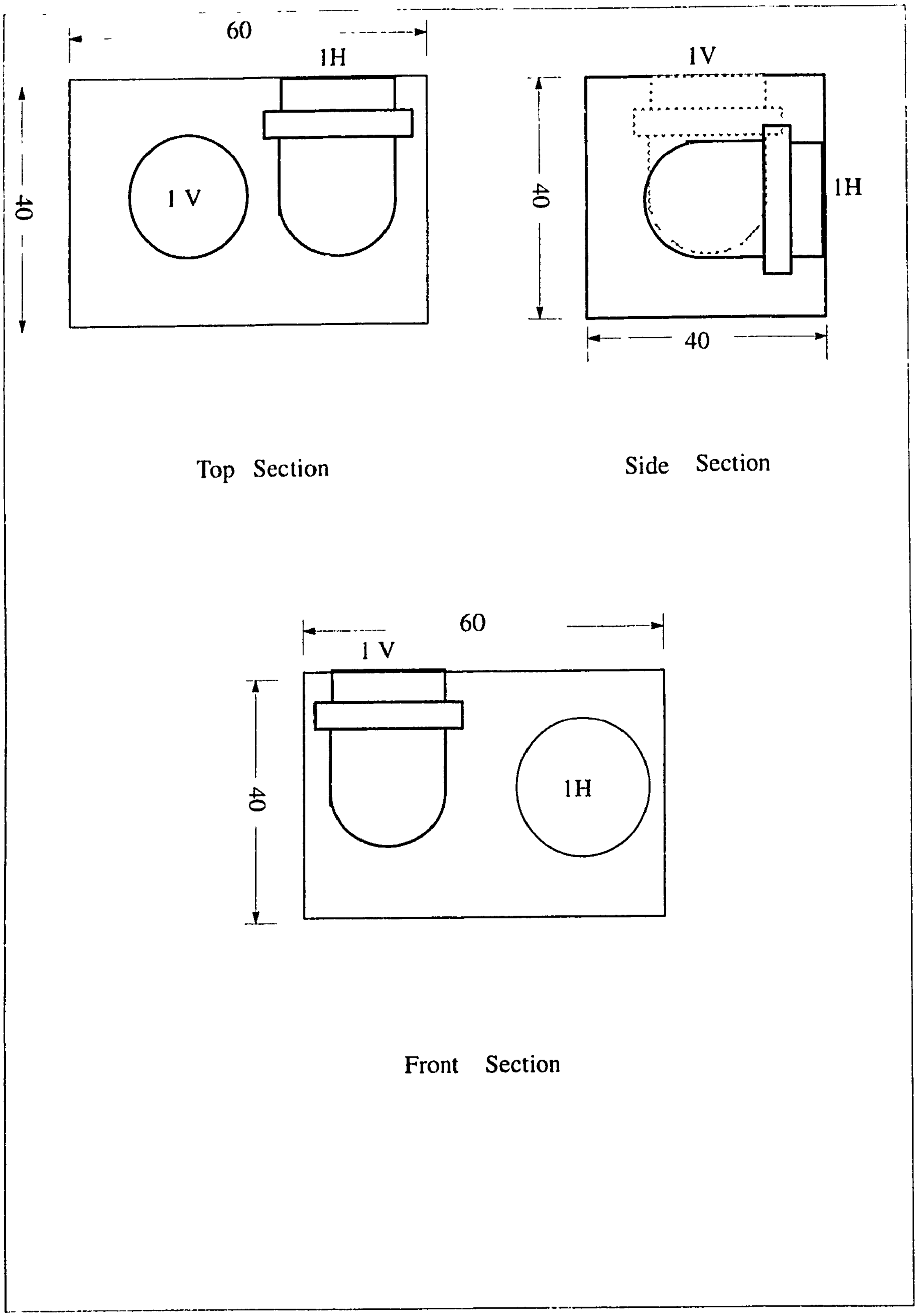

Figure 3 -14 Transducers box unit to measure Vertical and Horizontal stresses.

Figure 3-15 Photograph shows general view of the sand placing equipment

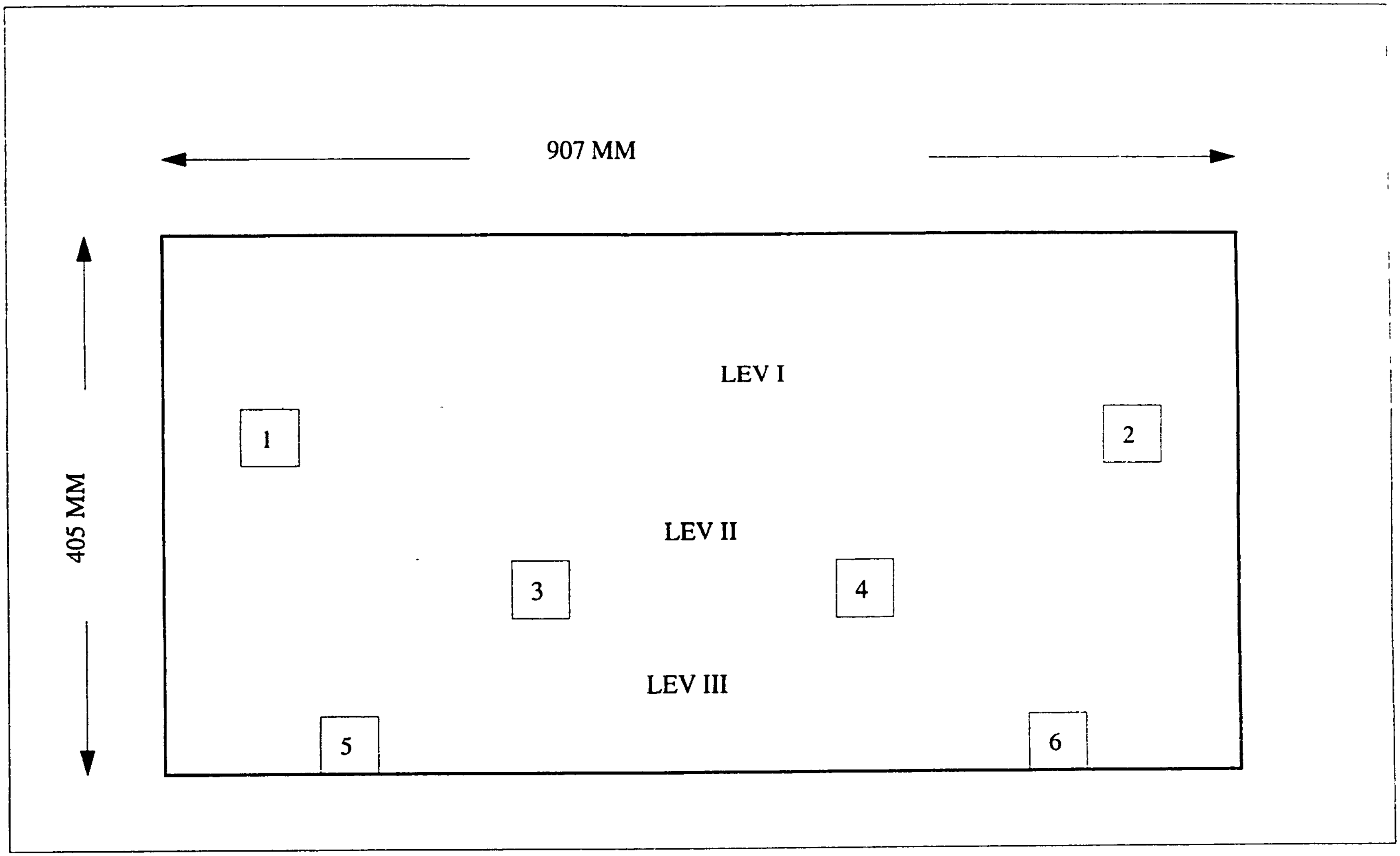

Figure (3-16) Sketch showing the location of containers to measure the unit weight of the sand after placing

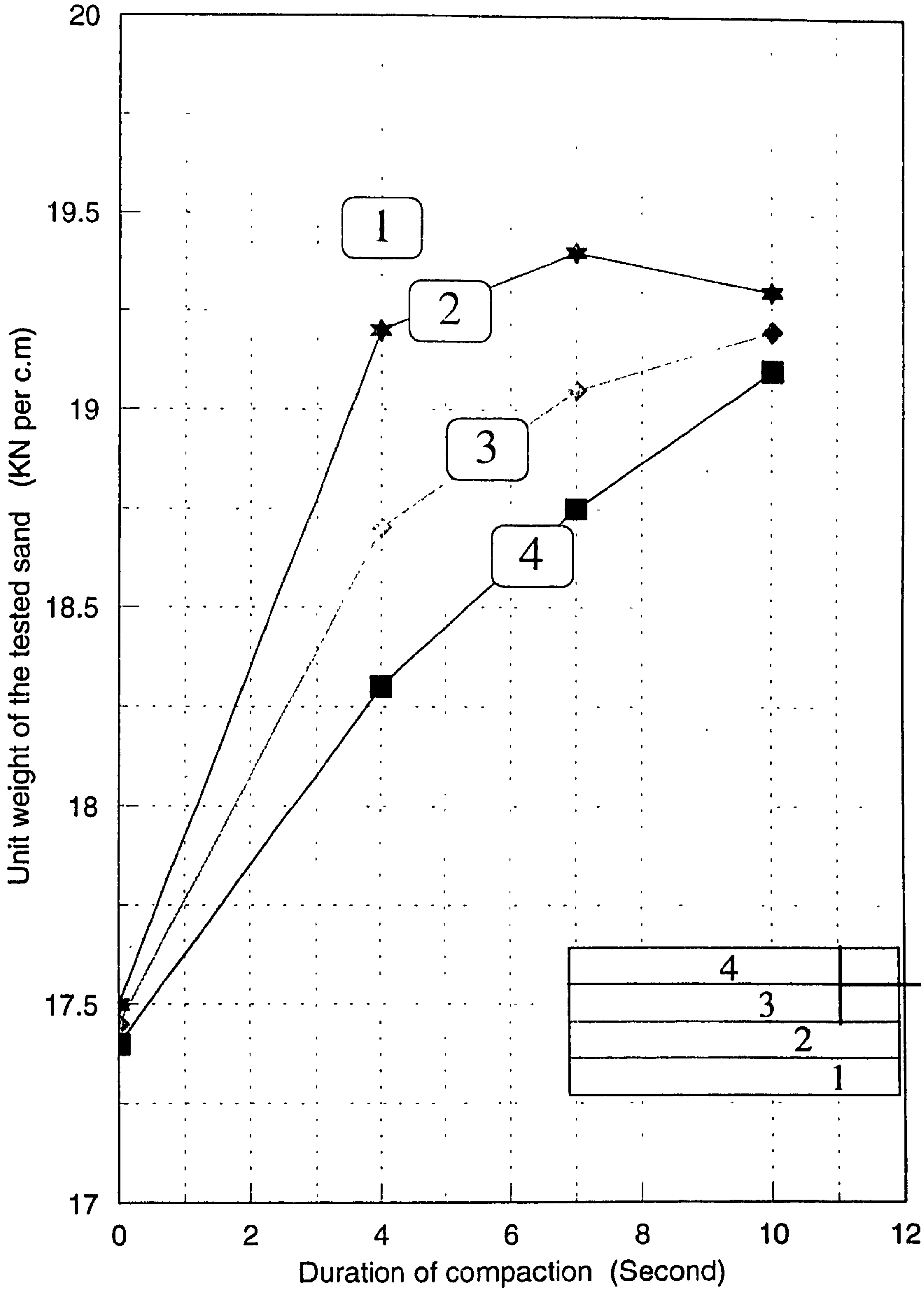

Figure 3-17 Unit weight of the sand versus duration of compaction

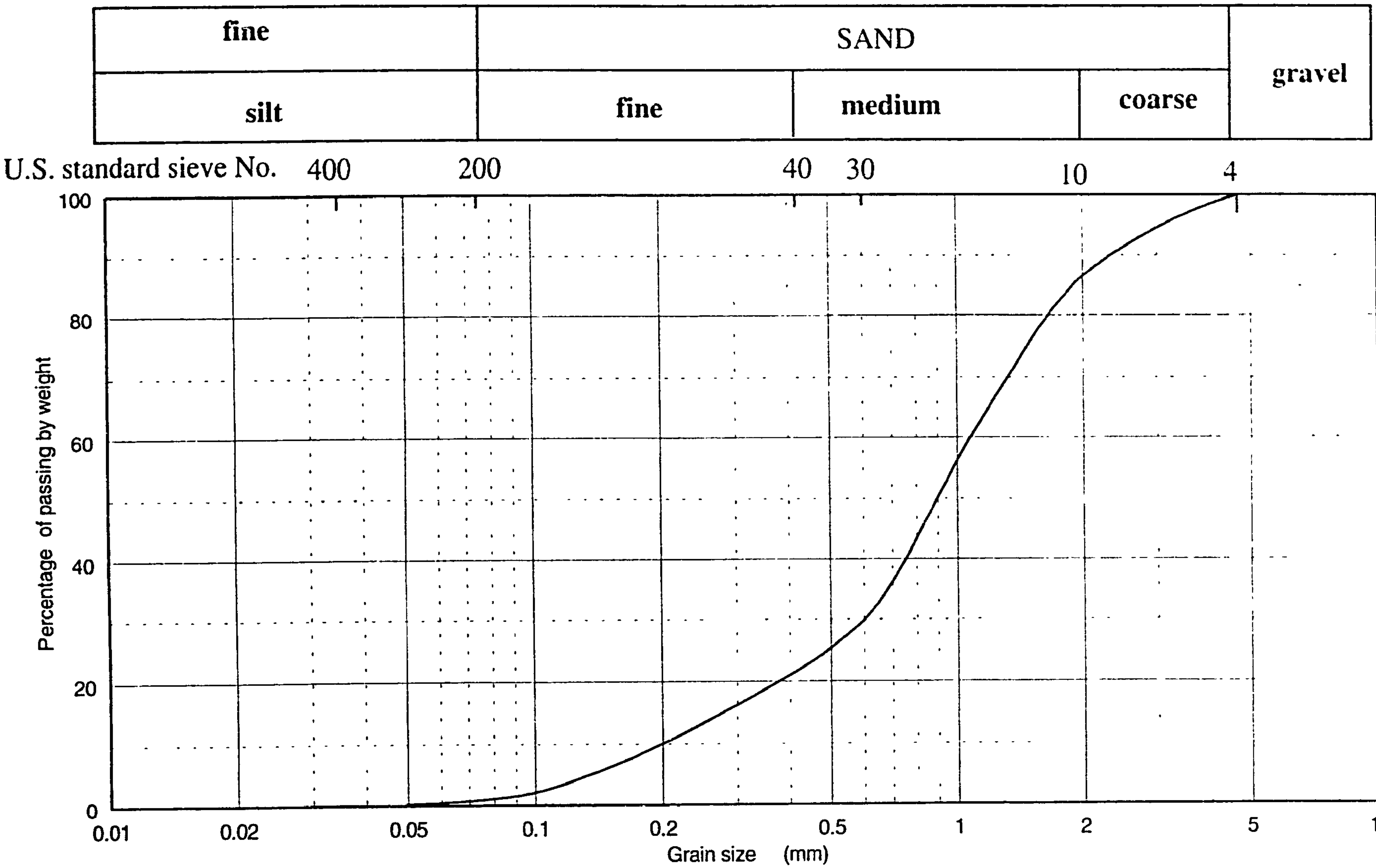

Fig 3-18 Grain size distribution of the tested sand

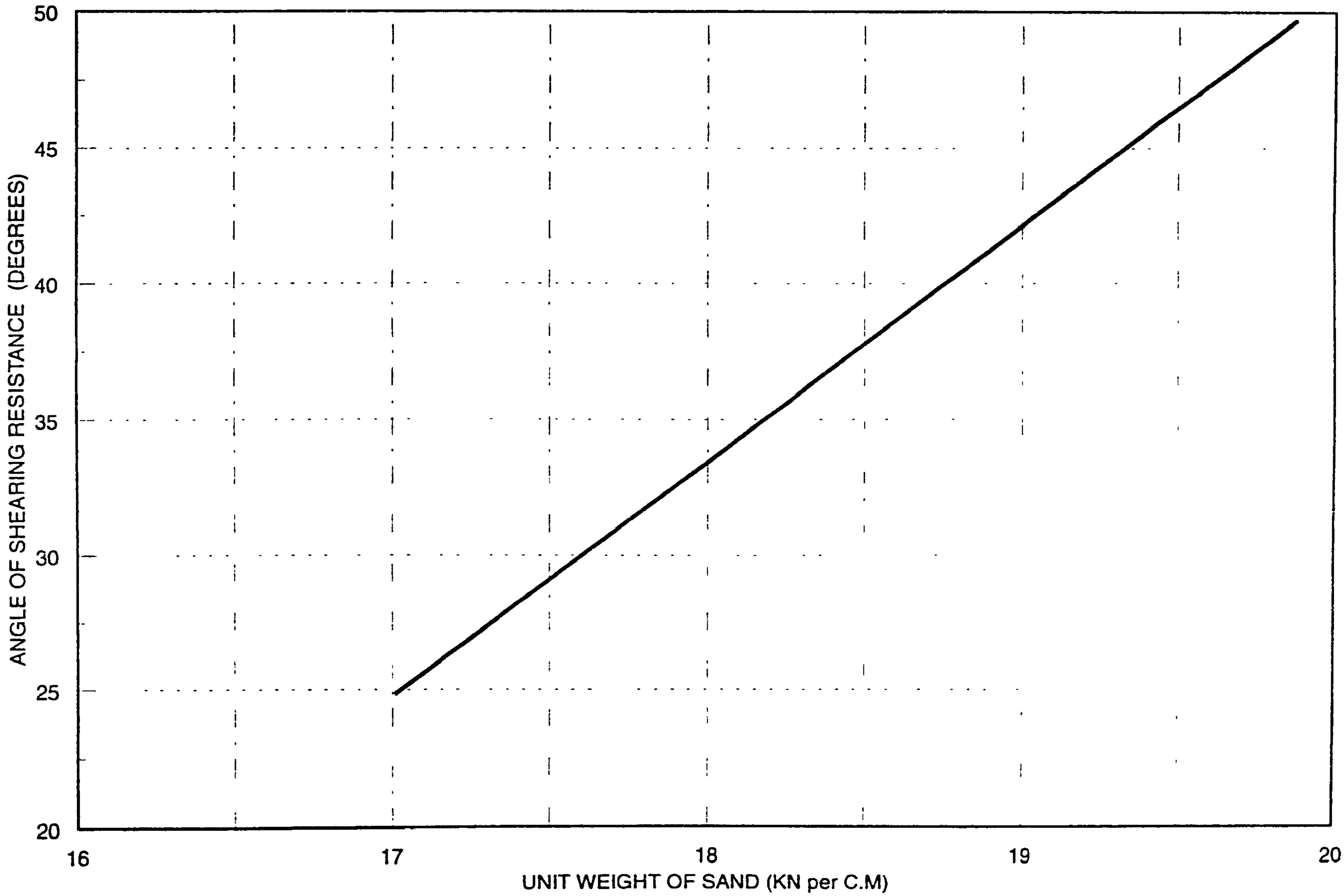

Figure 3-19 Angle of shearing resistance versus unit weight as deduced from shear box test results

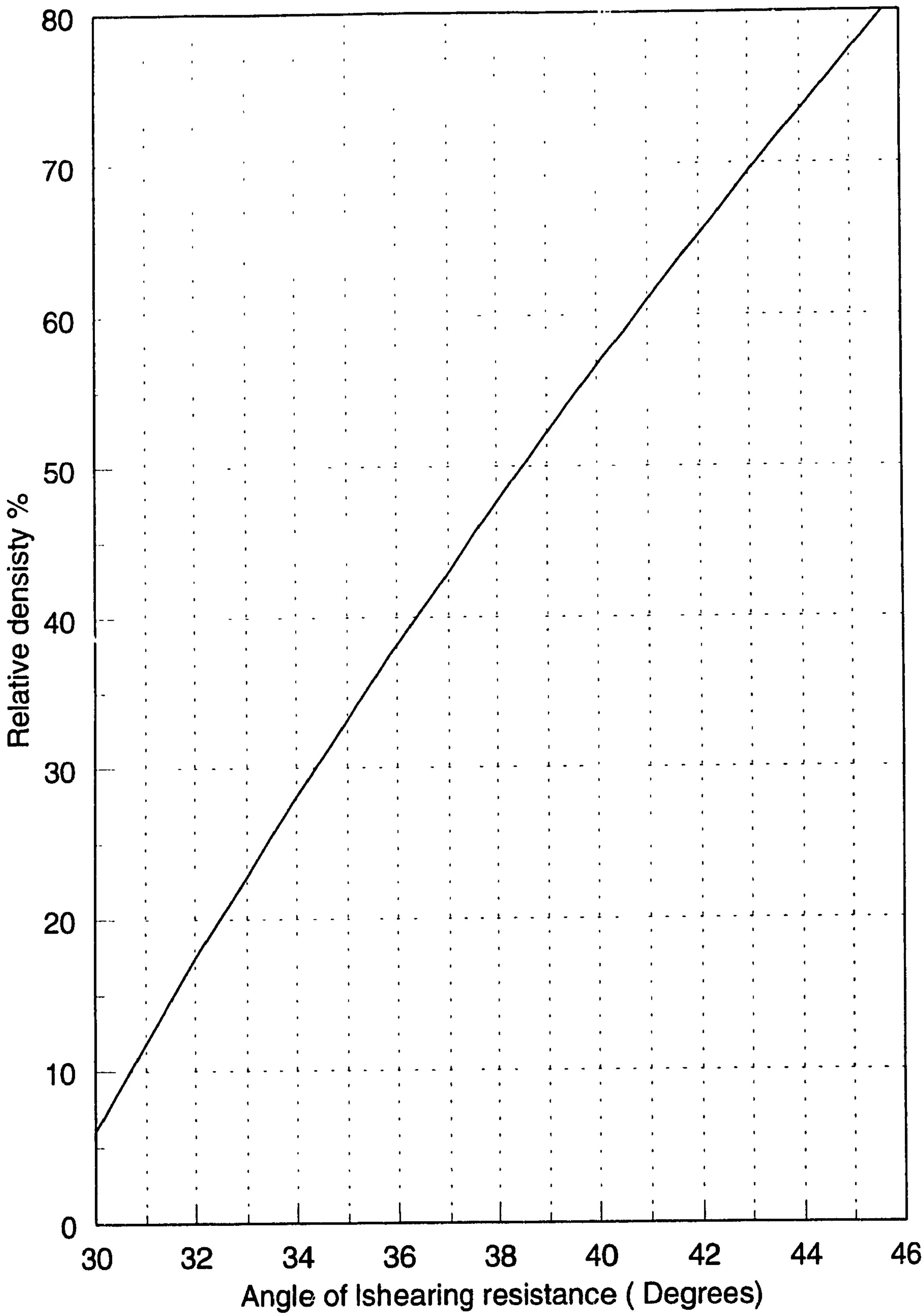

Fig 3-20 Angle lof Shearing resistance versus Relative density

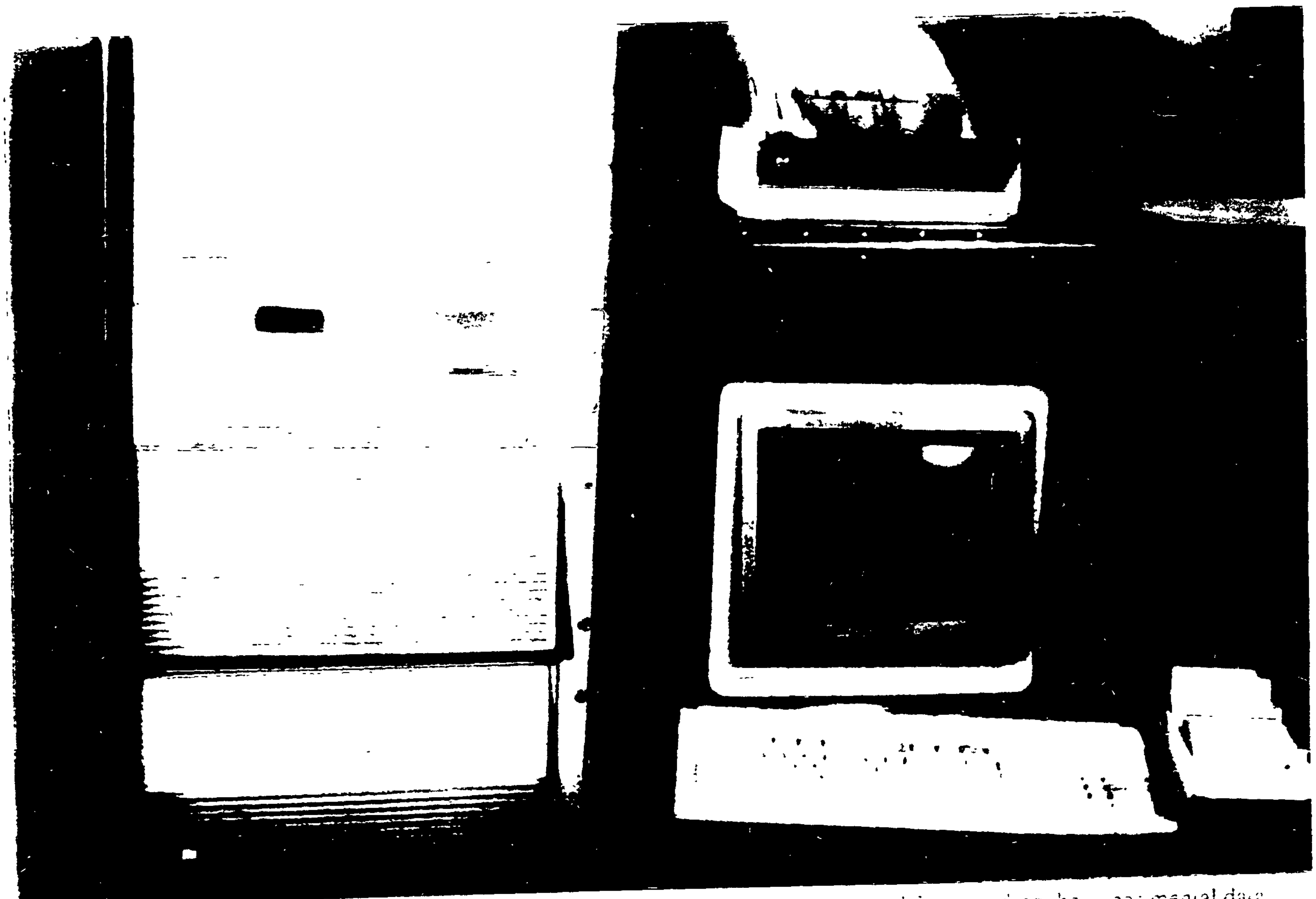

Figure 3-21 Photograph shows the Data Acquisition System (DAS) and the computer used for recording the experimental data.

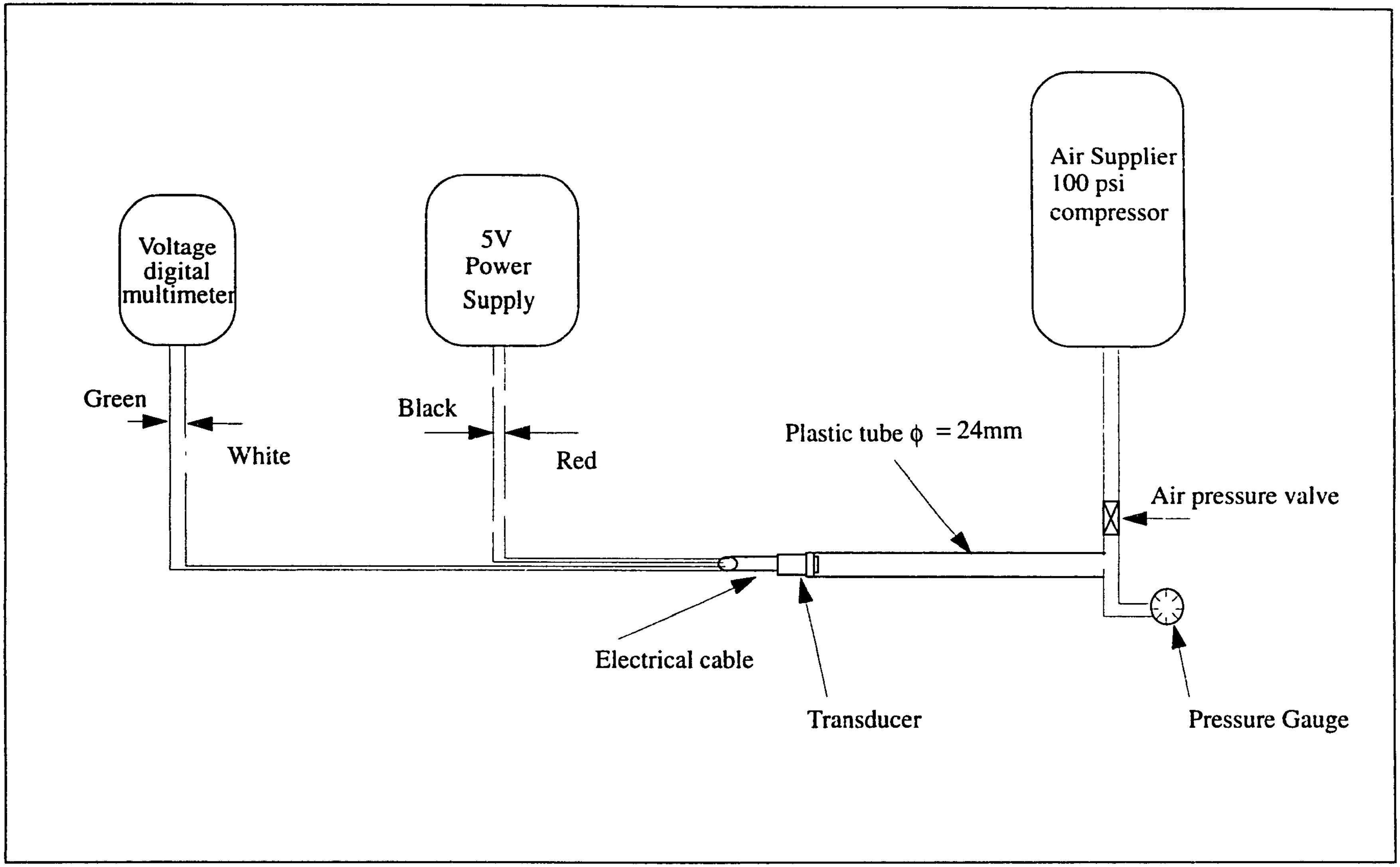

Figure 3-22 Lay - out of the transducer calibration.

Figure 3-23 Photograph shows the set-up used for Calibration of transducer

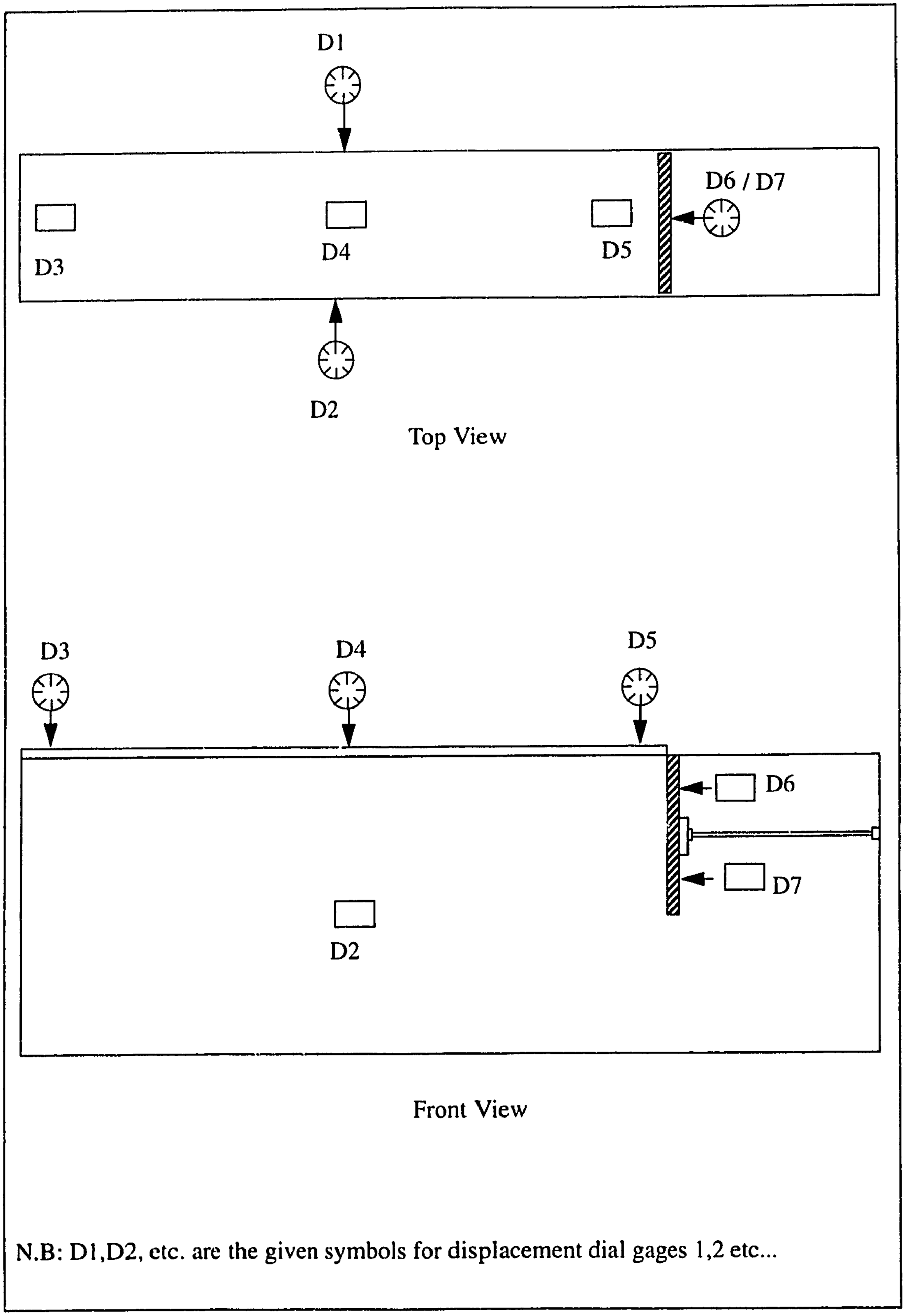

Figure 3-24 Location of the displacement dial gages.

CHAPTER 4

TEST RESULTS AND ANALYSIS

4-1 GENERAL

In this chapter, a summary of the test program is given as well as the experimental test results and analysis for the cases of the retaining wall subjected to at rest and active conditions.

4-2 Test Program

The following table show the test program followed in this experimental investigation:

Table (4-1) Schedule of the experimental investigation program.

Test No	maximum load (Kpa)	Tables No.	Results
1	0.0 Kpa	4-2 to 4-4 & A-1 to A-3	Ko, OCR, Ka
2	13.7 Kpa	4-5 to 4-9 & A-4 to A-7	Ko, OCR, Ka
3	26.2 Kpa	4-10 to 4-15 & A-8 to A-14	Ko, OCR, Ka
4	26.7 Kpa	4-17	Ko,OCR
Test No.	compaction duration	Table No.	Results
5	1 second	4-18	Ko, OCR
6	2 seconds	4-18	Ko, OCR
7	4 seconds	4-18	Ko, OCR
8	6 seconds	4-18	Ko, OCR

4-3 Test results

4-3-1 At rest condition

The test results are given in Tables for the at rest condition during and after the overconsolidation processes of the sand by both techniques:

For overconsolidation by means of applying surfaced loads the results are given in tables 4-2, 4-5, 4-6, 4-12, and 4-16;

For overconsolidation by means of compacting the sand by an air compressor the results are given in table 4-18.

The changes in the horizontal pressures on the wall as deduced from the transducer readings during each increment of loading and unloading for a period of 48 hours were also recorded. The results are given in tables: (4-10) & (4-11). Typical results are represented in a graphical form in figures: (4-1) and (4-2). The initial and the final readings registered on the transducers were plotted against load increment in figure (4-3). In this figure, the upper part shows the sequence of loading and unloading which was used to overconsolidate the sand. In the lower part of this figure, the transducer readings were given in the form of initial and final reading for every load increment. From the deduced pressure diagram on the wall, the earth pressure and the coefficient of earth pressure for the cases of the at rest and active cases were calculated.

Figure (4-4) to (4-6) show graphically the relation between the vertical pressure σ_v which is measured in the sand mass at the same level of the transducer in question versus the horizontal pressure measured by the transducers on the wall during loading and unloading. It can be noticed that the relationship during loading is linear, but, during unloading, is polynomial. Besides, the at rest lateral earth pressure, Ko increases due to the increase of the over consolidation ratio, OCR, which will be well documented in the test results analysis.

Furthermore, the displacements measured by the dial gages during loading and unloading of the surfaced loads are given in tables 4-9 and 4-15.

4-3-2 Active condition

The test results for the active case during retaining wall movement for both the pressures on the retaining wall and for the vertical and horizontal pressures in the soil mass are given in tables 4-3, 4-4, 4-7, 4-8, 4-13, 4-14, and 4-17.

Figures (4-7) shows the variation of the horizontal pressures measured by transducers on the wall versus the displacement of the wall. It can be noticed that the horizontal pressure decreases in proportion with the depth. Furthermore, the horizontal pressure decreases sharply at the beginning of the wall displacement until a minimum value which represents the active earth pressure on the wall.

Figure (4-8) shows a typical relationship for the displacement of the wall versus the horizontal force on the wall measured by the Load Cell. It can be noticed that the horizontal force decreases sharply at the beginning of the wall displacement until a minimum value which represents the active earth force on the wall.

Finally, all the deduced stresses of the transducers embedded in the sand mass are presented in appendix I tables A-1 to A-14.

Experimental Results of Test No1

Table (4-2):Horizontal pressure measured by transducers on the wall at the at rest condition (Test No.1)

Ps Static pressure (Kpa)	Time (hour)	Horizontal pressure measured by transducers on the wall (Kpa)				
		W1*	W2*	W3*	W4*	W5*
0	0	0.25	0.61	0.79	1.05	1.29
	4	0.25	0.62	0.8	1.05	1.29
	8	0.25	0.62	0.81	1.08	1.29
	24	0.26	0.64	0.83	1.1	1.35
	28	0.27	0.65	0.83	1.11	1.36
	32	0.28	0.66	0.85	1.13	1.38
	48	0.28	0.66	0.85	1.11	1.58

* For location of the transducers see figure (3-6).

Table (4-3):Horizontal pressure measured by transducers on the wall during displacement of the wall during the Active Case (TestNo.1).

Displacement of the wall (mm)	0.0	0.5	1.0	1.5	2.1	2.51	2.9	8.4
Horizontal pressure measured by transducers on the wall (Kpa)								
W1 *	0.28	0.20	0.13	0.12	0.12	0.115	0.115	0.115
W2*	0.66	0.52	0.38	0.37	0.37	0.37	0.37	0.37
W3 *	0.85	0.70	0.65	0.64	0.62	0.62	0.60	0.60
W4 *	1.19	0.98	0.93	0.89	0.88	0.87	0.85	0.85
W5 *	1.58	1.3	1.25	1.24	1.2	1.15	1.10	1.10

* For location of the transducers see figure (3-6).

Table (4-4): Forces measured by the load cell during displacement of the wall during the active case (Test No.1).

Displacement of the wall (mm)	0.0	0.5	1.0	1.5	2.1	2.51	2.9	8.4
Load cell force (Newton)	40.43	35.22	32.33	29.15	28.33	27.20	26.04	25.95

Experimental Results of Test No.2

Table(4-5):Horizontal pressure measured by transducers on the wall during loading at the at rest condition (Test No.2).

Ps Static pressure (Kpa)	Time (hour)	Horizontal pressure measured by transducers on the wall (Kpa).				
		W1*	W2*	W3*	W4*	W5*
0	0	0.2	0.68	0.95	1.22	1.46
	4	0.2	0.68	0.94	1.21	1.46
	8	0.2	0.68	0.94	1.21	1.45
	24	0.2	0.67	0.91	1.16	1.38
	28	0.2	0.66	0.91	1.16	1.38
	32	0.2	0.65	0.9	1 15	1.35
	48	0.2	0.65	0.9	1.15	1.35
6.3	0	3.45	3.71	3.99	4.45	4.71
	4	3.45	3.70	3.90	4.45	4.71
	8	3.45	3.70	3.90	4.41	4.65
	24	3.33	3.55	3.65	4.08	4.35
	28	3.31	3.55	3.62	4.08	4.31
	32	3.30	3.50	3.60	4.00	4.25
	48	3.30	3.50	3.60	4.00	4.25
13.7	0	6.73	7.04	7.45	7.71	7.98
	4	6.73	7.02	7.35	7.64	7.98
	8	6.68	7.00	7.35	7.61	7.98
	24	6.56	6.91	7.15	7.41	7.66
	28	6.54	6.83	7.15	7.35	7.63
	32	6.50	6.80	7.10	7.31	7.62
	48	6.50	6.80	7.10	7.30	7.60

* For location of the transducers see figure (3-6).

Table (4-6): Summary of the test results during loading and unloading at the at rest condition (Test No.2).

Ps Static pressure (Kpa)	Time (day)	Horizontal pressure measured by transducers on the wall (Kpa).				
		W1*	W2*	W3*	W4*	W5*
0.0	2	0.2	.65	.9	1.15	1.35
6.3	4	3.3	3.5	3.6	4.0	4.25
13.7	6	6.5	6.8	7.1	7.3	7.6
6.3	8	3.8	4.1	4.9	4.8	5.4
0.0	10	0.34	1.53	1.84	2.62	3.36

* For location of the transducers see figure (3-6).

Table (4-7): Horizontal pressure measured by transducers on the wall during the displacement of the wall during the active case (Test No.2) .

Displacement of the wall (mm)	0.0	0.5	1.0	1.5	2.1	2.51	2.9	8.4
Horizontal pressure measured by transducers on the wall (Kpa)								
W1*	.34	0.2	0.13	0.12	0.12	0.11	0.11	0.11
W2*	1.53	0.55	0.37	0.36	0.36	0.36	0.35	0.35
W3 *	1.85	0.98	0.65	0.62	0.63	0.58	0.58	0.58
W4 *	2.62	1.2	1.1	0.87	0.86	0.85	0.82	0.82
W5 *	3.36	1.7	1.12	1.11	1.09	1.08	1.05	1.05

* For location of the transducers see figure (3-6).

Table (4-8): Forces measured by the Load cell during displacement of the wall during the Active case (Test No.2).

Displacement of the wall (mm)	0.0	0.5	1.0	1.5	2.1	2.51	2.9	8.4
Load cell force (Newtons)	70	39	31.25	27.75	25.15	24.75	24.00	24.00

Table (4-9): Displacement measured by dial gages during loading and loading of the surfaced loads at the at rest condition (Test No.2).

Ps Static pressure (Kpa)	Time (day)	Displacement measured by dial gages (1/100 mm)						
		D1*	D2*	D3*	D4*	D5*	D6*	D7*
0.0	2	9.51	5.92	xx	xx	xx	6.05	11.00
0.0	4	9.54	5.93	xx	xx	xx	6.05	11.00
1.0	6	9.55	5.93	7.18	0.44	1.2	6.05	11.00
6.3	8	9.55	5.93	6.89	0.14	0.9	6.05	11.00
13.7	10	9.55	5.93	6.73	14.94	0.72	6.05	11.00
6.3	12	9.55	5.93	6.79	0.04	0.81	6.05	11.00
1.0	14	9.54	5.93	6.85	0.07	0.87	6.05	11.00
0.2	16	9.54	5.93	6.86	0.11	0.88	6.05	11.00
0.0	18	9.54	5.93	6.87	0.14	0.89	6.05	11.00

* For location of the dial gages see figure (3-24)

Experimental Results of Test No3.

Table(4-10): Horizontal pressure measured by transducers on the wall during loading at the at rest condition (Test No.3).

Ps Static pressure	Time	Horizontal pressure measured by transducers on the wall (Kpa)				
Kpa	hours	W1*	W2*	W3*	W4*	W5*
	0	0.3	0.6	0.8	1.0	1.3
	4	0.3	0.61	0.80	1.0	1.3
	8	0.3	0.62	0.81	1.05	1.31
0	24	0.3	0.63	0.84	1.08	1.37
	28	0.3	0.64	0.845	1.09	1.38
	32	0.3	0.65	0.85	1.1	1.4
	48	0.3	0.65	0.85	1.1	1.4
	0	3.0	3.3	3.5	4.2	4.3
	4	3.0	3.3	3.48	4.15	4.25
	8	2.95	3.28	3.4	4.1	4.2
5.4	24	2.94	3.15	3.25	3.85	3.91
	28	2.92	3.12	3.22	3.82	3.89
	32	2.9	3.1	3.2	3.8	3.86
	48	2.9	3.1	3.2	3.8	3.86
	0	5.7	6.0	6.3	6.9	6.9
	4	5.7	6.0	6.3	6.9	6.85
	8	5.65	5.9	6.2	6.85	6.7
11.3	24	5.58	5.85	6.05	6.6	6.65
	28	5.55	5.82	6.03	6.55	6.62
	32	5.5	5.8	6.0	6.5	6.6
	48	5.5	5.8	6.0	6.5	6.55

* For location of the transducers see figure (3-6)

Table(4-10)continued: Horizontal pressure measured by transducers on the wall during loading at the at rest condition (Test No.3).

Ps Static pressure Kpa	Time hours	Horizontal pressure measured by transducers on the wall (Kpa)				
		W1*	W2*	W3*	W4*	W5*
16.9	0	8.6	9.0	9.0	9.6	9.8
	4	8.5	8.9	9.0	9.6	9.7
	8	8.5	8.85	8.9	9.5	9.6
	24	8.3	8.6	8.5	9.2	9.3
	28	8.25	8.55	8.45	9.1	9.3
	32	8.2	8.5	8.4	9.0	9.2
	48	8.2	8.5	8.4	9.0	9.2
20.5	0	10.3	10.6	10.8	11.2	11.33
	4	10.2	10.6	10.7	11.1	11.21
	8	10.2	10.5	10.6	11.0	11.19
	24	9.9	10.1	10.3	10.6	10.85
	28	9.85	10.1	10.25	10.58	10.75
	32	9.8	10.0	10.2	10.5	10.73
	48	9.8	10.0	10.2	10.5	10.73
26.2	0	13.0	13.7	14.0	14.3	14.7
	4	12.9	13.6	13.8	14.1	14.5
	8	12.8	13.5	13.6	13.9	14.3
	24	12.2	12.8	12.7	13.0	13.6
	28	12.1	12.7	12.5	12.9	13.5
	32	12.0	12.3	12.4	12.8	13.4
	48	12.0	12.3	12.4	12.8	13.4

* For location of the transducers see figure (3-6)

Table(4-11): Horizontal pressure measured by transducers on the wall during unloading at the at rest condition (Test No.3).

Ps Static pressure Kpa	Time hours	Horizontal pressure measured by transducers on the wall (Kpa)				
		W1*	W2*	W3*	W4*	W5*
20.5	0	11.5	11.8	12.0	12.7	13.0
	4	11.4	11.7	11.9	12.6	13.0
	8	11.3	11.6	11.8	12.5	12.9
	24	11.25	11.4	11.7	11.8	12.85
	28	11.2	11.35	11.65	11.7	12.83
	32	11.2	11.3	11.6	11.6	12.8
	48	11.2	11.3	11.6	11.6	12.8
16.9	0	10.9	10.9	11.1	11.7	12.7
	4	10.8	10.9	11.0	11.6	12.7
	8	10.7	10.7	10.9	11.5	12.6
	24	10.3	10.4	10.5	10.7	12.4
	28	10.25	10.3	10.3	10.6	12.4
	32	10.2	10.2	10.2	10.4	12.3
	48	10.2	10.2	10.2	10.4	12.3
11.3	0	8.8	9.0	9.3	9.6	11.0
	4	8.7	9.0	9.2	9.5	11.0
	8	8.6	8.9	9.1	9.4	10.9
	24	8.5	8.7	8.9	9.3	10.7
	28	8.5	8.6	8.8	9.3	10.7
	32	8.4	8.6	8.7	9.2	10.6
	48	8.4	8.6	8.7	9.2	10.6

* For location of the transducers see figure (3-6).

Table (4-11) continued: Horizontal pressure measured by transducers on the wall during unloading at the at rest condition (Test No.3)).

Ps Static pressure Kpa	Time hours	Horizontal pressure measured by transducers on the wall (Kpa)				
		W1*	W2*	W3*	W4*	W5*
5.4	0	6.4	6.8	7.1	7.2	8.3
	4	6.3	6.2	7.0	7.1	8.2
	8	6.0	6.2	6.9	6.8	8.1
	24	4.8	4.8	5.1	6.0	6.9
	28	4.5	4.7	4.9	5.9	6.7
	32	4.4	4.6	4.74	5.8	6.4
	48	4.4	4.6	4.74	5.8	6.4
0	0	2.73	2.6	2.85	3.6	4.43
	4	2.6	2.4	2.6	3.4	4.2
	8	2.2	2.2	2.4	3.2	4.0
	24	1.05	1.4	1.9	2.9	3.2
	28	0.65	1.3	1.7	2.5	3.0
	32	0.45	1.2	1.65	2.3	2.93
	48	0.45	1.2	1.65	2.3	2.93

* For location of the transducers see figure (3-6).

Table (4-12): Horizontal pressure measured by transducers on the wall during loading and unloading of the static pressures at the at rest condition (Test No.3).

Ps Static pressure (Kpa)	Time (day)	Horizontal pressure measured by transducers on the wall (Kpa)				
		W1*	W2*	W3*	W4*	W5*
0	2	.3	.65	.85	1.10	1.4
1.0	4	.75	1.1	1.4	1.6	1.85
3.2	6	1.76	2.1	2.2	3.4	2.76
5.4	8	2.9	3.1	3.2	4.2	3.86
9.5	10	4.7	4.9	5.1	5.7	5.72
11.3	12	5.5	5.8	6.0	6.5	6.55
13.2	14	6.3	6.6	6.9	7.2	7.4
15.15	16	7.2	7.6	7.7	8.3	8.6
16.9	18	8.2	8.5	8.4	9.0	9.2
18.7	20	9.3	9.2	9.4	9.75	9.9
20.5	22	9.8	10.0	10.2	10.5	10.73
23.9	24	11.4	11.4	11.5	11 8	12.22
26.2	26	12.0	12.3	12.4	12.8	13.4
23.9	28	11.8	11.9	12.0	12.2	13.0
20.5	30	11.2	11.3	11.6	11.6	12.8
18.7	32	10.3	10.4	10.2	10.5	12.6
16.9	34	10.2	10.2	10.2	10.4	12.3
15.1	36	10.0	10.0	10.0	10.3	11.7
13.2	38	8.9	8.7	8.9	9.9	11.2
11.3	40	8.4	8.6	8.7	9.2	10.6
9.5	42	7.9	8.0	8.2	8.8	9.8
7.7	44	6.8	7.1	7.3	7.4	7.5
5.4	46	4.4	4.6	4.74	5.8	6.4
3.2	48	2.7	2.8	3.74	4.8	5.4
0	50	.55	1.71	2.44	4.14	5.16

* For location of the transducers see figure (3-6).

Table (4-13): Horizontal pressure measured by transducers on the wall during the displacement of the wall during the active case.(Test No.3)

Displacement of the wall(mm)	0.0	0.5	1.0	1.5	2.1	2.51	2.9	8.4
Horizontal pressure measured by transducers on the wall (Kpa).								
W1 *	0.55	0.23	0.17	0.12	0.12	0.12	0.115	0.1
W2*	1.71	0.63	0.46	0.39	0.36	0.36	0.35	0.34
W3 *	2.44	1.02	0.64	0.59	0.55	0.55	0.51	0.50
W4 *	4.14	1.3	0.9	0.85	0.79	0.79	0.75	0.74
W5 *	5.16	1.81	1.32	1.14	1.0	1.0	0.99	0.98

* For location of the transducers see figure (3-6)

Table (4-14): Forces measured by the Load cell during displacement of the wall during the Active Case (Test No.3).

Displacement of the wall(mm)	0.0	0.5	1.0	1.5	2.1	2.51	2.9	8.4
Load cell force (Newtons)	82	51.5	37.3	32.2	24.4	23.3	23	21

Table (4-15): Displacement measured by dial gages during loading and unloading at the at rest condition (Test No.3).

Ps Static pressure (Kpa)	Time (day)	Displacement measured by the dial gages (1/100 mm)						
		D1*	D2*	D3*	D4*	D5*	D6*	D7*
0	2	10.03	8.15	xxx	xxx	xxx	0.73	4.78
1.0	4	10.07	8.21	5.50	3.78	0.00	0.73	4.78
3.2	6	10.07	8.21	5.35	3.74	14.96	0.73	4.78
5.4	8	10.07	8.21	5.18	3.69	14.88	0.73	4.78
9.5	10	10.07	8.21	4.99	3.62	14.65	0.73	4.78
11.3	12	10.07	8.21	4.91	3.47	14.58	0.73	4.78
13.2	14	10.07	8.21	4.86	3.41	14.51	0.73	4.78
15.15	16	10.07	8.21	4.80	3.32	14.43	0.73	4.78
16.9	18	10.07	8.21	4.66	3.22	14.37	0.73	4.78
18.7	20	10.07	8.21	4.67	3.16	14.30	0.73	4.78
20.5	22	10.07	8.21	4.66	3.08	14.27	0.73	4.78
23.9	24	10.07	8.21	4.57	2.90	14.10	0.73	4.78
26.2	26	10.07	8.21	4.51	2.76	14.01	0.73	4.78
23.9	28	10.07	8.21	4.51	2.76	14.01	0.73	4.78
20.5	30	10.07	8.21	4.51	2.76	14.02	0.73	4.78
18.7	32	10.07	8.21	4.51	2.76	14.03	0.73	4.78
16.9	34	10.07	8.21	4.52	2.76	14.03	0.73	4.78
15.1	36	10.07	8.21	4.52	2.77	14.03	0.73	4.78
13.2	38	10.07	8.21	4.53	2.77	14.03	0.73	4.78
11.3	40	10.07	8.21	4.54	2.78	14.04	0.73	4.78
9.5	42	10.07	8.21	4.56	2.78	14.06	0.73	4.78
7.7	44	10.07	8.21	4.57	2.81	14.10	0.73	4.78
5.4	46	10.07	8.21	4.60	2.82	14.12	0.73	4.78
3.2	48	10.07	8.21	4.66	2.83	14.17	0.73	4.78
0.2	50	10.07	8.21	4.81	3.01	14.36	0.73	4.78

* For location of dial gages see figure (3-24)

Experimental Results of Test No4.

Table (4-16): Horizontal pressure measured by transducers on the wall during loading and unloading of the static pressures at the at rest condition (Test No.4).

Ps Static pressure (Kpa)	Horizontal pressure measured by transducers on the wall (Kpa)				
	W1*	W2*	W3*	W4*	W5*
0		.5	.81	1.16	1.39
23.3		9.9	10.4	12.2	12.3
26.78		11.4	11.9	13.3	13.7
14.7		9.5	10	10.4	10.8
9.81		7.1	7.6	8.1	8.6
7.36		5.9	6.5	7.1	7.55
5.89		5.3	5.8	6.5	7.0
4.91		4 7	5.3	6.0	6.5
4.43		4.5	5.05	5.8	6.3
3.94		4.15	4.8	5.5	6.05
3.45		3.9	4.55	5.3	5.8
2.96		3,6	4.2	5.0	5.6
2.47		3 3	3.9	4.7	5.3
1.98		2.9	3.6	4.4	5.05
1.49		2..6	3.3	4.1	4.8
1.0		2.2	2.9	3.8	4.45
0.386		1.7	2.5	3.5	4.2
0.155		1.45	2.3	3.3	4.0
0.0		1.35	2.15	3.2	3.9

* For location of the transducers see figure (3-6).

Table (4-17): Summary of the test results performed on the wall during the active case.

Test No.	1	2	3
Maximum Ps (Kpa)	0	13.7	26.2
ϕ (Degree)	30	32	33
W1* (Kpa)	0.115	0.11	0.10
W2 *(Kpa)	0.37	0.35	0.34
W3 *(Kpa)	0.60	0.58	0.50
W4 *(Kpa)	0.85	0.82	0.74
W5 *(Kpa)	1.1	1.05	0.98
Load cell force P (Newtons)	25.95	25.00	21.00

*For location of the transducers see figure (3-6)

Table (4-18): Test results performed on the compacted sands at the at rest condition.

Compaction (second)	TEST NO.	Depth H (mm)	Angle of shearing resistance, ϕ, (Degrees)	Unit weight γ (KN/m^3)	Horizontal pressure σ_h (Kpa)
1	5	144	30.5	17.55	1.60
		265	31	17.75	3.52
		365	32	17.80	5.72
3	6	144	34	18.25	1.73
		265	36	18.7	3.76
		365	42	19.02	6.4
4	7	144	36	18.69	1.82
		265	43.3	19.2	3.87
		365	45.5	19.6	6.49
6	8	144	41.3	18.92	1.83
		265	44	19.35	3.9
		365	46	19.7	6.6

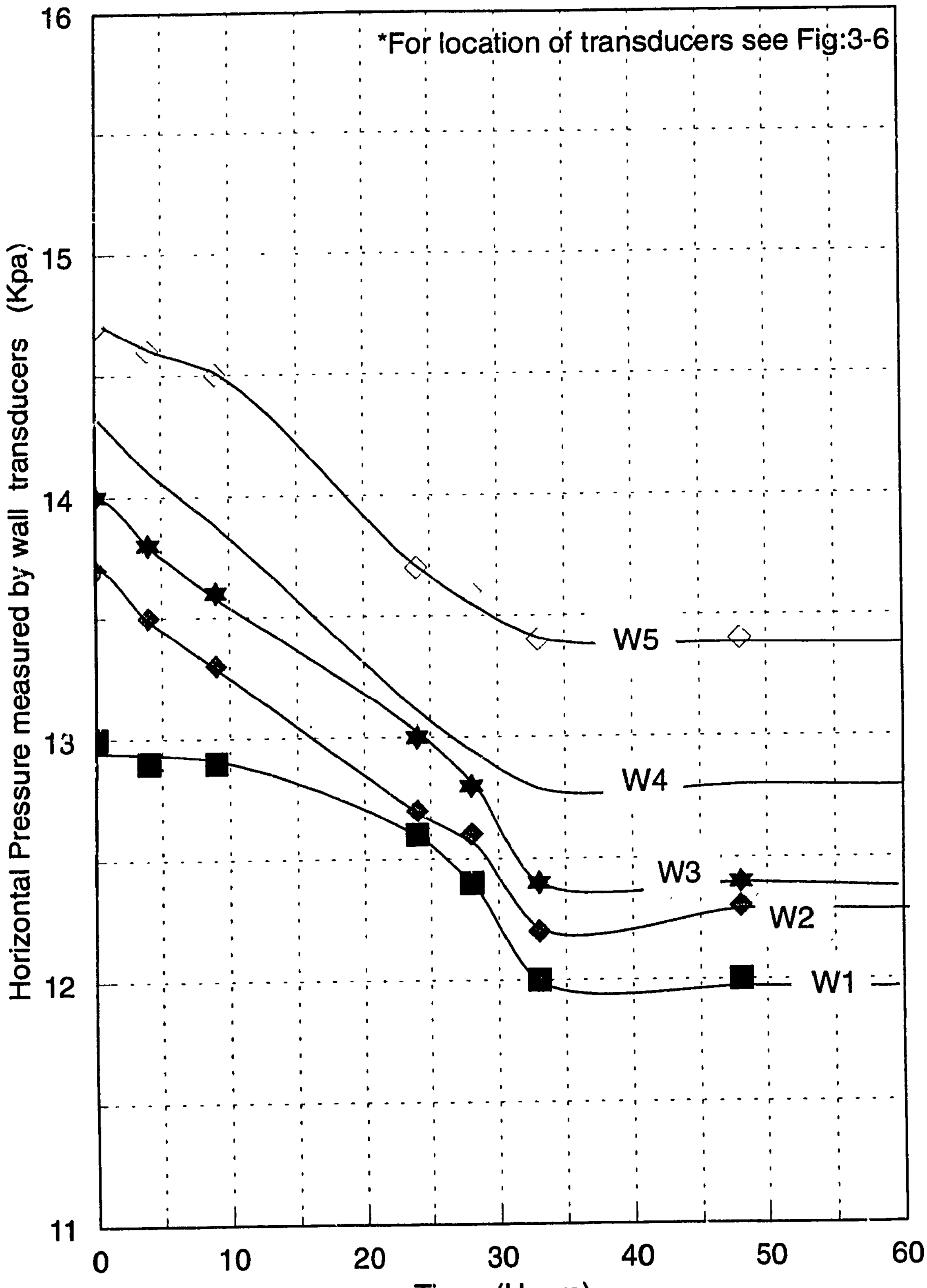

Figure 4-1 Horizontal pressure measured by wall transducers versus time during loading of ps= 26.2 Kpa

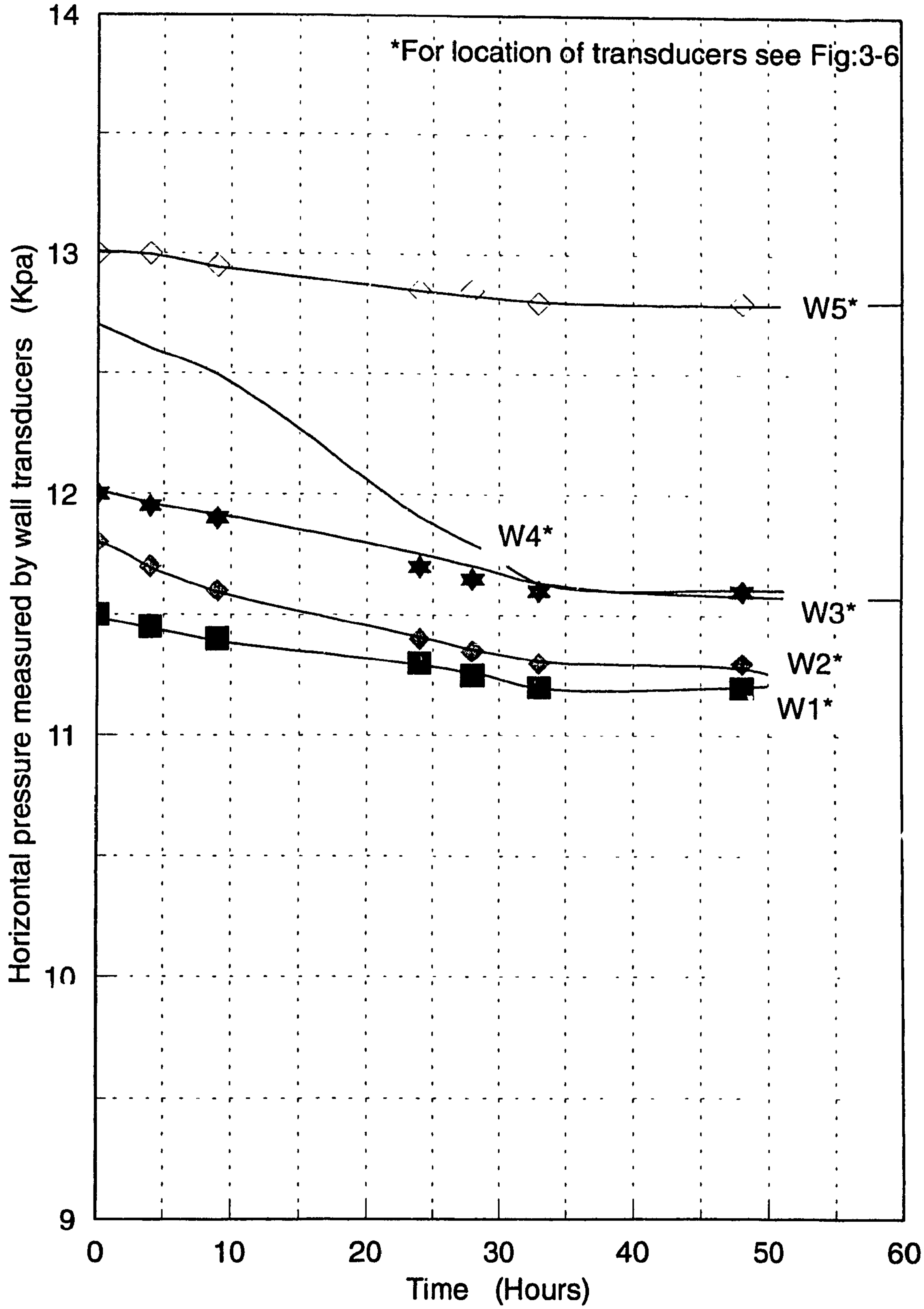

Figure 4-2 Horizontal pressure measured by wall transducers versus time during unloading ps=20.5 kpa

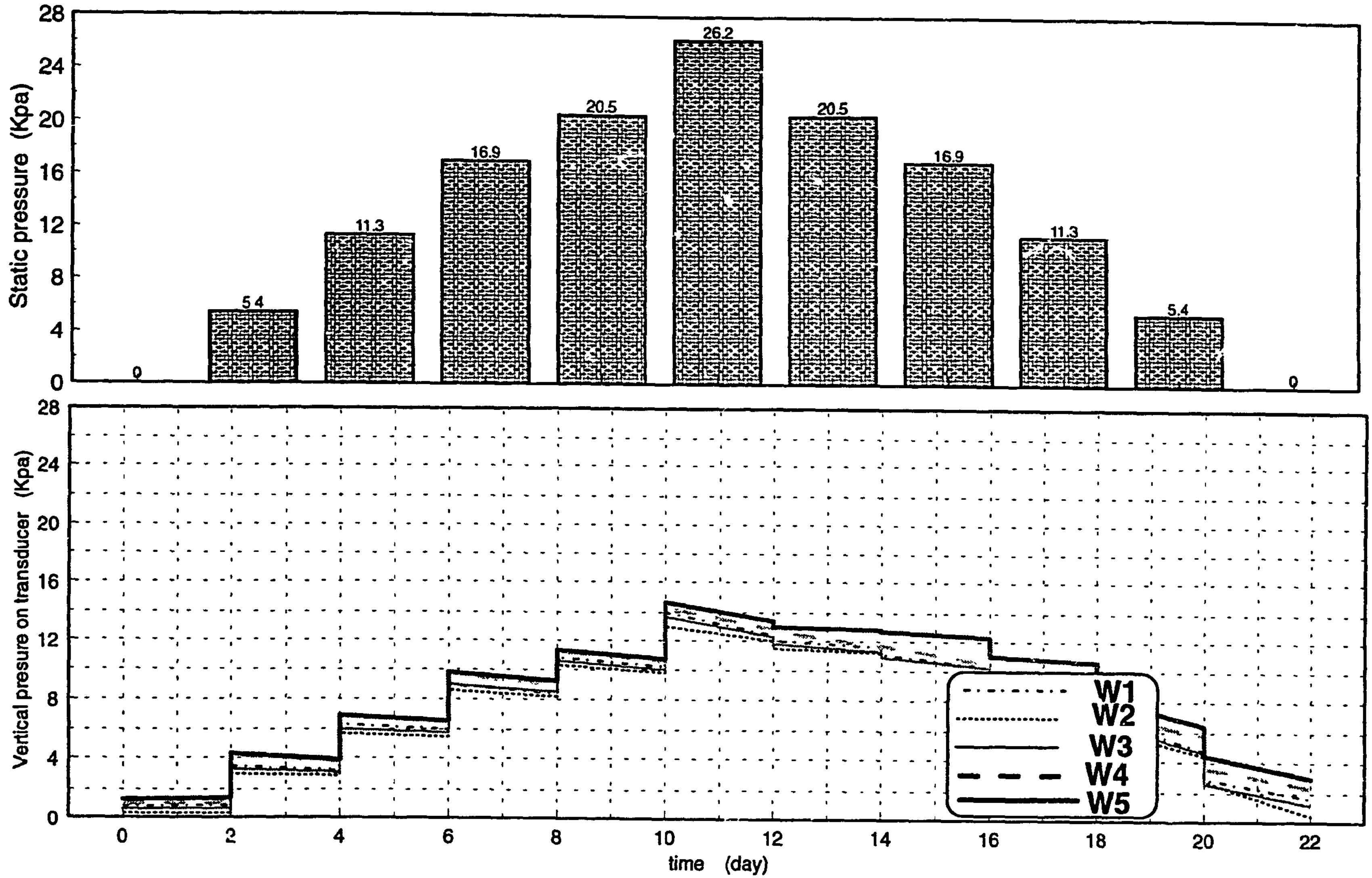

Figure 4-3 Initial and final reading of transducers on the wall for all increments during loading and unloading.

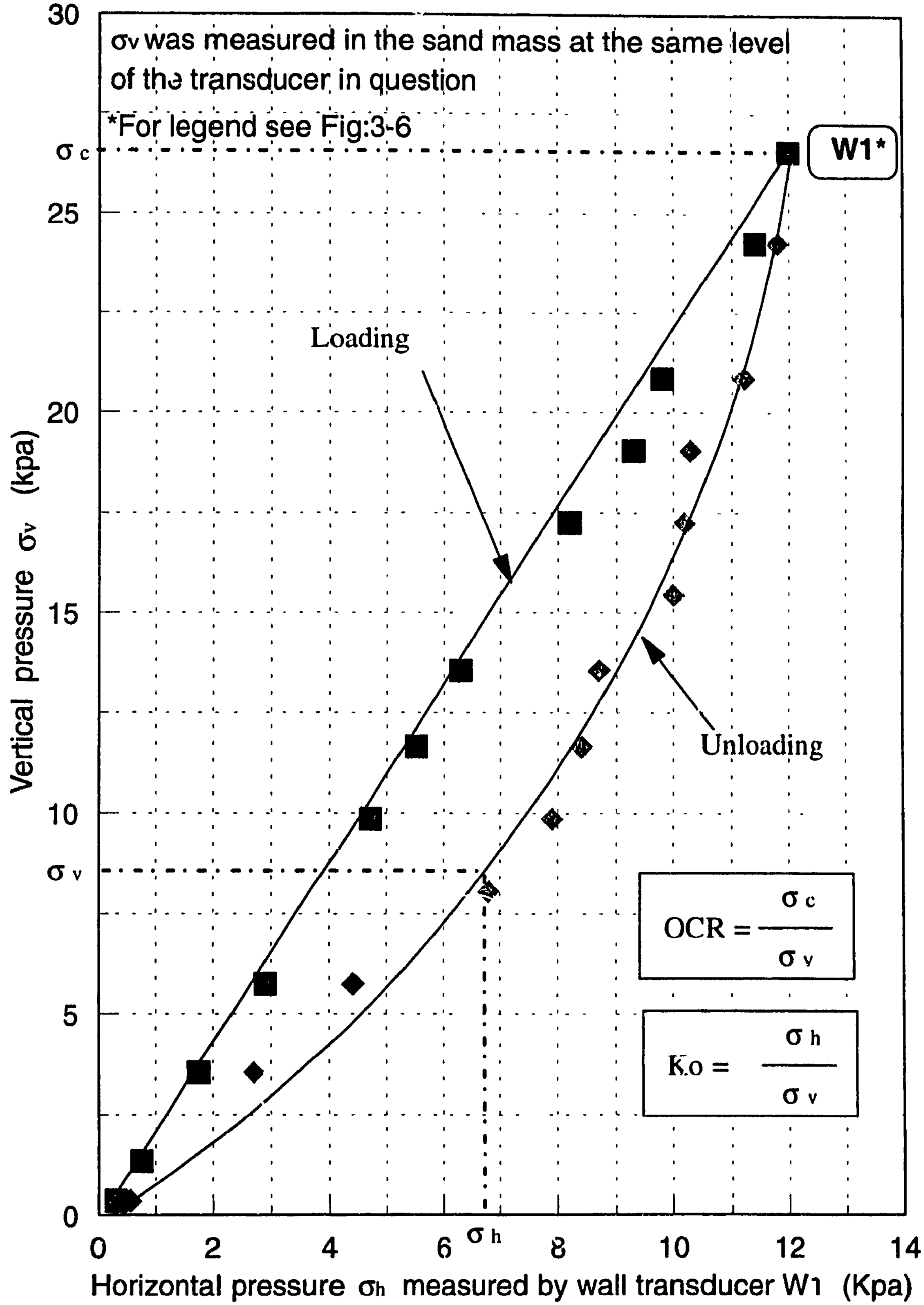

Figure 4 - 4 Vertical pressure σv versus horizontal pressure σh measured by transducer W1.

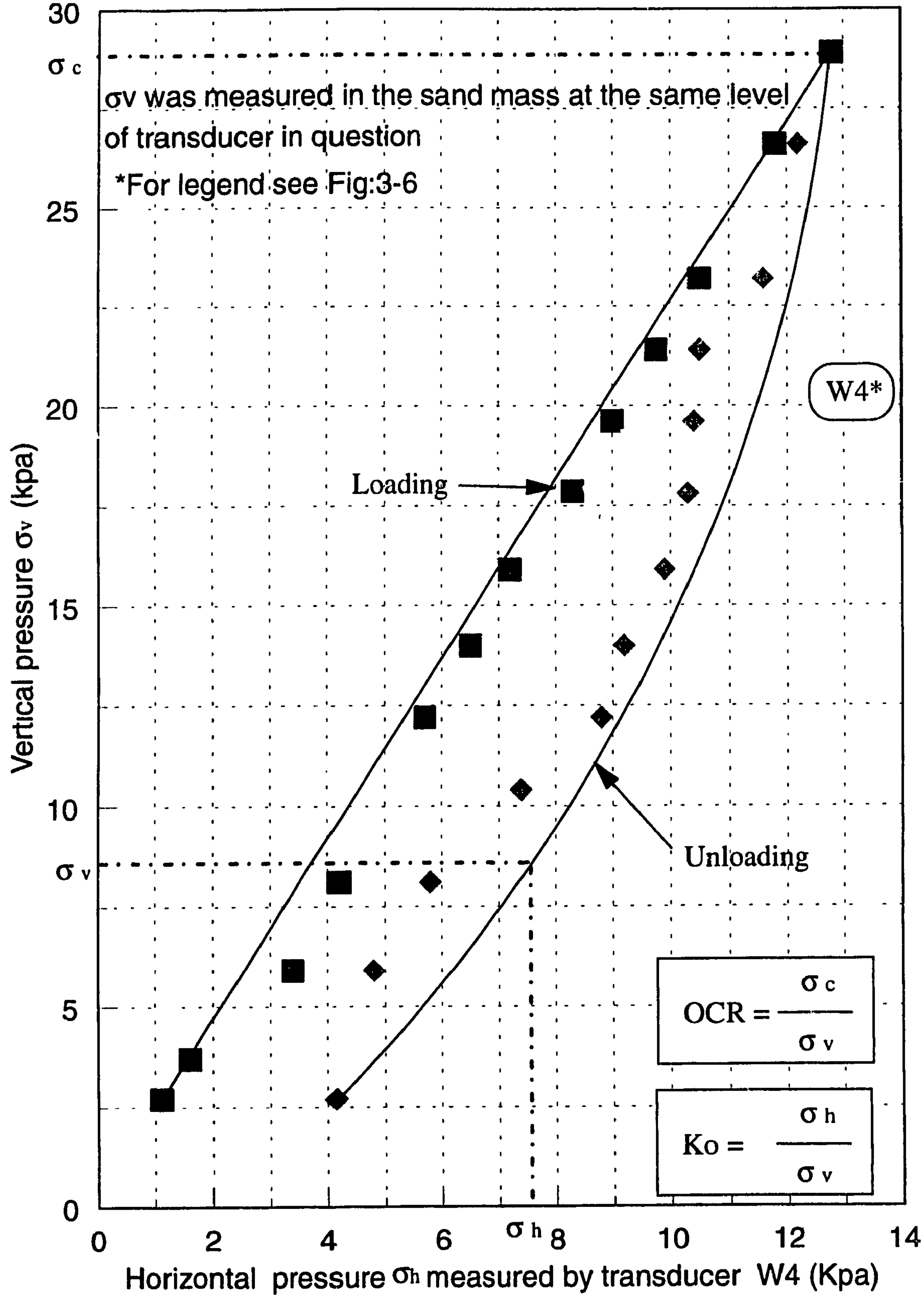

Figure 4 -5 Vertical pressure σv versus horizontal pressure σh measured by transducer W4.

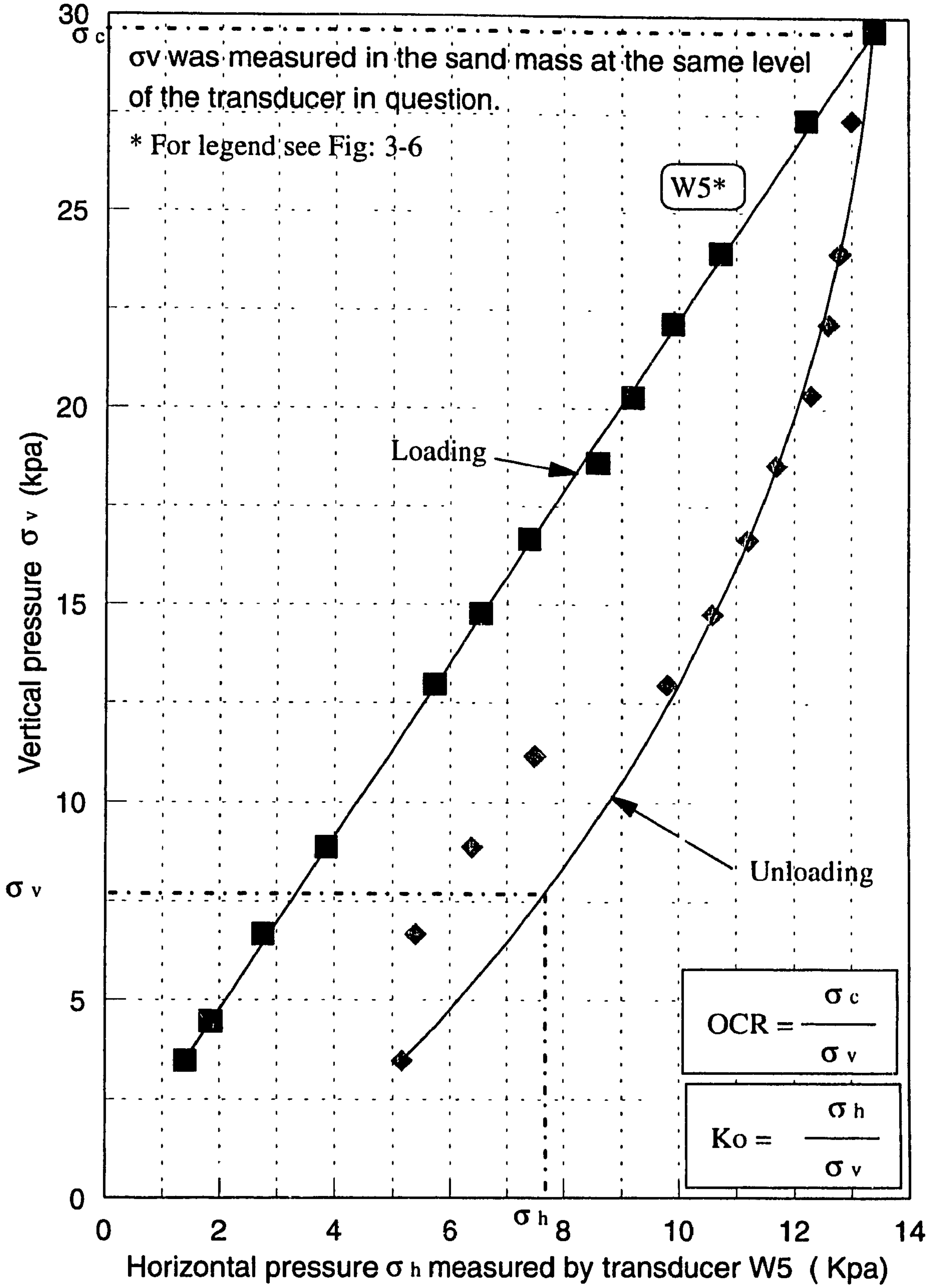

Figure 4 - 6 Vertical pressure σv versus horizontal pressure σh measured by transducer W5.

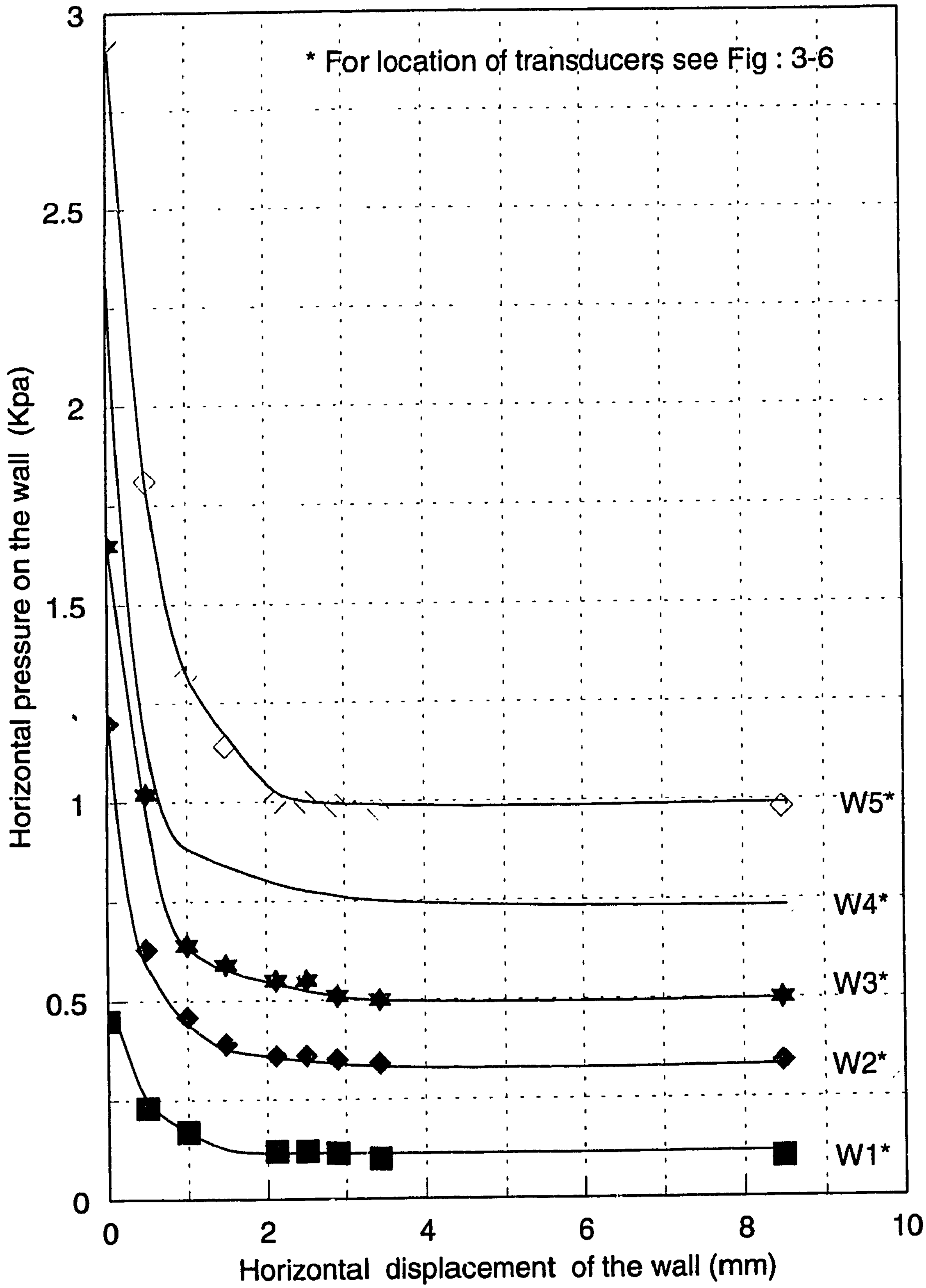

Figure 4-7 Horizontal pressure versus displacement of the wall

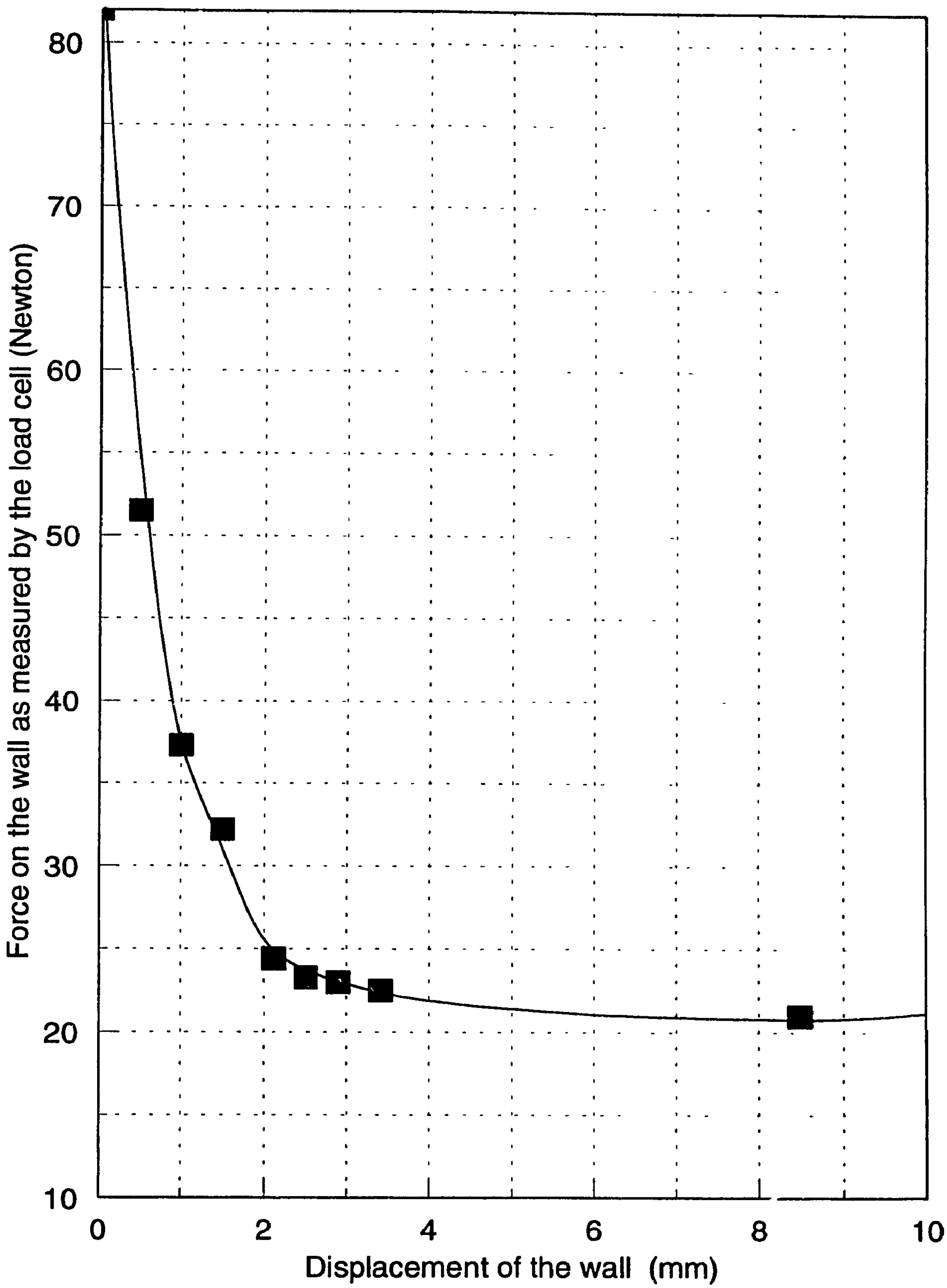

Figure 4-8 Displacement of the wall versus force on the wall as measured by the load cell

4-4 Analysis of the test results

4-4 -1 General

In the present investigation the at rest lateral earth pressure and the active earth pressure for homogeneous sand behind the retaining wall were studied as a function of the overconsolidation ratio, OCR, and the angle of shearing resistance, ϕ.

In this section, the experimental results for the homogenous normally consolidated and overconsolidated sands were compared with the available theories for the case of at rest and active earth pressures. A semi-empirical formula is proposed to predict the values of the coefficient of earth pressure at rest, Ko, for normally and overconsolidated sands.

4-4-2 Determination of OCR.

In this analysis the overconsolidation ratio, OCR, as a result of surfaced load for a given element at a depth h from the surface is defined as:

$$OCR = \frac{\sigma_c}{\sigma_v} \quad \text{.......... 4-1}$$

where, σ_c is the maximum vertical pressure ever applied on this element.

σ_v is the existing vertical pressure on the same element.

Besides, for overconsolidated sand by means of compaction OCR is calculated from Wroth's equation (2-22).

4-4-3 Determination of Ko

The earth pressure coefficient at rest, Ko, for a given element is given by:

$$K_o = \frac{\sigma_h}{\sigma_v} \qquad \text{.......... 4-2}$$

where, σ_h is the horizontal pressure as deduced from the transducer reading at this element (At the rest condition).

4-4-4 Analyzing the Lateral earth pressure results for the case of at rest condition.

The test results were analyzed and compared with the available theories. The results are presented in tables: (4-19) to (4-22).

Table (4-19): Analysis of the test results for the lateral earth pressure of at rest condition, for overconsolidated sands by means of surfaced loads(Test No.2)

Ps Static pressure	OCR	Ko
(Kpa)		
0	1	.48
6.3	1	.45
13.7	1	.45
6.3	1.44	.558
0.0	6.35	0.97

Table (4-20): Analysis of the test results for the lateral earth pressure of at rest condition, for overconsolidated sands by means of surfaced loads(Test No.3)

Ps Static pressure	OCR	Ko
(Kpa)		
0	1	.4
23.9	1	.44
26.2	1	.45
23.9	1.09	.47
20.5	1.27	.5
18.7	1.4	.5
16.9	1.53	.53
15.1	1.71	..57
13.2	1.96	.62
11.3	2.37	.66
9.5	2.69	.72
7.7	3.29	.72
5.4	4.61	.72
3.2	7.47	.81
0.0	11.5	1.47

Table (4-21): Analysis of the test results for the lateral earth pressure of at rest condition, for overconsolidated sands by means of surfaced loads(Test No.4)

Ps Static pressure	OCR	Ko
(Kpa)		
0	1	.4
23.3	1	.41
26.78	1	.41
14.7	1.7	.6
9.81	2.37	.65
7.36	2.95	.7
5.89	3.47	.75
4.91	3.93	.78
4.43	4.2	.8
3.94	4.51	.82
3.45	4.89	.85
2.96	5.32	.87
2.47	5.84	.90
1.98	6.48	.93
1.49	7.26	.97
1.0	8.26	1.0
0.386	9.99	1.1
0.155	10.88	1.12
0.0	11.5	1.14

Table (4 -22): Analysis of test results for the lateral earth pressure of at rest condition, for overconsolidated sands by means of compaction.

Compaction (second)	TEST NO.	Depth H (mm)	angle of shearing resistance, ϕ, (Degrees)	OCR	K_{oc} $\sigma_h/\gamma H$
		144	30.5	1.37	.62
1	5	265	31	1.78	.75
		365	32	2.22	.88
		144	34	175	.66
3	6	265	36	2.34	.76
		365	42	4.7	.9
		144	36	2.03	.68
4	7	265	43.3	4.35	.76
		365	45.5	8.0	.91
		144	41.3	3.52	.67
6	8	265	44	5.18	.76
		365	46	8.11	.92

The vertical pressures σ_v deduced by the transducers within the sand mass for the case of normally consolidated sand is represented in figure (4-9). The results showed good agreement with the classical evaluation of $\sigma_v = \gamma H$. This confirm the suitability of the use of transducers in this investigation.

The lateral earth pressures on the wall for the case of at rest condition, for normally consolidated sand are represented in figure (4-10) the results are in agreement with Jaky equation (1944).

The lateral earth pressure on the wall for the case of at rest condition, for the overconsolidated sand are represented in figures (4-11). It can be noticed that the horizontal pressures for overconsolidated sands are higher than those for the normally consolidated sand. This confirm that the overconsolidation ratio, OCR, has great effect on the lateral earth pressure for the at rest condition.

The changes of the lateral earth pressure on the wall during static loading are presented in figures (4-12) to (4-15). From these figures it can be noticed that the changes of the lateral earth pressures on the wall during loading are in agreement with jaky equation and with the available methods for estimating the lateral earth pressure for normally consolidated sand, $\sigma_h = Ko(\gamma H + Ps)$.

The deformation of the sand during loading and unloading are represented in figure (4-16). It can be noticed that the sand doesn't return to its original state, and further the sand behaves as elastic-plastic material. There is some recovery due to the elastic properties of the sand, and there is residual plastic deformation due to its plastic properties. This residual plastic deformation is locked into the sand particles and results in the overconsolidation of the sand.

4-5-5 Proposed method

The analysis of the test results are presented graphically In Figures: (4-17) to (419) for test No. 2,3,4 respectively These graphs enabled to propose the following semi-empirical formula to predict the coefficient of lateral earth pressure at rest condition for the overconsolidated sand by means of surfaced loads :

$$K_{oc} = K_o OCR^m \qquad \text{...4-6}$$

Where the exponent m could be estimated from Figure: (4-20) and Ko is the coefficient of earth pressure at rest condition which is evaluated from Jaky's equation: (Ko=1- sin ϕ)

Figure (4-21) shows graphically the test analysis of the test results of the overconsolidated sand by means of compaction.

Figure (4-22) present design charts showing the lateral earth pressure coefficient for the at rest condition, as function of the angle of shearing resistance, ϕ, and the overconsolidation ratio, OCR, for sand which was overconsolidated by means of surfaced loads.

4-5-6 Determination of Ka

In the present investigation the active lateral earth pressure Ka is calculated from the following

$$K_a = \frac{\sigma_h}{\sigma_v} \quad \text{.......... 4 - 7}$$

where, σ_h is the horizontal pressure deduced by transducer on the wall under the active condition.

Furthermore, the lateral earth pressure could be calculated from the following equation:

$$K_a = \frac{P}{0.5\gamma H^2 b} \quad \text{.......... 4 - 8}$$

where, P is the total load deduced by the load cell after reaching its minimum value;

b is the width of the retaining wall 197 mm;

H is the height of the retaining wall 215 mm.

4-5-7 Analysis of the lateral earth pressure for the case of active condition.

The test results were analyzed and compared with the available methods. The results of the active condition analysis are presented in table (4-23).

The minimum lateral earth pressures deduced by the wall transducers due to the wall displacement are plotted against the depth in figure (4-23) which shows that the test results are in accordance with Rankine's theory for the active condition.

Table (4 -23) Analysis of the test results for the case of active lateral earth pressure.

Ps(Kpa)	0	13.7	26.2
ϕ	30	32	33
Transducer	Ka		
W1	0.33	0.30	0.28
W2	0.33	0.30	0.29
W3	0.32	0.29	0.26
W4	0.32	0.29	0.274
W5	0.32	0.29	0.282

Table (4 -23) continued: Analysis of the test results for the case of active lateral earth pressure.

Test No.	1	2	3
Ka calculated from best fitting line	0.32	0.29	0.28
Ka calculated from the total load deduced by the load cell	0.33	0.302	0.289

a)-The Coulomb's and Rankine's methods:

Both Rankine's and Coulomb's method are similar for the case of no friction on the vertical retaining wall and horizontal backfill which is the case of the present investigation. Using equation 2-1, 2-2 and 2-7 we get:

P_a=.5x.197x.2948x17.75x.215^2= 0.0238 KN. or 23,8 N.

b)-The trial wedges method.

Let us take as a first trial the plane on which failure occurs the plane that has θ equals to 60^0. Then, by increasing it until 64^0, we find that Pa is maximum at a θ equals to 62^0. Figure (4-24) and tables (4-24) shows all the results and calculations.

$W = .5\ \gamma\ d\ h^2 \cot\theta$

$Pa = W \tan\beta$

where. $\beta = 90 - (\phi + 90 - \theta) = \theta - \phi$

$= W \tan(\theta - \phi)$

$= .5\ \gamma\ d\ h^2 \cot\theta \tan(\theta - \phi)$

Table (4-24) Trial wedges method for loose sand. ϕ=33 γ= 17.9 KN/c.m

θ	cotθ	tan(θ-33)	product	Pa / KN
60	.57735	.509	.294173	.02399
61	.5543	.532	.294473	.02403
62	.5317	.5543	.2947313	.02403
63	.509	.578	.294175	.02399
64	.4887	.60	.2868	.023178

From table 4-24 it can be noticed that the experimentally calculated Ka is in accordance with the Rankine values. This result means that the interlocking between the overconsolidated sand particles returns to its previous consolidation state after the movement of the wall.

The importance of studying the influence of OCR on sands is represented in figure (4-25) where the influence of OCR on the earth pressure is illustrated. As the OCR increases Ko and Kp increase, but, Ka doesn't change. This imply that all sands with same ϕ and different OCR have the same Ka. Furthermore, in the case of overconsolidated sand, higher OCR necessitates a longer displacement for the wall in order to achieve either the minimum or the maximum earth pressures which represent the case of Ka or Kp respectively.

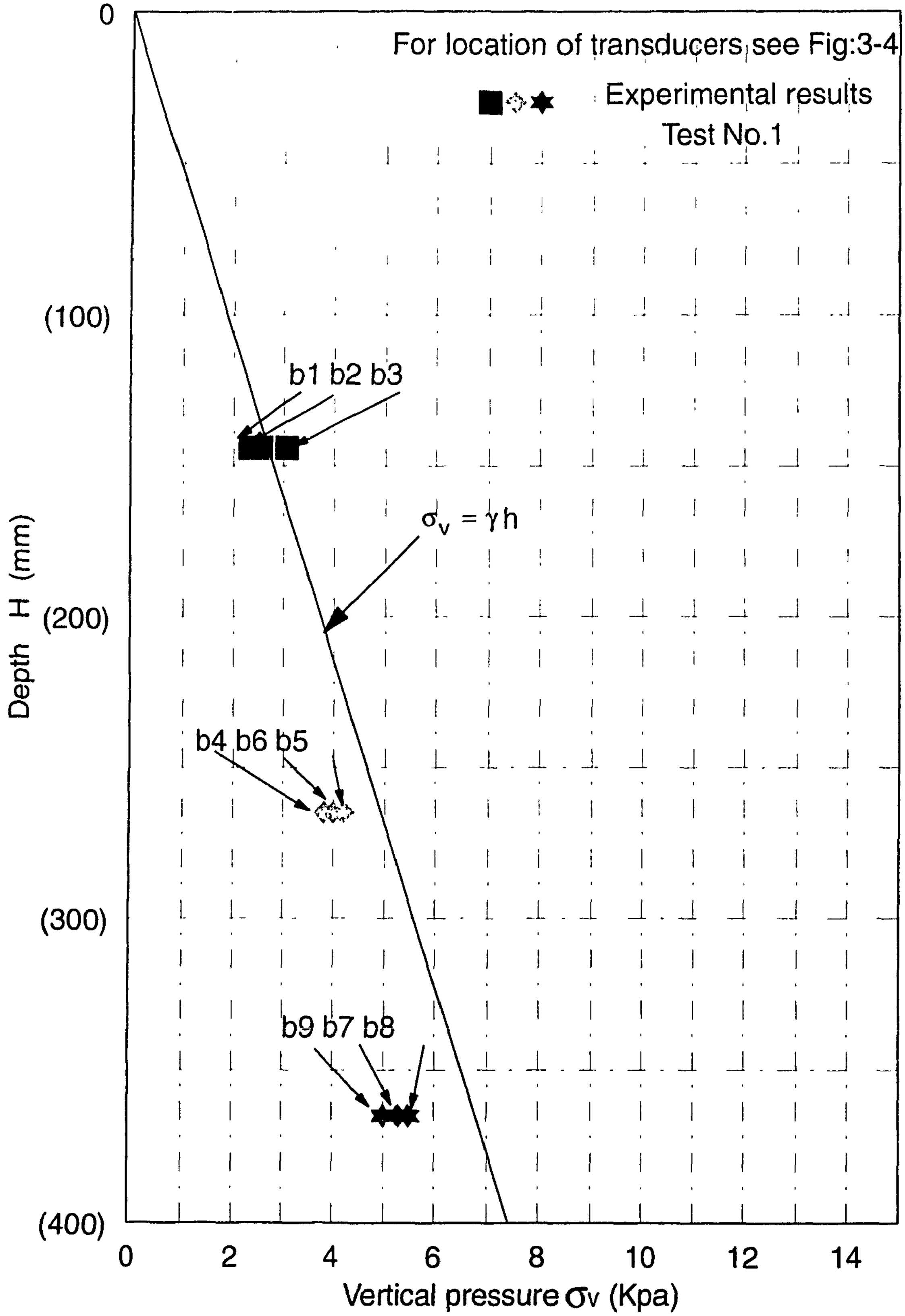

Figure 4-9 Vertical pressure for the case of normally consoildated sand versus depth

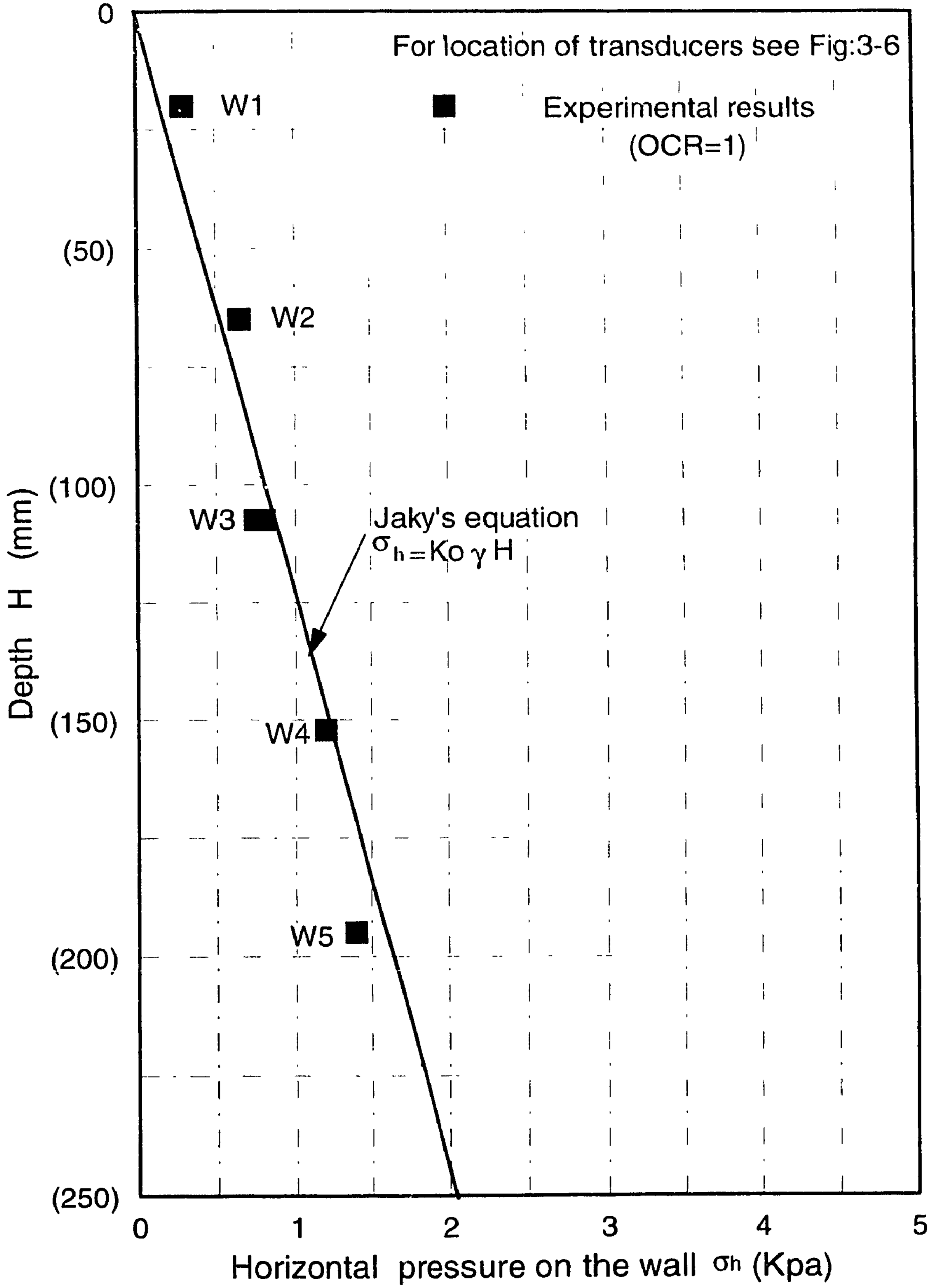

Figure 4-10 Horizontal pressure on the wall for the Ko Condition for normally consolidated sand versus depth.

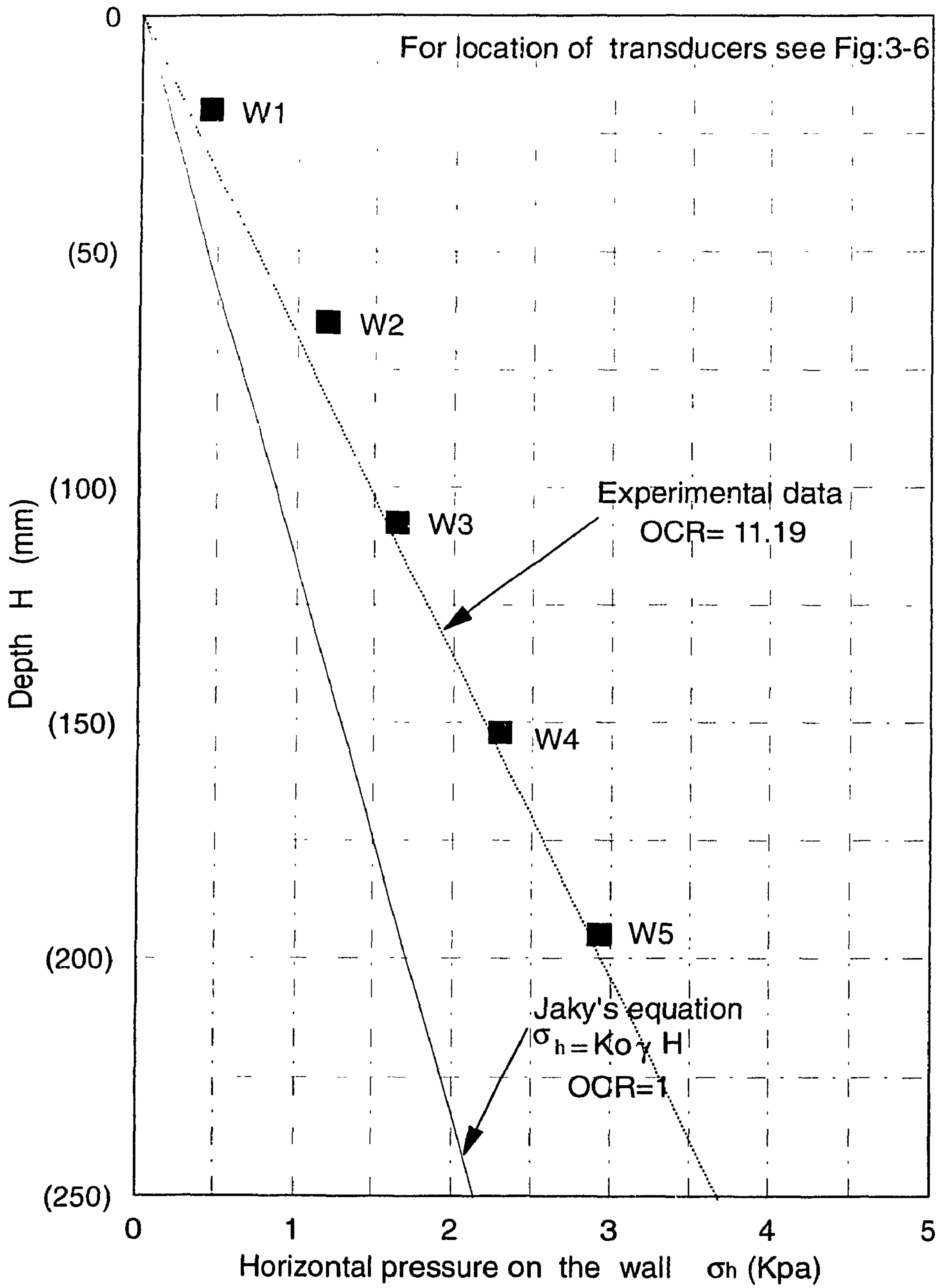

Figure 4-11 Horizontal pressure on the wall for the Ko condition for overconsolidated sand versus depth.

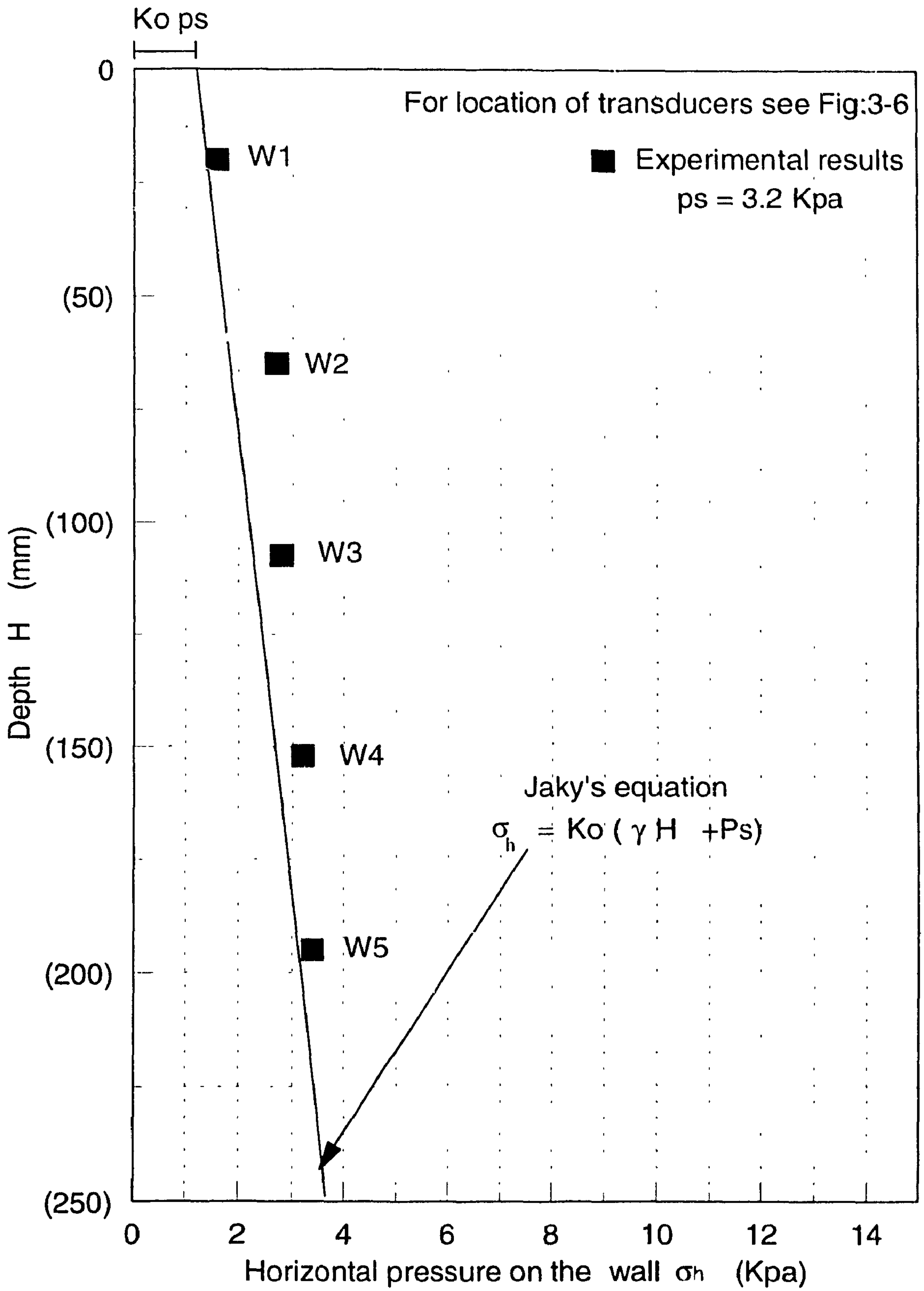

Fig 4-12 Horizontal pressure on the wall versus depth during loading ps=3.2 Kpa.

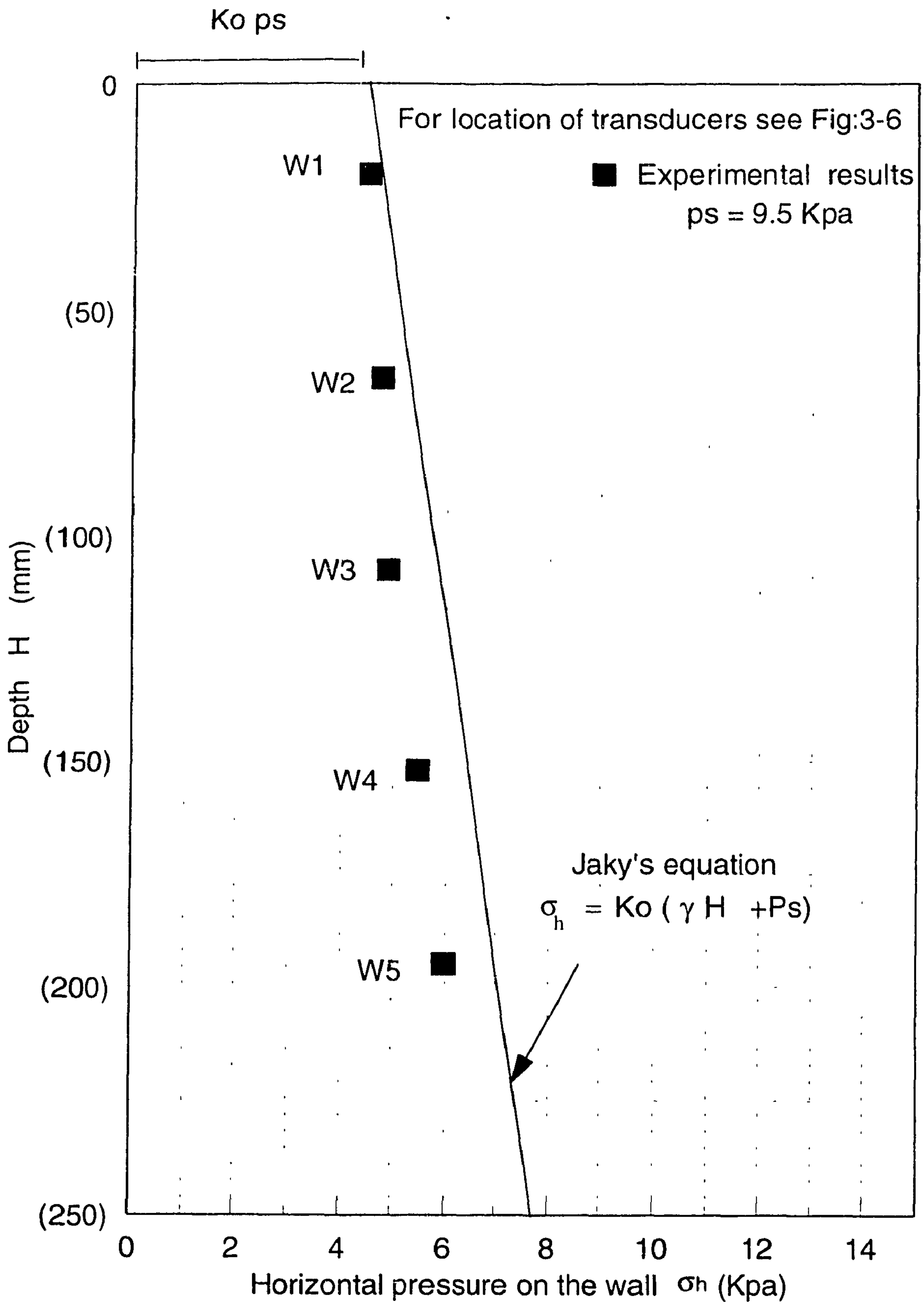

Figure 4-13 Horizontal pressure on the wall versus depth during loading ps=9.5 Kpa.

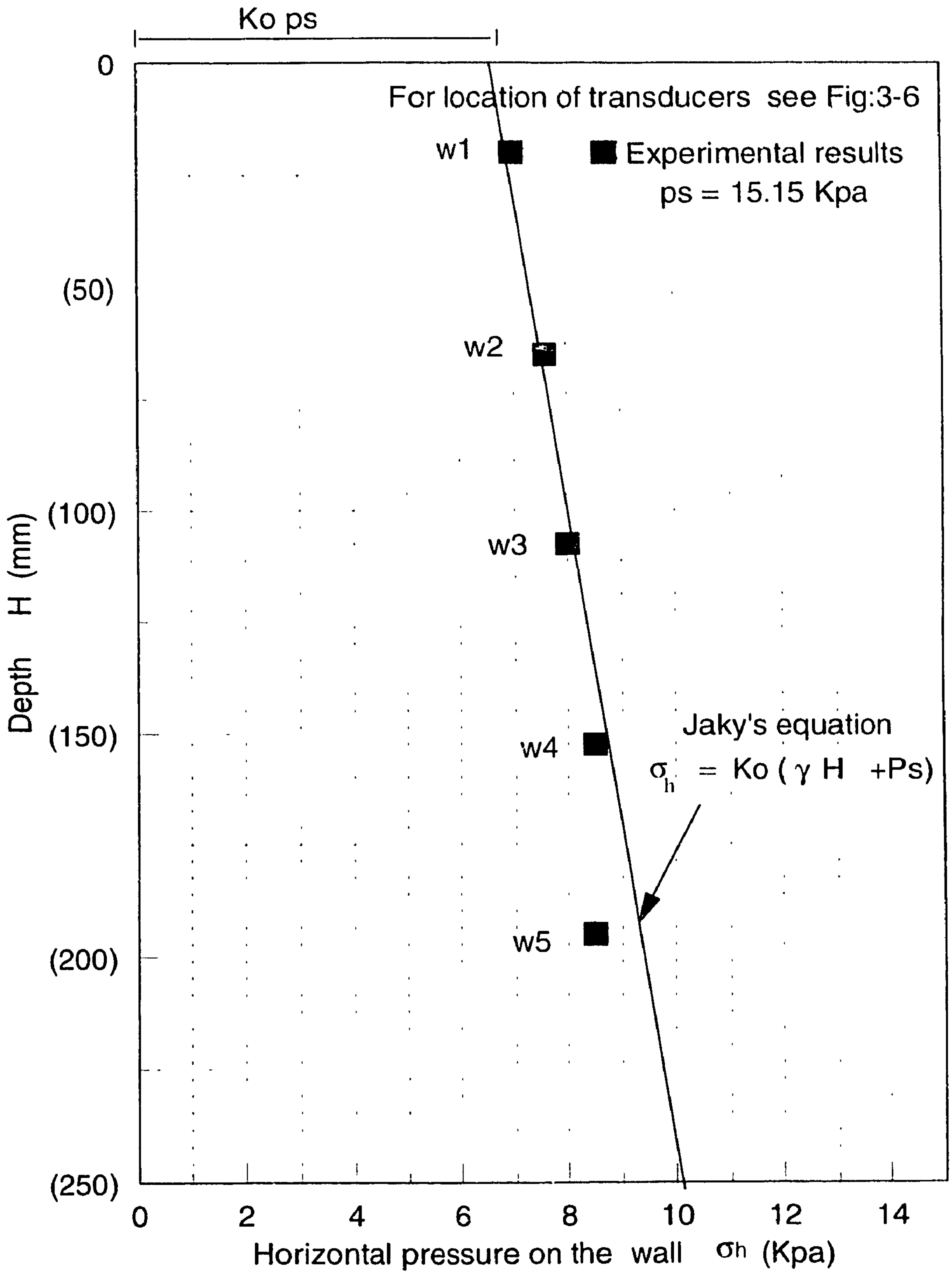

Figure 4-14 Horizontal pressure on the wall versus depth during loading ps=15.15 Kpa.

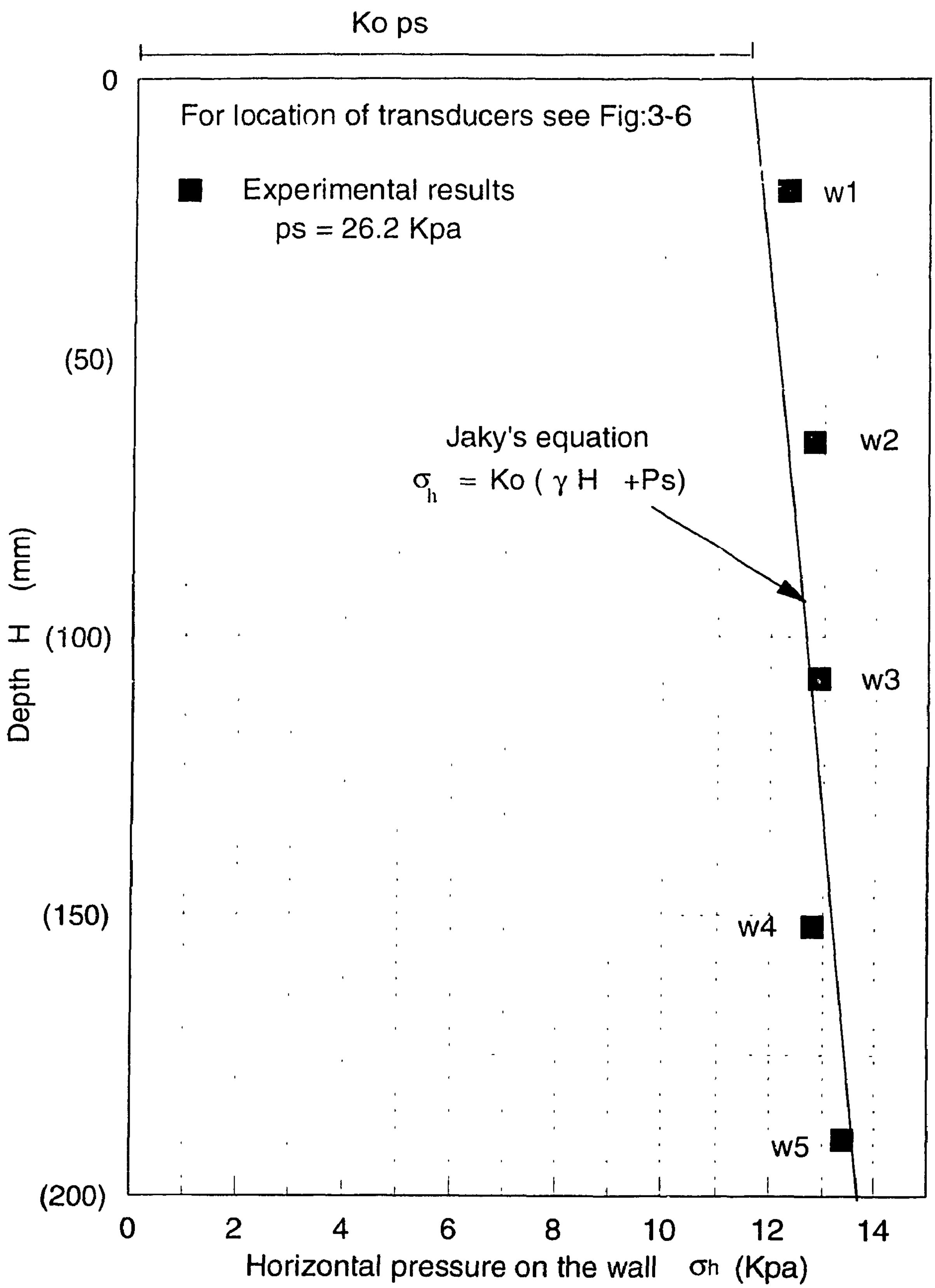

Figure 4-15 Horizontal pressure on the wall versus depth during loading ps=26.2 Kpa.

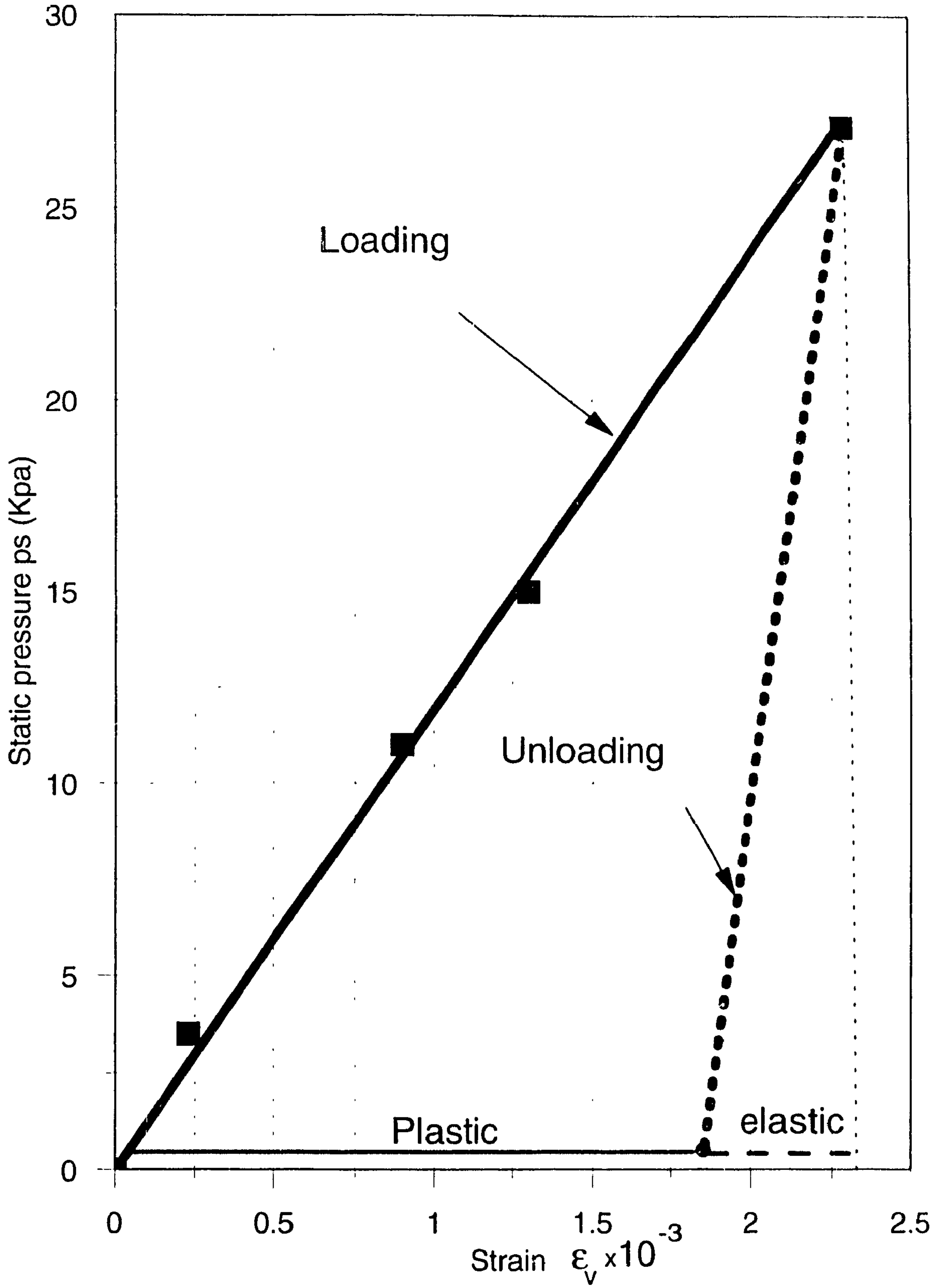

Figure 4-16 Stress strain Relationship

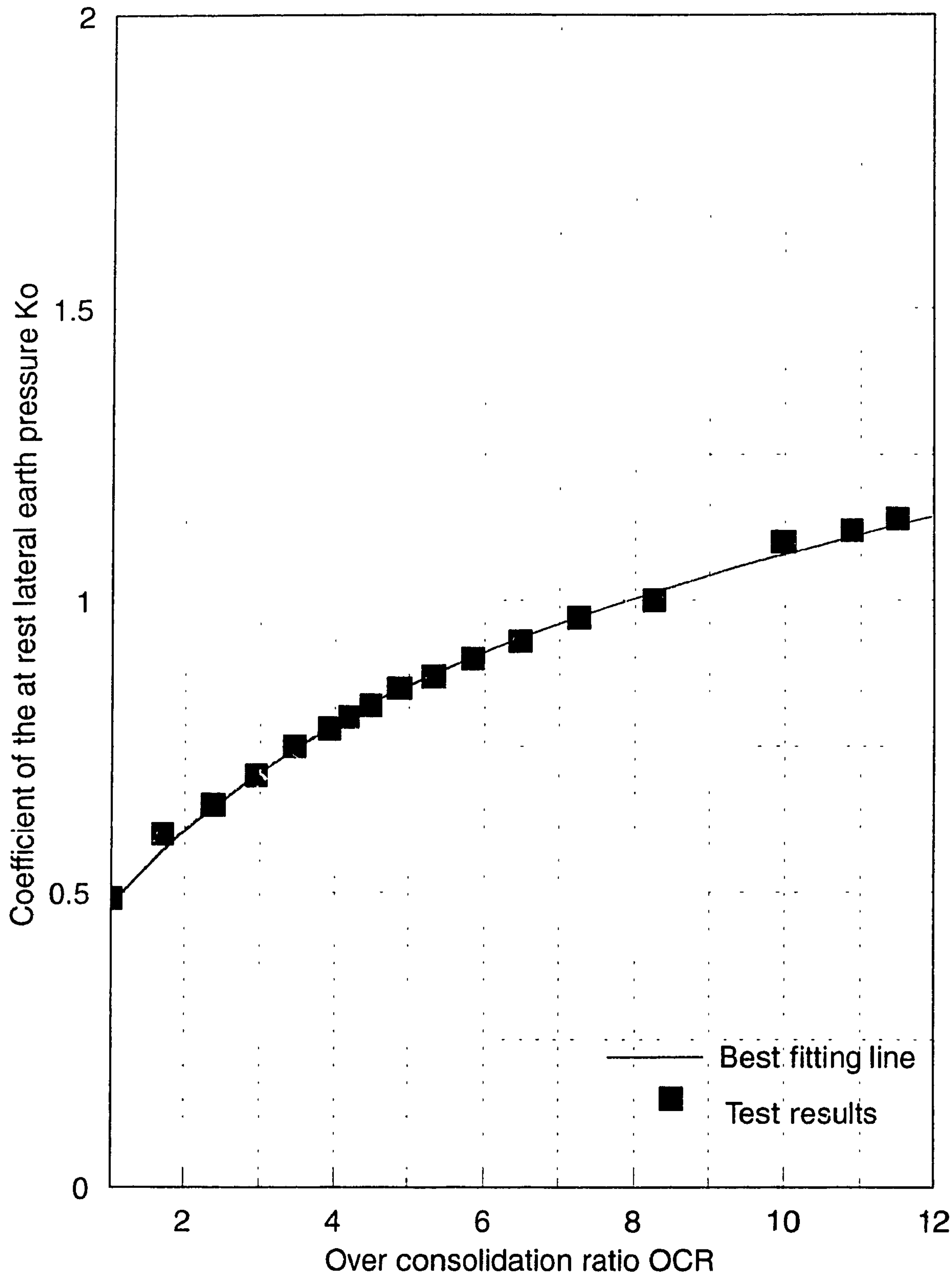

Figure 4-17 Coefficient of the at rest lateral earth pressure Ko versus OCR for over consolidated sand by surfaced loads $\phi = 31$ Degrees

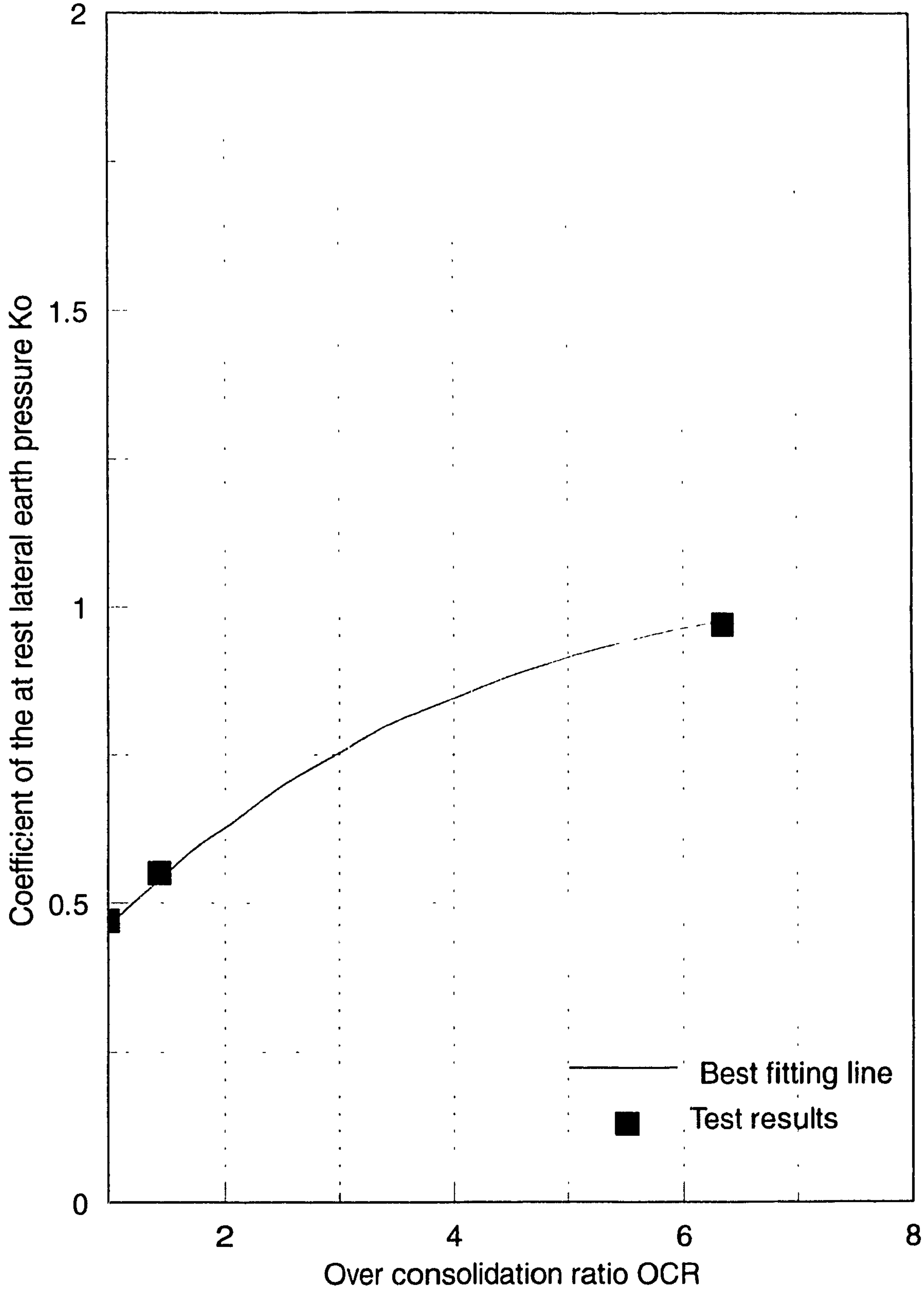

Figure 4-18 Coefficient of the at rest lateral earth pressure Ko versus OCR for overconsolidated sand by surfaced loads ϕ = 32 Degrees

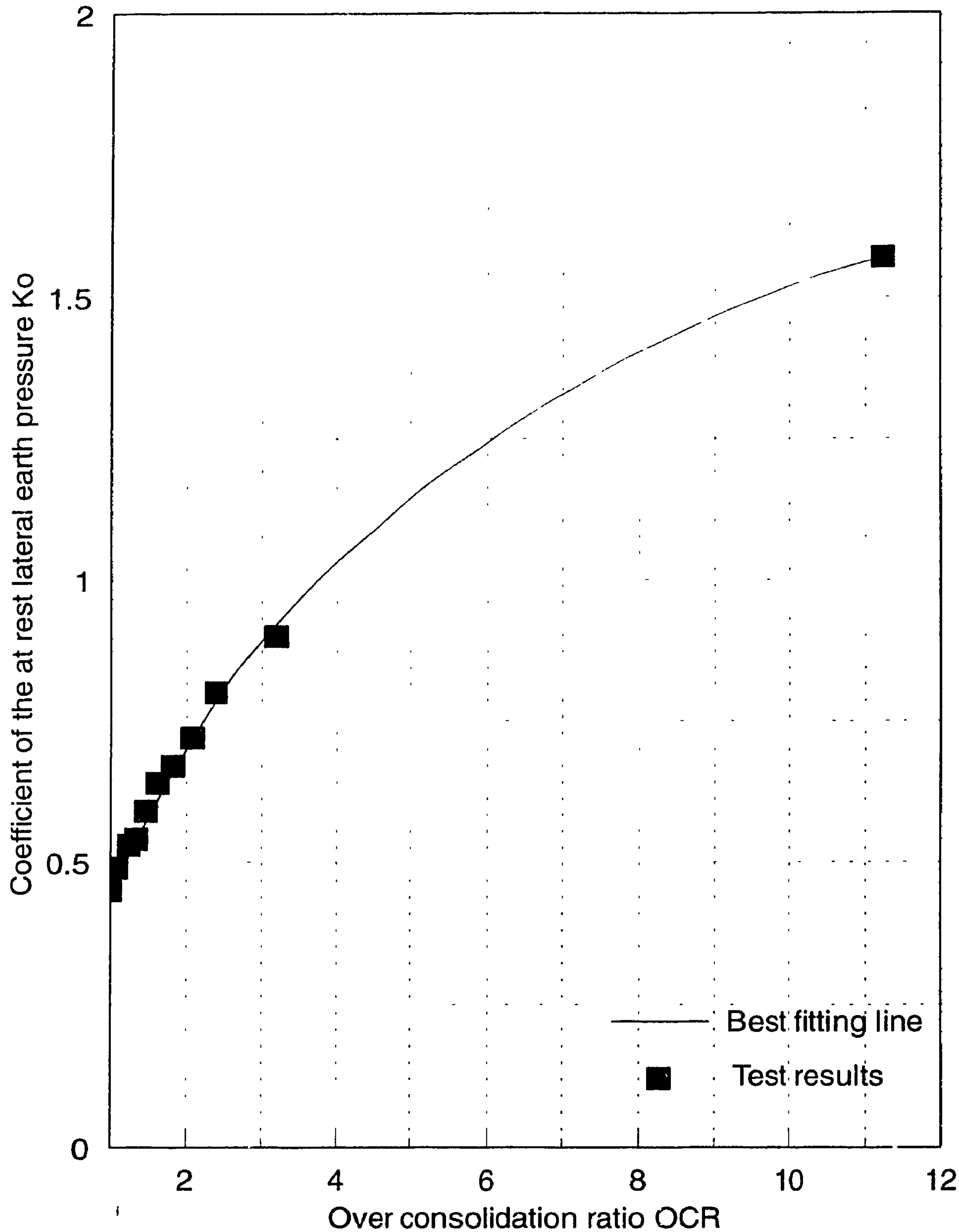

Figure 4-19 Coefficient of the at rest lateral earth pressure Ko versus OCR for over consolidated sand by surfaced loads $\phi = 33$ Degrees

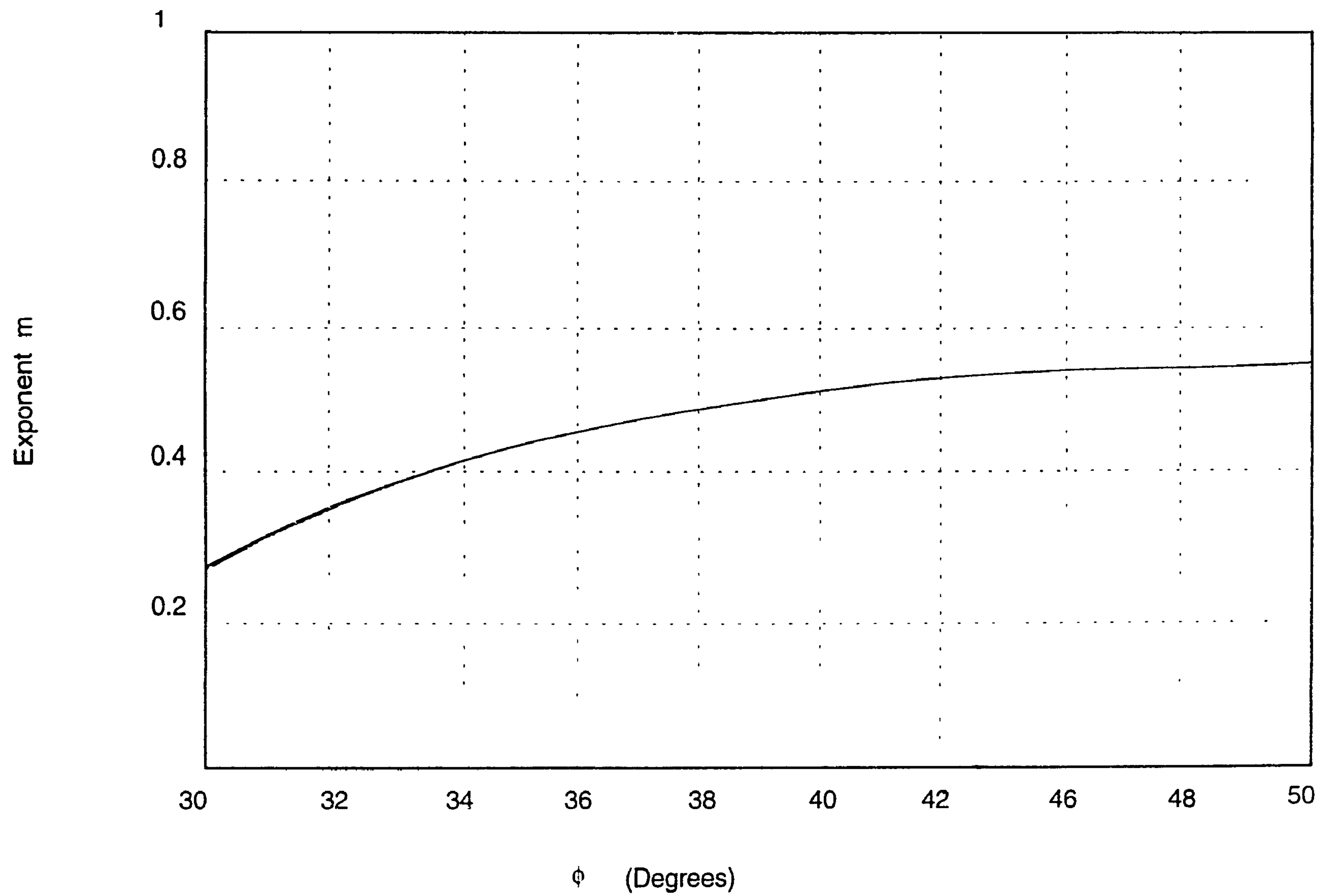

Figure 4-20 Proposed method exponent m Versus ϕ

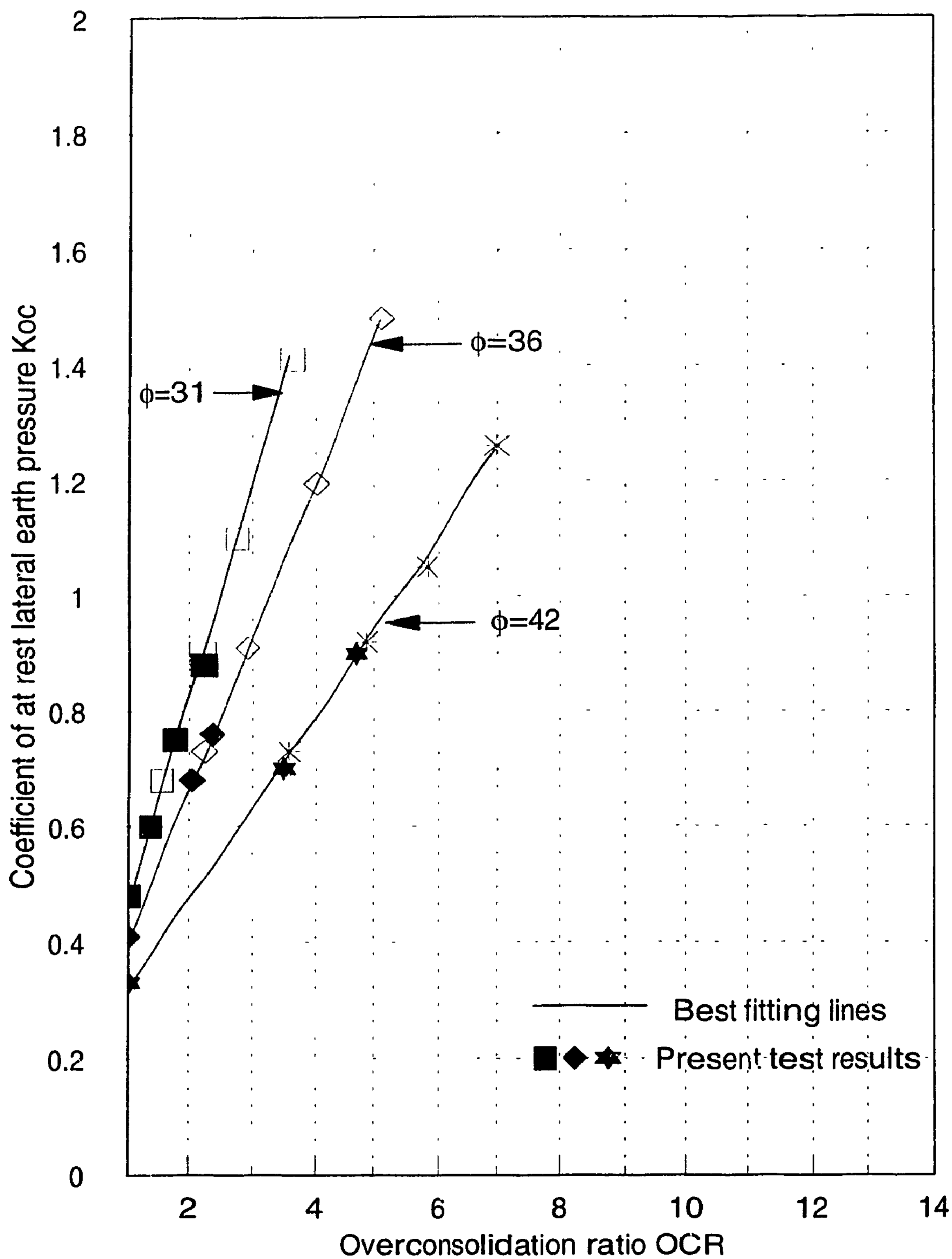

Figure 4-21 Ko versus OCR for the overconsolidated sands by means of compaction.

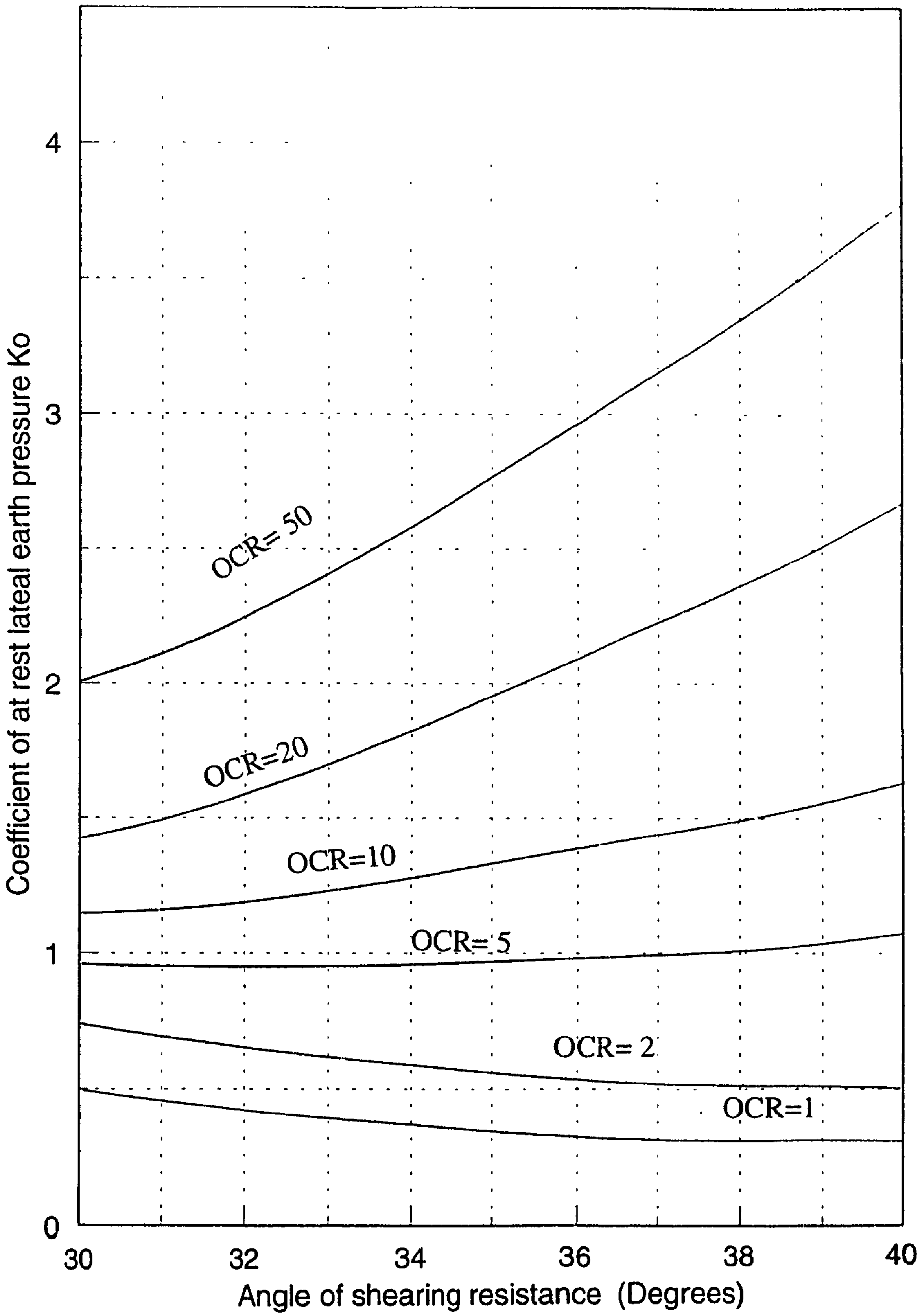

Figure 4-22 Design chart for overconsolidated sand by surfaced loads

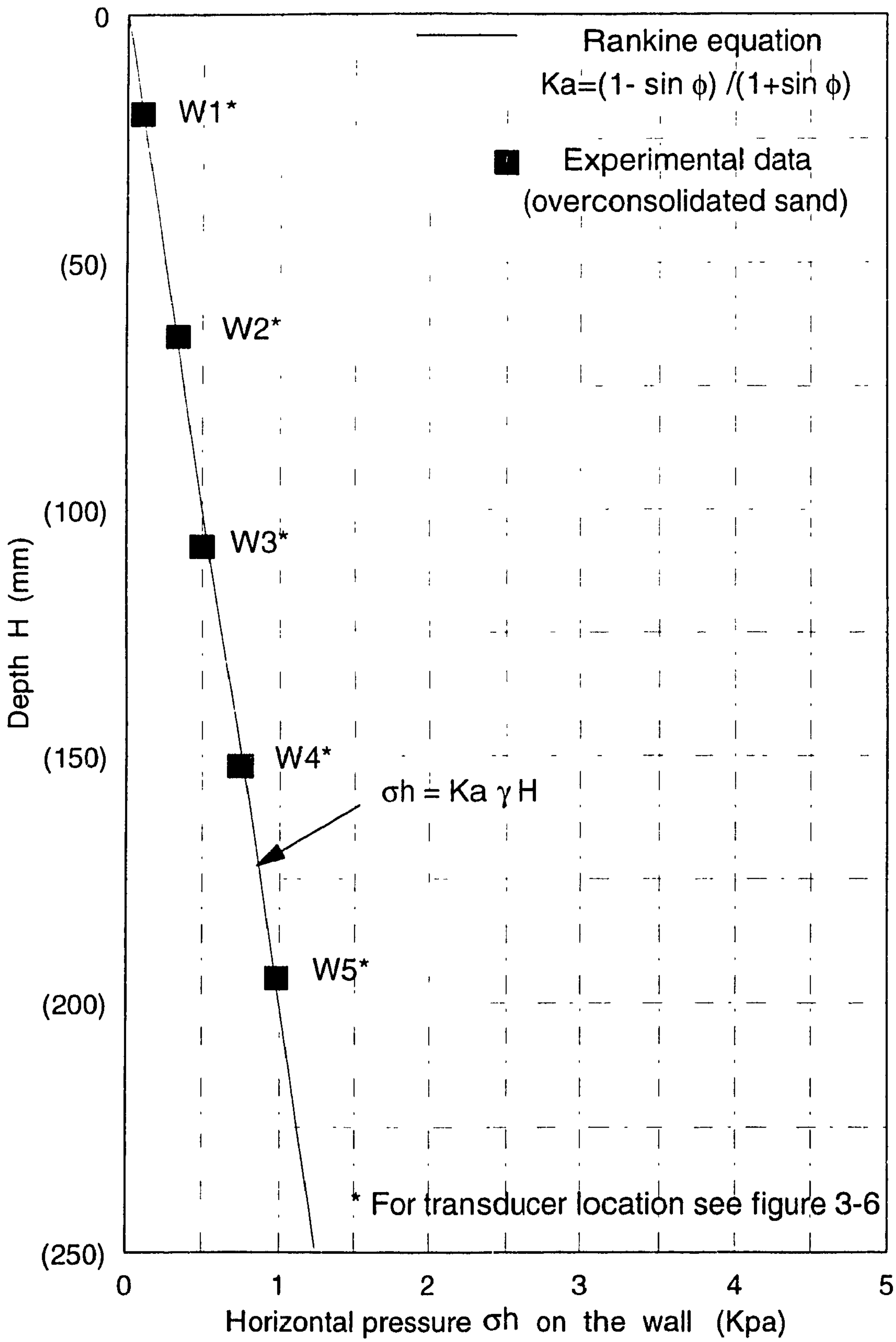

Figure 4-23 Horizontal pressure on the wall for over consolidated sand versus depth (active case).

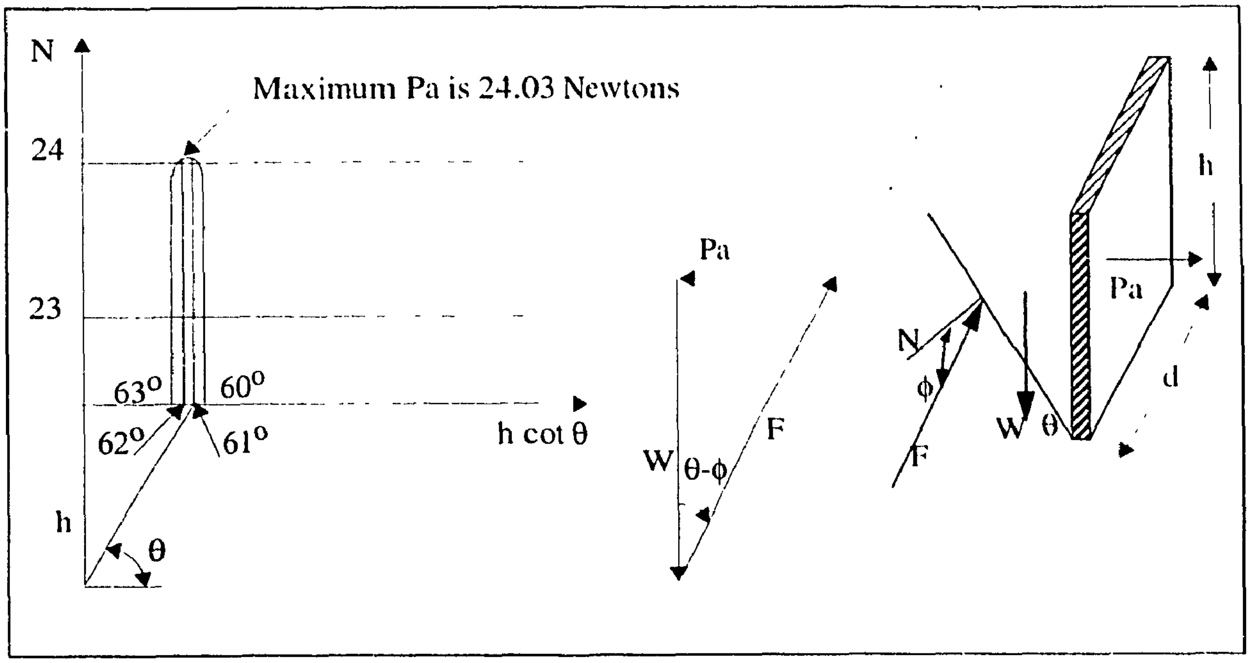

Figure (4-24) Trial wedges method

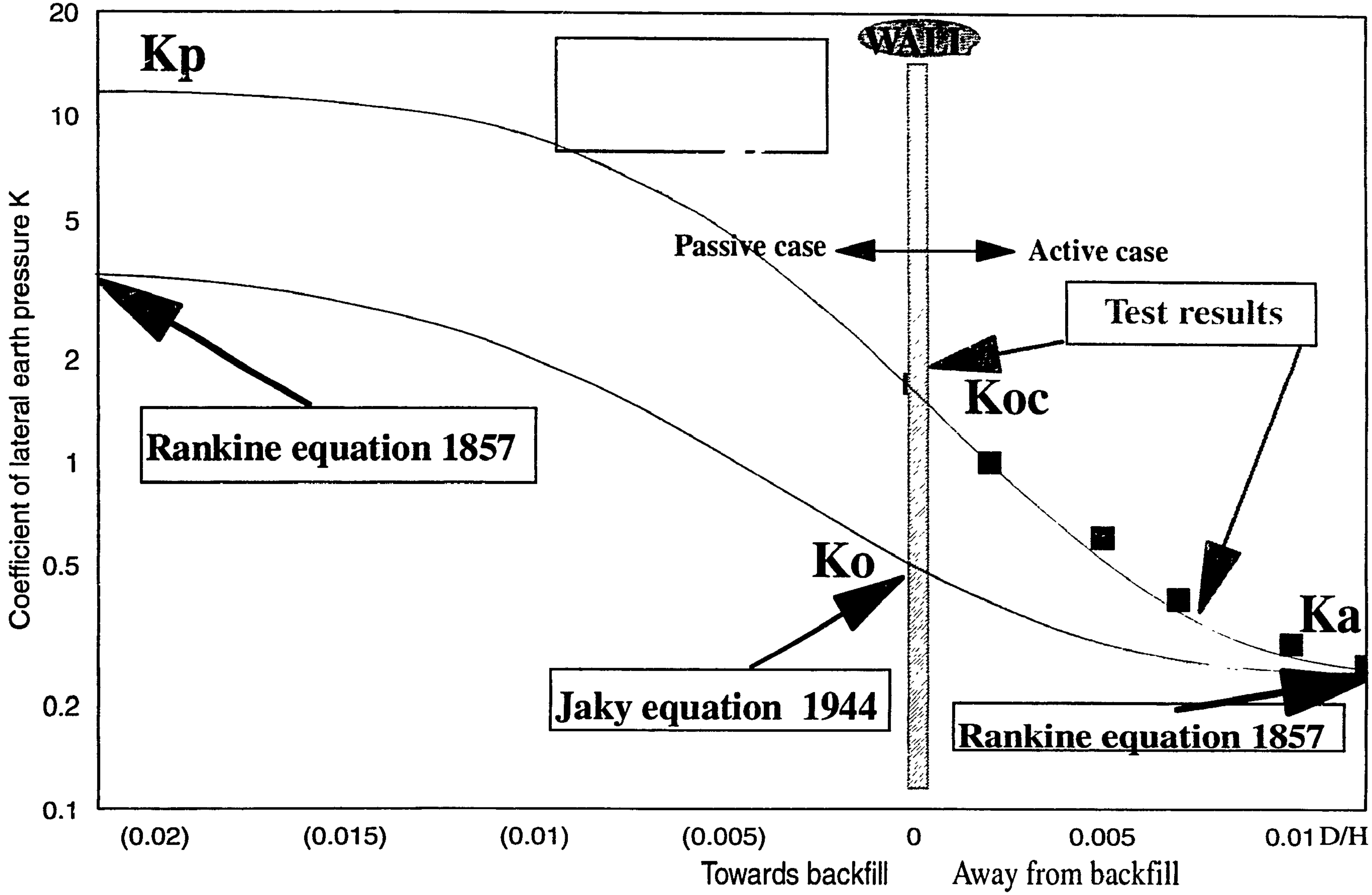

Figure 4-25 Variation of lateral earth pressures due to overconsolidation and wall movements

CHAPTER 5

CONCLUSION

Based on the results of the present experimental investigation on at rest and active earth pressures of overconsolidated sand, the following can be concluded:

1-The coefficient of lateral earth pressure (at rest condition) depends on the angle of shearing resistance ,ϕ, and the overconsolidation ratio, OCR.

2-The coefficient of lateral earth pressure for the active case Ka, is independent of the overconsolidation ratio OCR. This is based on the fact that due to the displacement of the wall, the particles interlocking which was produced during the overconsolidation processes is destroyed and accordingly the OCR is reduced to a value of one. At which, the overconsolidated sand behaves similar to that of normally consolidated sand under the active condition.

3-A semi-empirical formula was developed to predict the lateral earth pressure coefficient (at the rest condition), Ko, as a function of the overconsolidation ratio, OCR and the angle of shearing resistance, ϕ.

4- A design chart was developed to provide directly the Ko value for given values of the angle of shearing resistance, ϕ, and the overconsolidation ratio, OCR.

RECOMMENDATION FOR FUTURE RESEARCH.

Based on the results of the present experimental investigation on the at rest and active earth pressures of overconsolidated sand, the following can be recommended for future investigation:

1- Conduct field test on full-scale retaining wall.

2- Develop numerical models such as a finite element model to study the stresses in the soil mass as well as on the wall.

3- Conduct tests on different types of sands, and on partially or fully saturated sands.

4- Extend the study to include cohesive soil.

REFERENCES

1. Al-Khoury I.(1994),"Passive earth pressure of overconsolidated homogeneous and layered cohesionless material." M.A.Sc. Thesis, University of Concordia Montreal.

2. Alpan.I.(1967)," The empirical evaluation of coefficient Ko and Kor. "Journal of Soil mechanics and Foundations. Tokyo, Japan Vol.7, No.1, pp:31-40.

3. Andrawes.K.&El-sohby.M.(1973)," Factors affecting coefficient of earth pressure Ko.", Journal of Soil Mechanics and Foundations, ASCE. Vol.99, No.7, pp:527-539.

4. Bishop,A.W.(1958)," Test requirements for measuring Ko." Proceedings, Brussels conference on Earth Pressure Problems, Brussels, Belgium Vol.1, pp:2-14.

5. Bishop & Henkel, (1957), "The measurement of soil properties in the triaxial test "Publisher Edward Arnold.

6. Bjerrum.L,Kringstad.S and Kummeneje.O.(1961)," The Shear Strength of a Fine Sand." Proceedings, 5th international conference of soil mechanics and foundations engineering. Vol. 1 Paris, France. pp:23-28.

7. Clough.G. & Duncan.J, (1971), "Finite element analysis of retaining wall behavior. "Journal Of Geotechnical Engineering, ASCE. Vol 97, pp: 1657-1673.

8. Coulomb,C.A.(1776)," Essai sur une application des Regles des Maximis et minimis a quelque problemes de Statique." Memoire Academic Royale des sciences, No.7, Paris.

9. Daramola.O.(1980)," On Estimating Ko for Overconsolidated Soils." Geotechnique, Vol.30, No.2, pp:310-313.

10. Darwin.G.M.(1883)," On The Horizontal Thrust of a Mass of Sand." Proceedings of the Institution of Civil Engineers,Vol.71, pp:351-378.

11. Donath.A.(1891)," Untersulchengen Uber den Eidruck auf Stutzwande." Zeitschrift fur Bawesen, 41 pp: 491-518.

12. Feda.(1984)." Ko Coefficient of sand in Triaxial Apparatus." Journal of Geotechnical Engineering, ASCE, Vol. 110 No.4, pp:519-524.

13. Handy.R.L.(1983)," Discussion of Ko-OCR Relationship in Soil." Journal of Geotechnical Engineering, ASCE. Vol.109, No.6, pp:862-863.

14. Hendron.A.J.(1963)." The behavior of sand in one-dimensional compression." Ph.D. Thesis, University of Illinois at Urbana Campaign, Urbana.Ill.

15. Jaky.J.(1944),"A Myygalmi nyomas tenyezoje (The coefficient of earth pressure at Rest.)" Magyar Mermok es Epitesz-Egylet Kozlonye, pp:355-358.

16. Janbu.J.(1957)," Earth Pressures and Bearing Capacity Calculations by Generalized Procedure of Slices." Proceedings of the Fourth International Conference on Soil Mechanics and Foundation Engineering. London Vol II. pp:207-212.

17. Kjellman,Walter.(1936)," Report on an Apparatus for Consummate Investigation of The Mechanical Properties of Soils." Proceedings of the 1st Int.Conf. on Soil Mechanics and Foundationn.Eng.June 1936, Cambridge Mass, Vol.2, pp:16-20.

18. Mayne & Kulhawy (1982)," Ko-OCR Relationships in Soils." Journal of the Geotechnical Engineering, ASCE. Vol.108, No.6, pp:851-872.

19. Mesry.G.&Hayat.T.M (1993)," The coefficient of earth pressure at rest." Canadian Geotechnical Journal.Vol30, pp:647-666.

20. Meyerhof.G.G.(1976)," Bearing Capacity and Settlement of Pile Foundation." Journal of Soil Mechanic And foundations ASCE Vol.102. No 3, pp:195-228

21. Rahardjo.H & Al (1984), "General limit equilibrium method for lateral earth force." Canadian Geotechnical Journal.Vol 21, pp:166-175-.

22. Rankine.W.J.M.(1857)."On the Stability of Loose Earth. "Trans Royal Soc London, Vol.147.

23. Rowe.P.W.(1963)," Stress-Dilatancy, Earth Pressures, and Slopes." Journal of Soil Mechanics and Foundations, ASCE.Vol. 89, No.3, pp:37-61.

24. Saglamer.A.(1975), "Soil parameters affecting coefficient of earth pressure at rest of cohesionless soils."Proceedings, Istanbul Conference on Soil mechanics and Foundations Engineering Ankara, Turkey Vol.1 pp:9-16.

25. Schmidt. Birger (1966), "Earth Pressures At rest Related To Stress History." Canadian Geotechnical Journal.Vol.3, No.4, pp:239 -245.

26. Sherif.M.&Fang.Y&Sherif.R.(1984), "Ka and Ko Behind rotating and non-yielding wall. "Journal of Geotechnical Engineering ASCE. Vol.110, No.1, pp:41-56

27. Terzaghi.K. (1920)." Old Earth - Pressure Theories and New Test Results." Engineering News Record, 85 No.14, pp:632-637.

28. Ting.C.M.R. & AL (1994) "Development of Ko in Soft Soils." Geotechnique, Vol.44, No.1, pp:101-109.

APPENDIX I

Experimental Results of Test No1

for the transducers' measurements in the sand mass

Table (A-1): Vertical pressure measured by transducers in the soil mass at the at rest condition (Test No.1).

Ps Static pressure (Kpa)	Time (hour)	Vertical pressure measured by transducers in the sand (Kpa)								
		B1*	B2*	B3*	B4*	B5*	B6*	B7*	B8*	B9*
		V	V	V	V	V	V	V	V	V
0	0	2.15	2.46	2.85	3.85	3.91	3.7	5.35	5.02	4.95
	4	2.15	2.48	2.87	3.87	3.91	3.72	5.35	5.02	4.95
	8	2.25	2.5	2.9	3.92	3.95	3.75	5.38	5.12	4.98
	24	2.3	2.53	2.95	3.95	3.96	3.81	5.42	5.2	5.00
	28	2.33	2.55	2.97	3.98	3.97	3.87	5.44	5.25	5.05
	32	2.35	2.58	3.00	4.1	4.0	3.9	5.45	5.35	5.1
	48	2.40	2.50	2.55	4.4	4.3	4.2	5.45	5.35	5.55

Table (A-2): Horizontal pressure measured by transducers in the soil mass at the At rest condition (Test No.1).

Ps Static pressure (Kpa)	Time (hour)	Horizontal pressure measured by transducers in the sand (Kpa)					
		B4*	B5*	B6*	B7*	B8*	B9*
		H	H	H	H	H	H
0	0	1.85	1.95	1.82	1.92	2.05	1.96
	4	1.90	1.98	1.85	1.95	2.10	1.99
	8	1.92	2.05	1.93	1.95	2.12	2.02
	24	1.99	2.20	2.01	2.05	2.25	2.10
	28	2.05	2.22	2.04	2.07	2.28	2.13
	32	2.10	2.25	2.05	2.10	2.30	2.15
	48	2.10	2.09	2.05	2.40	2.55	2.45

* For location of the transducers see figure (3-4)

Table (A-3): Pressures measured by transducers in the sand during displacement of the wall during the Active Case (TestNo.1).

Displacement (mm)	0.0	0.5	1.0	1.5	2.1	2.51	2.9	8.4
Pressure measured by transducers in the sand (Kpa)								
V1*	2.40	2.40	2.40	2.40	2.40	2.40	2.40	2.40
V2*	2.50	2.40	2.38	2.37	2.36	2.35	2.35	2.35
V3*	2.55	2.35	2.30	2.27	2.26	2.25	2.25	2.25
V4*	4.40	4.40	4.40	4.40	4.40	4.40	4.40	4.40
V5*	4.3	4.18	4.17	4.16	4.15	4.12	4.10	4.10
V6*	4.2	4.07	3.99	3.95	3.89	3.85	3.85	3.85
V7*	5.45	5.45	5.45	5.45	5.45	5.45	5.45	5.45
V8*	5.35	5.27	5.26	5.25	5.25	5.25	5.25	5.25
V9*	5.55	5.41	5.39	5.37	5.36	5.35	5.35	5.35
H4*	2.10	2.10	2.10	2.10	2.10	2.10	2.10	2.10
H5*	2.09	1.95	1.92	1.90	1.89	1.89	1.89	1.89
H6*	2.05	1.89	1.84	1.81	1.79	1.77	1.75	1.75
H7*	2.40	2.40	2.40	2.40	2.40	2.40	2.40	2.40
H8*	2.55	2.45	2.38	2.37	2.36	2.36	2.35	2.35
H9*	2.45	2.32	2.30	2.27	2.26	2.25	2.25	2.25

* For location of the transducers see figure (3-4)

Experimental Results of Test No.2

for the transducers' measurements in the sand mass

Table (A-4): Vertical pressure measured by transducers in the sand during loading of the static pressure on the sand mass (Test No.2).

Ps Static pressure (Kpa)	Time (hour)	Pressure measured by transducers in the sand (Kpa)								
		B1*	B2*	B3*	B4*	B5*	B6*	B7*	B8*	B9*
		V	V	V	V	V	V	V	V	V
0	0	2.28	2.37	2.41	4.01	3.8	3.71	5.25	5.00	4.81
	4	2.28	2.45	2.47	4.01	3.8	3.75	5.3	5.05	4.85
	8	2.28	2.45	2.47	4.03	3.9	3.77	5.35	5.09	4.90
	24	2.31	2.59	2.50	4.08	3.95	3.91	5.45	5.20	4.95
	28	2.32	2.54	2.53	4.09	3.97	3.93	5.47	5.25	4.99
	32	2.33	2.56	2.50	4.1	4.01	3.95	5.50	5.30	5.00
	48	2.33	2.56	2.50	4.1	4.00	3.95	5.50	5.30	5.00
6.3	0	7.85	7.95	8.4	6.7	6.90	6.90	8.40	8.61	8.55
	4	7.85	7.90	8.3	6.7	6.90	6.80	8.30	8.61	8.45
	8	7.80	7.90	8.3	6.6	6.90	6.80	8.25	8.52	8.35
	24	7.60	7.75	8.0	6.0	6.30	6.20	7.90	8.057	7.92
	28	7.57	7.73	7.95	5.95	6.20	6.10	7.80	7.85	7.83
	32	7.55	7.70	7.90	5.90	6.10	6.00	7.73	7.92	7.81
	48	7.55	7.70	7.90	5.90	6.1	6.00	7.70	7.90	7.80
13.7	0	12.61	12.95	11.85	10.00	10.10	10.10	10.30	10.40	10.50
	4	12.45	12.92	11.65	9.95	10.05	10.05	10.15	10.35	10.40
	8	12.25	12.90	11.61	9.92	9.95	9.95	10.05	10.05	10.35
	24	11.82	11.85	11.45	9.70	9.30	9.20	9.50	9.60	9.80
	28	11.74	11.65	11.39	9.60	9.20	9.05	9.40	9.35	9.65
	32	11.55	11.45	10.37	9.40	9.00	8.90	9.20	9.30	9.50
	48	11.5	11.45	10.35	9.40	9.00	8.90	9.20	9.30	9.50

* For location of the transducers see figure (3-4)

Table (A-5): Horizontal pressure measured by transducers in the sand during loading of the static pressure on the sand mass.(Test No.2).

Ps Static pressure (Kpa)	Time (hour)	Pressure measured by transducers in the sand (Kpa)					
		B4*	B5*	B6*	B7*	B8*	B9*
		H	H	H	H	H	H
0	0	2.11	2.0	2.15	2.90	2.83	2.90
	4	2.11	2.05	2.17	2.90	2.83	2.90
	8	2.12	2.07	2.19	2.95	2.85	2.90
	24	2.18	2.21	2.28	3.05	2.96	2.94
	28	2.19	2.24	2.29	3 07	2.98	2.94
	32	2.20	2.25	2.30	3.10	3.00	2.95
	48	2.20	2.25	2.30	3.10	3.00	2.95
6.3	0	2.92	3.15	3.28	4.62	4.73	5.15
	4	2.92	3.12	3.17	4.62	4.71	5.10
	8	2.85	3.10	3.13	4.57	4.71	5.02
	24	2.60	2.78	2.95	4.22	4.34	4.89
	28	2.57	2.73	2.93	4.16	4.27	4.86
	32	2.55	2.70	2.90	4.10	4.20	4.85
	48	2.55	2.70	2.9	4.10	4.20	4.85
13.7	0	5.11	4.86	4.92	7.75	7.93	7.99
	4	5.02	4.85	4.90	7.75	7.90	7.98
	8	4.95	4.80	4.88	7.71	7.88	7.90
	24	4.58	4.55	4.57	7.45	7.65	7.80
	28	4.55	4.48	4.38	7.42	7.55	7.78
	32	4.50	4.46	4.36	7.40	7.50	7.75
	48	4.50	4.46	4.36	7.40	7.50	7.75

* For location of the transducers see figure (3-4)

Table (A-6): Summary of the test results in the sand mass during loading and unloading test (No. 2).

Ps Static pressure (Kpa)	Time (day)	Vertical pressure measured by transducers in the sand (Kpa)								
		B1*	B2*	B3*	B4*	B5*	B6*	B7*	B8*	B9*
		V	V	V	V	V	V	V	V	V
0.0	2	2.33	2.56	2.5	4.1	4.0	3.95	5.5	5.3	5.0
6.3	4	7.55	7.7	7.9	5.9	6.1	6.0	7.7	7.9	7.8
13.7	6	11.5	11.45	10.35	9.4	9.0	8.9	9.2	9.3	9.5
6.3	8	8.3	8.25	8.1	7.4	7.23	7.6	8.6	8.7	8.9
0	10	3.98	3.75	3.6	5.55	5.45	5.4	7.2	7.15	7.1

Ps static pressure (Kpa)	Time (day)	Horizontal pressure measured by transducers in the sand (Kpa)					
		B4*	B5*	B6*	B7*	B8*	B9*
		H	H	H	H	H	H
0	2	2.2	2.25	2.3	3.1	3.0	2.95
6.3	4	2.55	2.7	2.9	4.1	4.2	4.85
13.7	6	4.5	4.45	4.35	7.4	7.5	7.75
6.3	8	4.3	4.25	4.1	5.4	5.3	5.84
0	10	3.16	3.14	3.13	3.82	3.85	3.88

* For location of the transducers see figure (3-4)

Table (A-7): Pressure measured by transducers during the displacement of the wall (Test No.2).

Displacement (mm)	0.0	0.5	1.0	1.5	2.1	2.51	2.9	8.4
Pressure measured by transducers in the sand (Kpa)								
V1*	3.98	3.98	3.98	3.98	3.98	3.98	3.98	3.98
V2*	3.75	3.18	3.10	2.96	2.93	2.89	2.86	2.86
V3*	3.6	3.69	3.69	3.6	3.5	3.5	3.5	3.5
V4*	5.55	5.42	5.39	5.39	5.39	5.39	5.39	5.39
V5*	5.45	5.36	5.30	5.25	5.20	5.19	5.15	5.15
V6*	5.4	5.3	5.25	5.20	5.15	5.10	5.0	4.9
V7*	7.2	6.95	6.85	6.84	6.84	6.84	6.84	6.84
V8*	7.15	7.15	7.10	7.10	7.10	7.10	7.10	7.10
V9*	7.1	6.95	6.90	6.85	6.85	6.85	6.85	6.85
H4*	3.16	2.85	2.85	2.85	2.85	2.85	2.85	2.85
H5*	3.14	2.52	2.46	2.46	2.46	2.46	2.46	2.44
H6*	3.13	2.70	2.67	2.67	2.67	2.67	2.67	2.67
H7*	3.82	3.63	3.53	3.51	3.51	3.51	3.51	3.51
H8*	3.85	3.60	3.05	3.05	3.05	3.05	3.05	3.05
H9*	3.88	3.6	3.06	3.06	3.06	3.06	3.06	3.06

* For location of the transducers see figure (3-4)

Experimental Results of Test No.3

for the transducers' measurements in the sand mass

Table (A-8): Vertical pressure measured by transducers in the sand during loading of the static pressure on the sand mass (Test No.3).

Ps Static pressure Kpa	Time hours	Pressure measured by transducers in the sand (Kpa)								
		B1*	B2*	B3*	B4*	B5*	B6*	B7*	B8*	B9*
		V	V	V	V	V	V	V	V	V
	0	2.22	2.44	2.95	3.9	3.8	3.6	5.3	5.1	4.9
	4	2.22	2.45	2.97	3.9	3.8	3.6	5.35	5.15	4.9
	8	2.25	2.5	3.01	4.0	3.9	3.7	5.4	5.2	4.92
0	24	2.3	2.53	3.04	4.2	4.0	3.8	5.45	5.25	4.98
	28	2.31	2.54	3.05	4.2	4.0	3.8	5.48	5.28	4.99
	32	2.33	2.56	3.06	4.2	4.0	3.8	5.5	5.3	5.0
	48	2.33	2.56	3.06	4.2	4.0	3.8	5.5	5.3	5.0
	0	7.1	7.2	8.2	7.5	7.9	8.2	8.5	8.2	8.4
	4	7.1	7.2	8.2	7.4	7.8	8.1	8.5	8.1	8.3
	8	7.1	7.2	8.2	7.3	7.8	8.0	8.4	8.05	8.25
5.4	24	6.9	7.0	8.0	7.0	7.3	7.5	8.0	7.7	7.9
	28	6.9	7.0	8.0	6.95	7.3	7.4	7.9	7.65	7.85
	32	6.9	7.0	8.0	6.9	7.2	7.3	7.8	7.6	7.8
	48	6.9	7.0	8.0	6.9	7.2	7.3	7.8	7.6	7.8
	0	11.83	10.38	12.4	11.6	12.7	12.9	9.7	9.2	9.5
	4	11.6	10.1	12.03	11.55	12.6	12.8	9.65	9.17	9.4
	8	11.4	10	12.25	11.5	12.5	12.7	9.61	9.1	9.35
11.3	24	11.0	9.3	11.8	11.2	12.0	12.0	9.05	8.8	9.0
	28	10.8	9.0	11.8	11.1	11.8	12.0	9.0	8.7	8.9
	32	10.7	8.9	11.7	11.0	11.7	11.9	8.9	8.6	8.8
	48	10.7	8.9	11.7	11.0	11.7	11.9	8.9	8.6	8.8

* For location of the transducers see figure (3-4)

Table (A-8) continued: Vertical pressure measured by transducers in the sand during loading of the static pressure on the sand mass (Test No.3).

Ps Static pressure Kpa	Time hours	Pressure measured by transducers in the sand (Kpa)								
		B1*	B2*	B3*	B4*	B5*	B6*	B7*	B8*	B9*
		V	V	V	V	V	V	V	V	V
16.9	0	15.3	12.6	16.2	15.1	17.7	17.7	12.2	12.6	12.5
	4	15.2	12.5	16.2	15.1	17.4	17.6	12.1	12.5	12.4
	8	15.1	12.45	16.1	15.05	17.3	17.5	12.0	12.4	12.3
	24	14.9	12.4	15.8	15.05	16.8	16.9	11.7	12.0	11.9
	28	14.9	12.4	15.8	15.0	16.4	16.7	11.68	11.95	11.85
	32	14.8	12.3	15.8	15.0	16.3	16.5	11.6	11.9	11.8
	48	14.8	12.3	15.8	15.0	16.3	16.5	11.6	11.9	11.8
20.5	0	17.7	15.95	17.6	18.2	20.7	20.3	14.9	14.5	14.5
	4	17.6	15.9	17.5	18.1	20.6	20.2	14.9	14.45	14.4
	8	17.55	15.8	17.5	18.0	20.5	20.1	14.8	14.4	14.3
	24	17.3	15.5	17.5	17.6	19.5	19.5	14.3	14.2	14.23
	28	17.25	15.4	17.5	17.55	19.3	19.4	14.25	14.15	14.11
	32	17.2	15.3	17.5	17.5	19.1	19.3	14.2	14.1	14.0
	48	17.2	15.3	17.5	17.5	19.1	19.3	14.2	14.1	14.0
26.2	0	22.35	19.55	21.3	22.8	24.7	25.2	20.6	20.3	20.2
	4	22.2	19.4	21.2	22.7	24.5	25.0	20.4	20.2	20.15
	8	22.1	19.3	21.1	22.6	24.2	24.9	20.3	20.1	20.02
	24	21.4	18.95	20.6	21.4	23.3	24.1	19.3	19.3	19.1
	28	21.3	18.8	20.55	21.3	23.2	24.0	19.2	19.25	18.95
	32	21.0	18.7	20.5	21.1	23.1	23.9	19.0	19.2	18.9
	48	21.0	18.7	20.5	21.1	23.1	23.9	19.0	19.2	18.9

* For location of the transducers see figure (3-4)

Table (A-9): Vertical pressure measured by transducers during unloading of the static pressure on the sand mass (Test No.3)

Ps Static pressure Kpa	Time hours	Pressure measured by transducers in the sand (Kpa)								
		B1*	B2*	B3*	B4*	B5*	B6*	B7*	B8*	B9*
		V	V	V	V	V	V	V	V	V
20.5	0	20.3	17.8	18.4	20.7	22.9	23.42	18.8	19.0	18.7
	4	20.3	17.8	18.4	20.7	22.8	23.4	18.8	19.0	18.7
	8	20.3	17.85	18.4	20.7	22.8	23.3	18.7	18.9	18.7
	24	20.4	17.9	18.5	20.7	22.6	23.1	18.5	18.8	18.7
	28	20.4	17.92	18.5	20.7	22.55	23.05	18.45	18.7	18.7
	32	20.4	17.92	18.5	20.7	22.5	23.0	18.4	18.6	18.7
	48	20.4	17.92	18.5	20.7	22.5	23.0	18.4	18.6	18.7
16.9	0	19.6	17.0	17.2	19.7	22.1	22.3	18.3	18.5	18.6
	4	19.6	17.0	17.2	19.6	22.1	22.2	18.25	18.45	18.6
	8	19.6	17.0	17.2	19.5	22.0	22.1	18.2	18.4	18.55
	24	19.6	17.0	17.2	19.3	21.2	21.5	18.08	18.38	18.52
	28	19.6	17.0	17.2	19.25	21.0	21.4	18.02	18.35	18.51
	32	19.6	17.0	17.2	19.2	20.8	21.2	18.0	18.3	18.5
	48	19.6	17	17.2	19.2	20.8	21.2	18.0	18.3	18.5
11.3	0	17.2	15.9	16.2	18.5	20.3	20.7	17.5	17.4	17.6
	4	17.2	15.9	16.1	18.5	20.3	20.6	17.4	17.3	17.5
	8	17.2	15.9	16.1	18.45	20.25	20.5	17.35	17.2	17.4
	24	17.2	15.8	15.9	18.2	20.1	19.7	17.1	17.1	17.3
	28	17.2	15.8	15.9	18.15	20.05	19.6	17.05	17.05	17.25
	32	17.2	15.8	15.8	18.1	20.0	19.5	17.0	17.0	17.2
	48	17.2	15.8	15.8	18.1	20.0	19.5	17.0	17.0	17.2

* For location of the transducers see figure (3-4)

Table (A-9) continued: Vertical pressure measured transducers in the sand during unloading of the static pressure on the sand mass (Test No.3).

Ps Static pressure Kpa	Time hours	Pressure measured by transducers in the sand (Kpa)								
		B*1	B2*	B3*	B4*	B5*	B6*	B7*	B8*	B9*
		V	V	V	V	V	V	V	V	V
5.4	0	12.2	12.5	12.4	15.8	17.1	17.2	16.9	16.8	16.5
	4	12.3	12.4	12.3	15.7	17.0	17.15	16.7	16.4	16.3
	8	12.3	12.4	12.3	15.7	16.9	17.1	16.5	16.1	16.1
	24	12.4	12	12	15.4	16.8	16.95	16.0	15.5	15.5
	28	12.4	11.9	12	15.35	16.8	16.95	15.5	15.2	15.3
	32	12.4	11.9	12	15.3	16.7	16.9	15.2	15.0	15.2
	48	12.4	11.9	12	15.3	16.7	16.9	15.2	15.0	15.2
0	0	5.12	5.91	5.9	10.1	10.3	10.2	13.8	14.2	13.8
	4	5.1	5.8	5.8	10.0	10.2	10.1	13.4	14.0	13.4
	8	5.0	5.7	5.7	10.0	10.1	10.0	13.2	13.6	13.1
	24	4.7	5.2	5.3	9.7	10.0	9.8	12.1	12.2	12.3
	28	4.6	5.1	5.3	9.7	10.0	9.8	12.0	12.0	12.0
	32	4.55.8	5.0	5.2	9.6	9.9	9.7	11.9	11.8	11.7
	48	4.4	5.0	5.2	9.6	9.9	9.7	11.9	11.8	11.7

* For location of the transducers see figure (3-4).

Table (A-10): Horizontal pressure measured by transducers in the sand during loading of the static pressure on the sand mass (test No.3)..

Ps Static pressure Kpa	Time hours	Pressure measured by transducers in the sand (Kpa)					
		B4*	B5*	B6*	B7*	B8*	B9*
		H	H	H	H	H	H
0	0	1.9	2.0	1.6	1.8	2.1	1.8
	4	1.9	2.1	1.7	1.8	2.12	1.81
	8	2.0	2.2	1.7	1.85	2.16	1.82
	24	2.1	2.3	1.8	1.95	2.18	1.88
	28	2.1	2.3	1.9	2.0	2.19	1.89
	32	2.1	2.3	1.9	2.0	2.2	1.9
	48	2.1	2.3	1.9	2.0	2.2	1.9
5.4	0	5.0	4.4	3.9	3.5	3.6	3.0
	4	5.0	4.4	3.9	3.4	3.6	2.95
	8	4.9	4.4	3.8	3.35	3.5	2.9
	24	4.8	4.3	3.6	3.1	3.45	2.8
	28	4.8	4.3	3.6	3.08	3.48	2.75
	32	4.7	4.2	3.6	3.0	3.4	2.7
	48	4.7	4.2	3.6	3.0	3.4	2.7
11.3	0	7.5	6.3	5.6	4.3	4.9	3.5
	4	7.4	6.3	5.5	4.25	4.85	3.5
	8	7.3	6.2	5.4	4.2	4.8	3.45
	24	7.2	6.0	5.2	4.1	4.65	3.4
	28	7.0	6.0	5.1	4.03	4.62	3.37
	32	7.0	5.9	5.1	4.0	4.6	3.3
	48	7.0	5.9	5.1	4.0	4.6	3.3

* For location of the transducers see figure (3-4)

Table (A-10) continued: Horizontal pressure measured by transducers during loading of the static pressure on the sand mass (Test No.3).

Ps Static pressure Kpa	Time hours	Pressure measured by transducers in the sand (Kpa)					
		B4*	B5*	B6*	B7*	B8*	B9*
		H	H	H	H	H	H
16.9	0	9.4	8.4	7.6	5.9	6.3	4.7
	4	9.4	8.3	7.5	5.8	6.2	4.6
	8	9.3	8.3	7.4	5.8	6.15	4.5
	24	9.25	8.0	7.2	5.6	6.0	4.0
	28	9.25	8.05	7.15	5.55	5.9	3.9
	32	9.2	7.9	7.1	5.5	5.8	3.8
	48	9.2	7.9	7.1	5.5	5.8	3.8
20.5	0	11.6	9.6	8.6	6.5	6.9	5.1
	4	11.5	9.5	8.5	6.45	6.9	5.1
	8	11.45	9.4	8.4	6.41	6.8	5.02
	24	11.3	9.0	8.2	6.12	6.65	4.5
	28	11.25	8.95	8.15	6.09	6.62	4.45
	32	11.2	8.9	8.1	6.0	6.6	4.4
	48	11.2	8.9	8.1	6.0	6.6	4.4
26.2	0	14.1	10.9	9.7	7.4	8.95	5.75
	4	14.0	10.8	9.6	7.3	8.9	5.7
	8	14.0	10.7	9.5	7.2	8.7	5.6
	24	13.8	10.3	9.3	7.0	8.4	5.2
	28	13.75	10.25	9.25	6.9	8.32	5.1
	32	13.7	10.2	9.2	6.8	8.3	5.0
	48	13.7	10.2	9.2	6.8	8.3	5.0

* For location of the transducers see figure (3-4)

Table (A-11): Horizontal pressure measured by transducers in the sand during unloading of the static pressure on the sand mass (Test No.3).

Ps Static pressure Kpa	Time hours	Pressure measured by transducers in the sand (Kpa)					
		B4*	B5*	B6*	B7*	B8*	B9*
		H	H	H	H	H	H
20.5	0	13.6	10.2	9.2	3.8	8.2	5.0
	4	13.6	10.2	9.2	3.75	8.2	4.98
	8	13.6	10.1	9.1	3.7	8.15	4.92
	24	13.55	10.05	8.95	3.66	8.12	4.85
	28	13.5	10.0	8.95	3.62	8.07	4.81
	32	13.5	10.0	8.9	3.6	8.0	4.8
	48	13.5	10.0	8.9	3.6	8.0	4.8
16.9	0	13.4	9.9	8.8	3.2	7.8	4.6
	4	13.4	9.9	8.8	3.1	7.7	4.55
	8	13.4	9.9	8.8	3.05	7.6	4.5
	24	13.3	9.85	8.7	2.9	7.3	4.4
	28	13.3	9.85	8.7	2.85	7.25	4.35
	32	13.3	9.8	8.7	2.8	7.2	4.3
	48	13.3	9.8	8.7	2.8	7.2	4.3
11.3	0	12.7	9.7	8.4	3.8	6.8	4.1
	4	12.7	9.7	8.4	3.75	6.7	4.1
	8	12.7	9.6	8.35	3.7	6.6	4.0
	24	12.65	9.5	8.25	3.66	6.48	3.95
	28	12.65	9.45	8.25	3.62	6.45	3.93
	32	12.6	9.4	8.2	3.6	6.4	3.9
	48	12.6	9.4	8.2	3.6	6.4	3.9

* For location of the transducers see figure (3-4)

Table (A-11) continued: Horizontal pressure measured by transducers during unloading of the static pressure on the sand mass (Test No.3)..

Ps Static pressure Kpa	Time hours	Pressure measured by transducers in the sand (Kpa)					
		B4*	B5*	B6*	B7*	B8*	B9*
		H	H	H	H	H	H
5.4	0	11.7	7.2	7.1	4.8	6.2	3.8
	4	11.711.7	7.2	7.1	4.7	6.1	3.75
	8	11.65	7.2	7.05	4.6	6.05	3.7
	24	11.6	7.15	7.0	4.55	5.9	3.66
	28	11.6	7.15	7.0	4.52	5.85	3.62
	32	11.6	7.1	7.0	4.5	5.8	3.6
	48	11.6	7.1	7.0	4.5	5.8	3.6
0	0	4.8	4.9	4.0	4.2	5.5	3.2
	4	4.8	4.9	4.0	4.1	5.4	3.1
	8	4.8	4.8	4.0	4.0	5.3	3.05
	24	4.6	4.84	3.9	3.8	5.2	2.9
	28	4.55	4.75	3.85	3.6	5.15	2.85
	32	4.5	4.7	3.8	3.5	5.1	2.8
	48	4.5	4.7	3.8	3.5	5.1	2.8

* For location of the transducers see figure (3-4).

Table (A-12): Vertical pressure measured by transducers in the sand mass during loading and unloading of the static pressure (Test No.3).

Ps Static pressure (Kpa)	Time (day)	Vertical pressure measured by transducers in the sand (Kpa)								
		B1*	B2*	B3*	B4*	B5*	B6*	B7*	B8*	B9*
		V	V	V	V	V	V	V	V	V
0	2	2.33	2.56	2.58	4.2	4.0	3.8	5.5	5.3	5.0
1.0	4	3.2	3.4	3.58	4.9	4.3	4.5	6.5	6.4	7.0
3.2	6	5.5	5.7	6.78	6.2	5.9	6.1	7.0	7.2	7.4
5.4	8	6.9	7.0	8.0	6.9	7.2	7.3	7.8	7.6	7.8
9.5	10	9.4	8.5	10.5	9.4	10.22	10.3	8.4	8.2	8.4
11.3	12	10.7	8.9	11.7	11.0	11.7	11.9	8.9	8.6	8.8
13.2	14	11.9	9.7	13.9	12.3	13.4	13.6	9.1	9.1	9.3
15.15	16	13.3	10.9	14.3	13.9	14.5	14.7	10.9	9.5	9.6
16.9	18	14.8	12.3	15.8	15.0	16.3	16.5	11.6	11.9	11.8
18.7	20	15.7	13.0	16.7	15.8	17.2	17.5	13.0	12.9	12.8
20.5	22	17.2	15.3	17.5	17.5	19.1	19.3	14.2	14.1	14.0
23.9	24	19.0	16.6	19.5	19.1	21.1	21.2	15.5	16.0	15.8
26.2	26	21.0	18.7	20.5	21.1	23.1	23.9	19.0	19.2	18.9
23.9	28	20.8	18.1	20.2	21.0	22.8	23.4	18.6	18.9	18.8
20.5	30	20.4	17.9	18.5	20.7	22.5	23.0	18.4	18.6	18.7
18.7	32	20.1	17.5	18.0	19.5	22.1	225	18.3	18.4	18.6
16.9	34	19.6	17.0	18.2	19.2	21.8	21.2	18.0	18.3	18.5
15.1	36	19.4	16.5	16.7	18.8	21.2	20.5	17.9	18.1	18.3
13.2	38	17.8	16.0	16.3	18.5	20.8	20.0	17.8	17.8	18.0
11.3	40	17.2	15.8	15.8	18.1	20.0	19.5	17.0	17.0	17.2
9.5	42	15.0	14.3	15.0	17.1	18.9	18.2	16.8	16.9	17.0
7.7	44	14.2	13.9	14.0	16.6	17.8	17.5	15.4	15.3	15.6
5.4	46	12.4	11.9	12.0	15.3	16.7	16.9	15.2	15.0	15.2
3.2	48	9.5	9.9	7.0	13.4	13.3	13.1	13.8	13.3	13.7
0	50	5.6	5.5	5.7	9.6	9.9	9.7	11.9	11.8	11.7

* For location of the transducers see figure (3-4).

Table (A-13): Horizontal pressure measured by transducers in the sand mass during loading and unloading of the static pressure (Test No.3).

Ps static pressure (Kpa)	Time (day)	Horizontal pressure measured by transducers in the sand (Kpa)					
		B4*	B5*	B6*	B7*	B8*	B9*
		H	H	H	H	H	H
0	2	2.4	2.3	2.3	3.0	2.95	2.7
1.0	4	2.6	2.4	2.5	3.3	3.2	3.1
3.2	6	3.8	3.0	3.1	4.4	4.3	4.2
5.4	8	4.7	4.2	4.4	5.35	5.2	5.1
9.5	10	6.3	6.3	6.1	7.3	7.2	7.1
11.3	12	7.0	7.1	6.9	8.0	7.9	7.65
13.2	14	8.1	8.13	7.9	8.8	8.7	8.55
15.15	16	8.7	9.1	8.6	9.1	9.05	8.95
16.9	18	9.2	9.8	8.9	10.15	10.2	9.9
18.7	20	10.1	10.75	9.9	10.7	11	10.3
20.5	22	11.2	11.6	10.9	11.1	11.2	10.6
23.9	24	12.9	13.1	12.8	12.1	12.3	11.85
26.2	26	13.7	14.1	13.5	12.9	13.1	12.7
23.9	28	13.6	14.0	13.5	12.9	13.0	12.7
20.5	30	13.5	13.9	13.5	12.8	12.9	12.6
18.7	32	13.4	13.9	13.4	12.8	12.8	12.5
16.9	34	13.3	13.8	13.2	12.7	12.7	12.4
15.1	36	13.0	13.2	12.9	12.5	12.4	12.3
13.2	38	12.8	12.7	12.8	12.3	12.1	12.0
11.3	40	12.6	12.2	12.7	11.7	11.6	11.1
9.5	42	12.0	11.7	12.1	10.9	11	10.4
7.7	44	11.7	11.3	11.6	9.5	9.6	9.3
5.4	46	11.6	10.2	11.5	8.6	8.65	8.5
3.2	48	9.6	9.2	9.4	7.65	7.75	7.5
0	50	6.5	6.6	6.4	7.51	7.55	7.42

* For location of the transducers see figure (3-4).

Table (A-14): Pressures measured by transducers in the sand during the displacement of the wall (Test No.3).

Displacement of the wall (mm)	0.0	0.5	1.0	1.5	2.1	2.51	2.9	8.4
pressure measured by transducers in the sand (Kpa)								
V1*	5.6	5.6	5.61	5.62	5.62	5.6	5.6	5.6
V2*	5.5	5.52	5.54	5.33	5.33	4.81	4.78	4.57
V3*	5.7	5.3	5.1	5.0	4.9	4.55	4.35	4.1
V4*	9.6	9.6	9.55	9.52	9.52	9.52	9.52	9.52
V5*	9.9	9.9	9.9	9.9	9.65	9.49	9.42	9.23
V6*	9.7	8.94	8.22	7.88	7.65	7.25	7.25	7.25
V7*	11.90	11.90	11.90	11.90	11.90	11.90	11.90	11.90
V8*	11.8	11.8	11.7	11.65	11.51	11.43	11.0	11.0
V9*	11.7	11.35	10.98	10.56	10.21	9.85	9.85	9.85
H4*	6.50	6.50	6.50	6.50	6.50	6.50	6.50	6.50
H5*	6.6	6.47	6.17	5.95	5.57	5.43	5.43	5.43
H6*	6.43	6.21	5.89	3.89	3.40	3.43	3.43	3.41
H7*	7.50	7.50	7.50	7.50	7.50	7.50	7.50	7.50
H8*	7.45	7.45	7.35	6.54	6.15	6.07	5.85	5.85
H9*	7.4	7.4	7.32	6.48	6.15	5.99	5.91	5.91

* For location of the transducers see figure (3-4).